Corrosion of W/Ts

Prof. Stephanos Tsinopoulos

Department of Mechanical Engineering,

University of Peloponnese, Greece

D.T. Kalovelonis

Department of Mechanical Engineering and Aeronautics,

University of Patras, Greece

Contents

Corrosion Principals

Significance and cost of Corrosion

Corrosion threats the overall integrity of:

- *Ships*
- *Offshore structures for oil and gas productions*
- *Offshore wind turbines*
- *Above and below ground storage tanks*
- *Underground pipelines*
- *Reinforced concrete structures (bridges, etc.)*
- *Nuclear facilities, etc.*

Corrosion consequences may be:

- *Catastrophic failure of structures*
- *Plant shutdowns*
- *Waste of resources*
- *Loss or contamination of product*
- *Reduction in efficiency*
- *Costly maintenance, etc.*

Estimated cost:

1) *About a quarter of the world's iron and steel production is destroyed by corrosion.*
2) *The annual global cost of corrosion is over 3% of the world's GDP, estimated at US$ 2.2 trillion.*





Definition of Corrosion

*Corrosion is the **spontaneous destruction** of **metals** and **alloys** caused by their:*

- ✓ *chemical,*
- ✓ *biochemical, or/and*
- ✓ ***electrochemical***

*interaction with the **surrounding environment**.*

.

*During corrosion, **metals** tend to **convert** to **more thermodynamically stable compounds**, such as oxides, hydroxides, salts, or carbonates. The original compounds (minerals and ores) are recovered from metals decreasing in free energy. Hence, **the energy used for forming the metals is emitted during corrosion reactions**. In other words, Metallurgy in reverse!*

Consequently, corrosion is a spontaneous, usually slow-progressing, chemical/electrochemical phenomenon

Corrosive environments

- ❑ Seawater
- ❑ Soil
- ❑ Sea mud
- ❑ Thin films

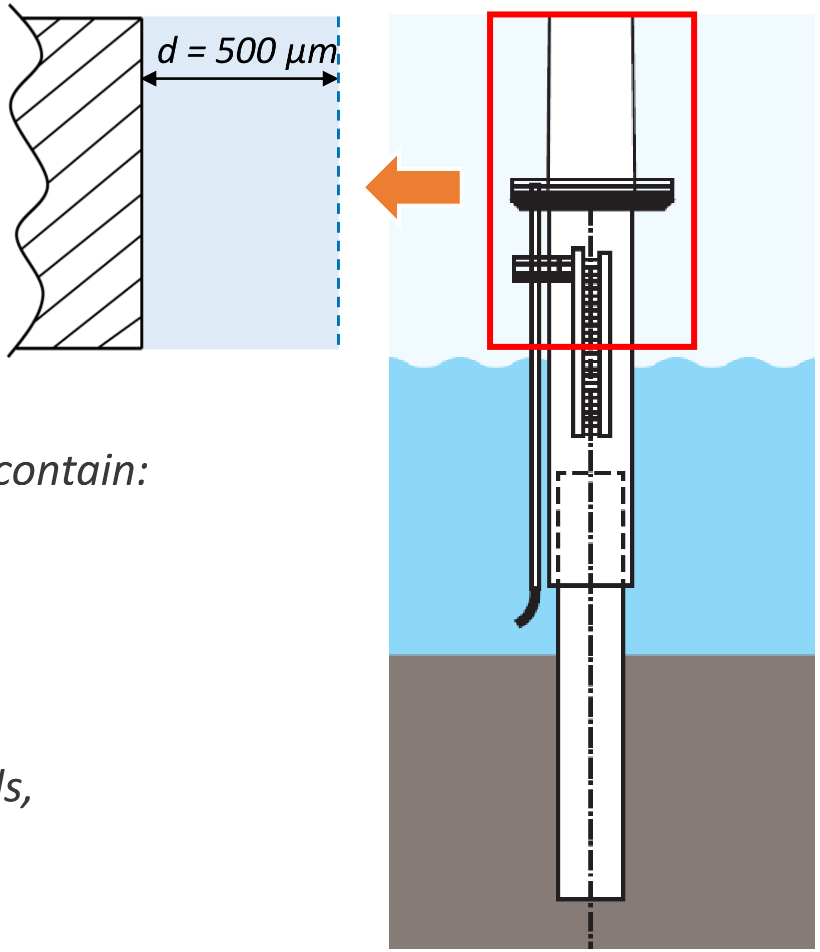

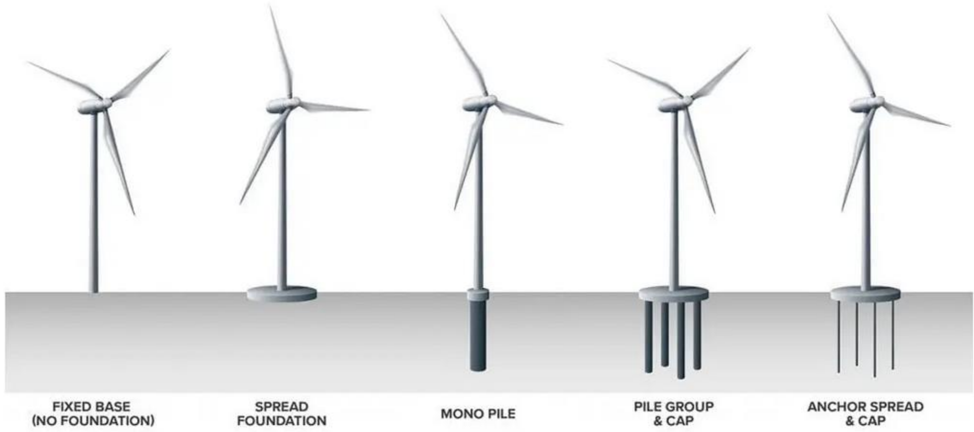

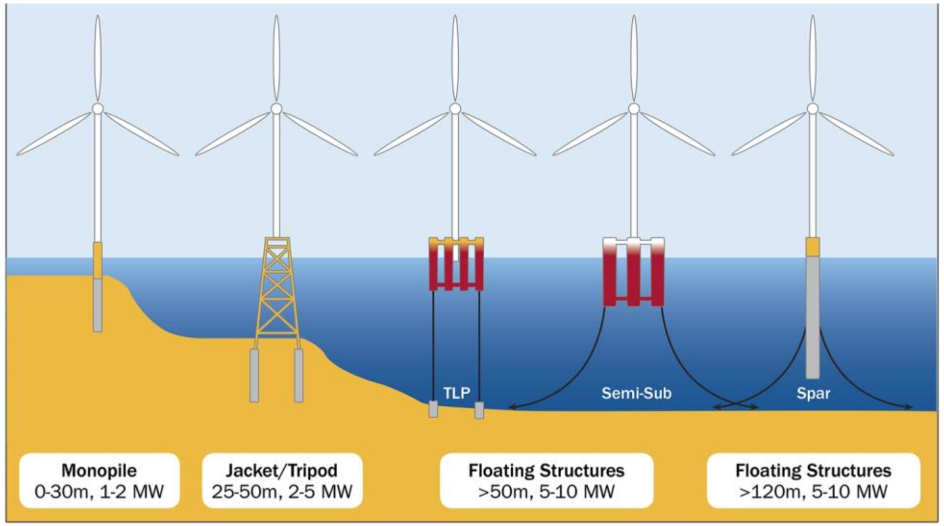

Corrosive environments may contain:

- ✓ *moisture,*
- ✓ *oxygen,*
- ✓ *chlorides*
- ✓ *inorganic and organic acids,*
- ✓ *high pressure, and/or*
- ✓ *high temperature*

Corrosion of steel in neutral or alkaline environment

- *The overall anodic reaction for the corrosion of iron in neutral or alkaline solutions is described:*

$$2Fe + 2H_2O + O_2 \rightarrow 2Fe^{2+} + 4OH^-$$

- *The above reaction may be separated into two partial reactions*

$$2Fe \rightarrow 2Fe^{2+} + 4e^-$$

$$O_2 + 2H_2O + 4e^- \rightarrow 4OH^-$$

- *In practice, the ferrous ion Fe^{2+} is likely to oxidize further to ferric ion Fe^{3+} then to react with the hydroxyl ion OH^- to produce insoluble ferric hydroxide $Fe(OH)_3$ which may loosely be called rust.*

$$Fe(OH)_2 + H_2 \rightarrow Fe(OH)_3 + H^+ + e^-$$

Corrosion of steel in acidic environment

- *The corrosion of iron in an acid environment occurs according to the following reaction:*

$$\mathrm{Fe} + 2\mathrm{HCl} \overset{\pm ne}{\rightleftarrows} \mathrm{FeCl_2} + \mathrm{H_2}$$

- *The dissolution of iron in an acidic solution releases hydrogen without the formation of any oxide barrier films on the surface.*
- *The above reaction may be separated into two partial reactions*

$$\mathrm{Fe} \longrightarrow \mathrm{Fe}^{2+} + 2\mathrm{e}^- \text{ (anodic partial reaction)}$$

$$2\mathrm{H}^+ + 2\mathrm{e}^- \longrightarrow \mathrm{H_2} \text{ (cathodic partial reaction)}$$

Overall reaction rate

The overall rate of the corrosion reaction is the given by the summation of the anodic and cathodic rates:

$$i = i_a - \sum_j i_{c,j}$$

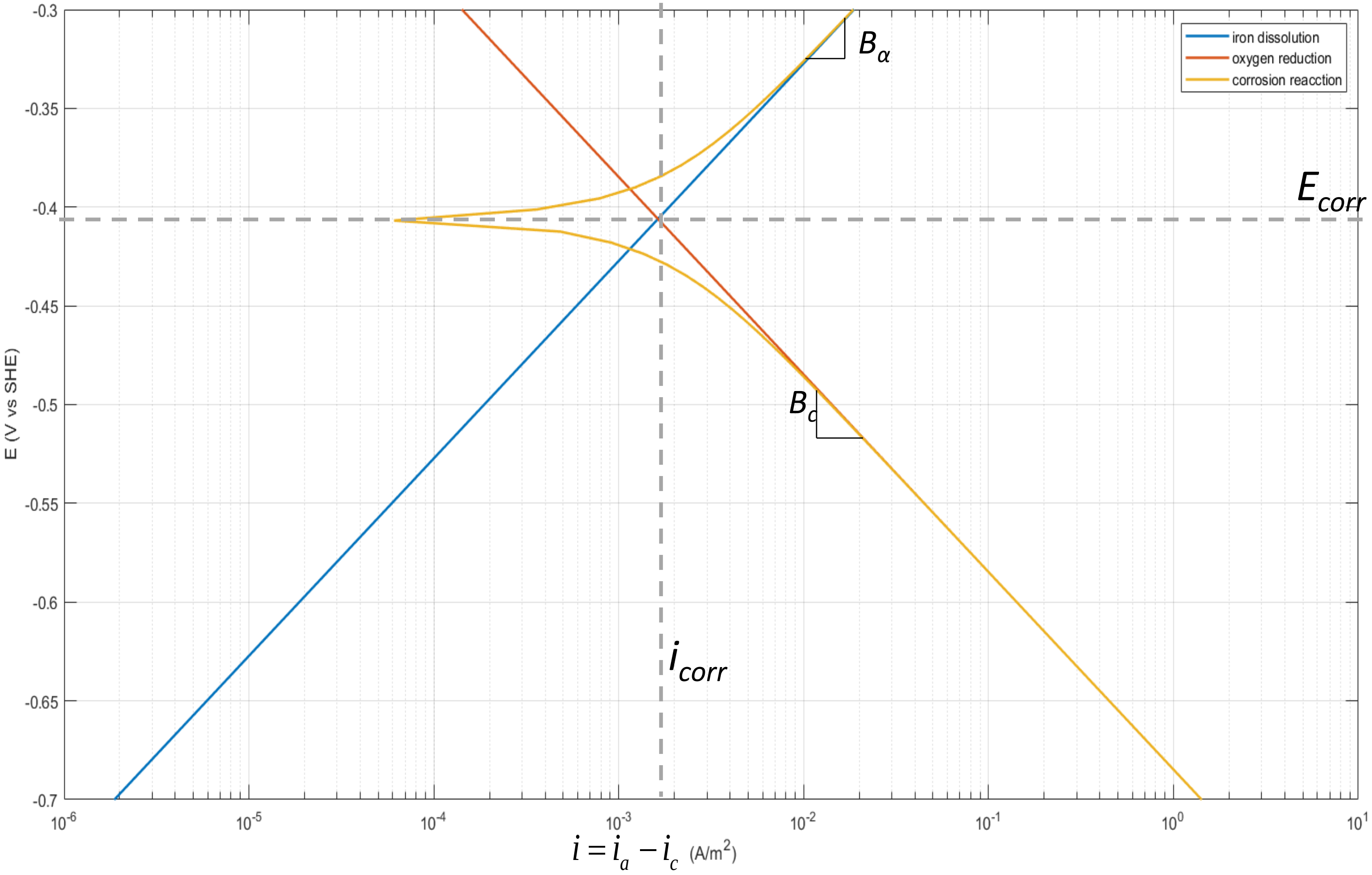

Active-passive behavior of steel

- ***Activity region***: *Active dissolution of steel.*
- ***Transition region***: *Unstable region, eventually steel will become either active or passive.*
- ***Passivity region***: *A protective barrier film is sustained.*
- ***Transpasive region***: *Pitting corrosion occurs.*

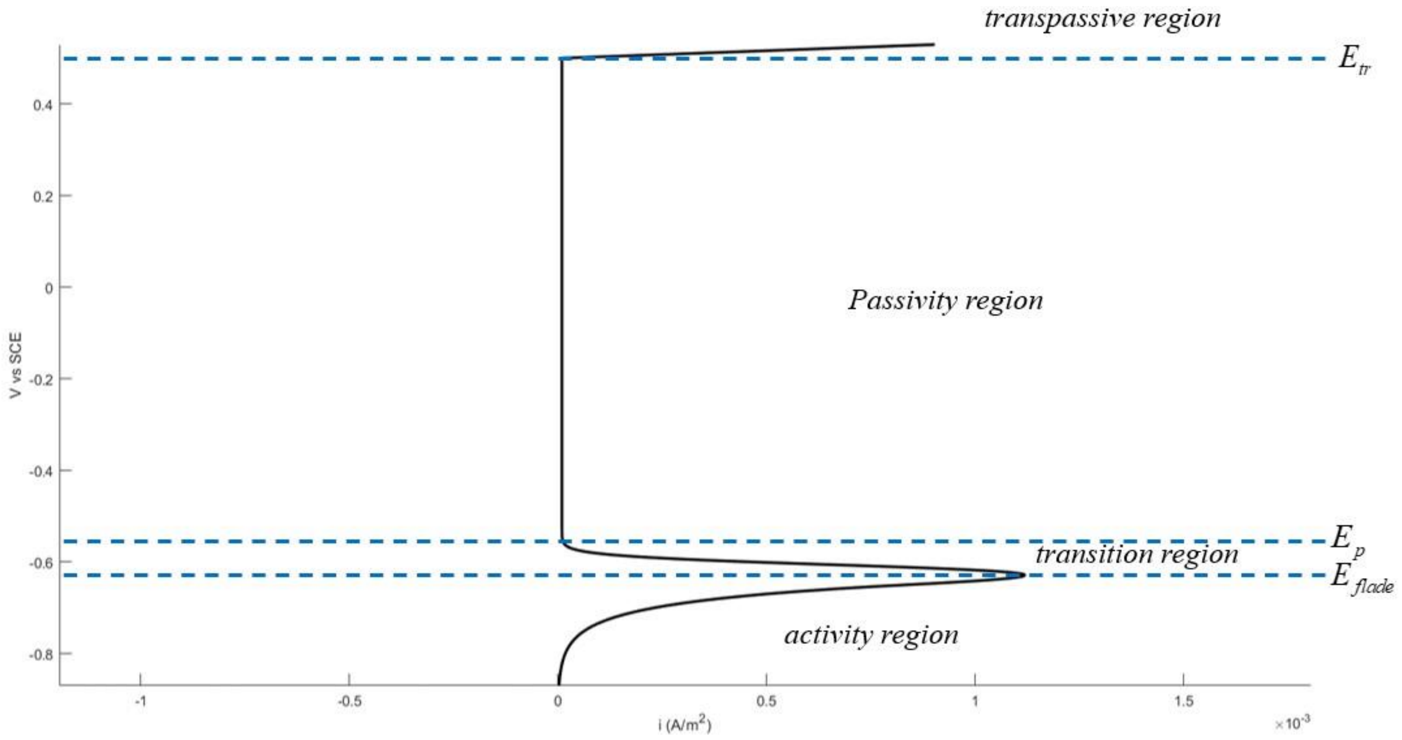

Active-passive behavior of steel

$$E_{Tr} = f\left(\left[Cl^{-}\right], T, pH\right)$$

- *Decrease of pH causes a decrease of the transpassive potential.*
- *Increase of chloride content causes a decrease of the transpassive potential.*

$$E_{flade} = f\left(\left[Cr\right], pH\right)$$

- *Decrease of pH causes an increase at the Flade potential.*

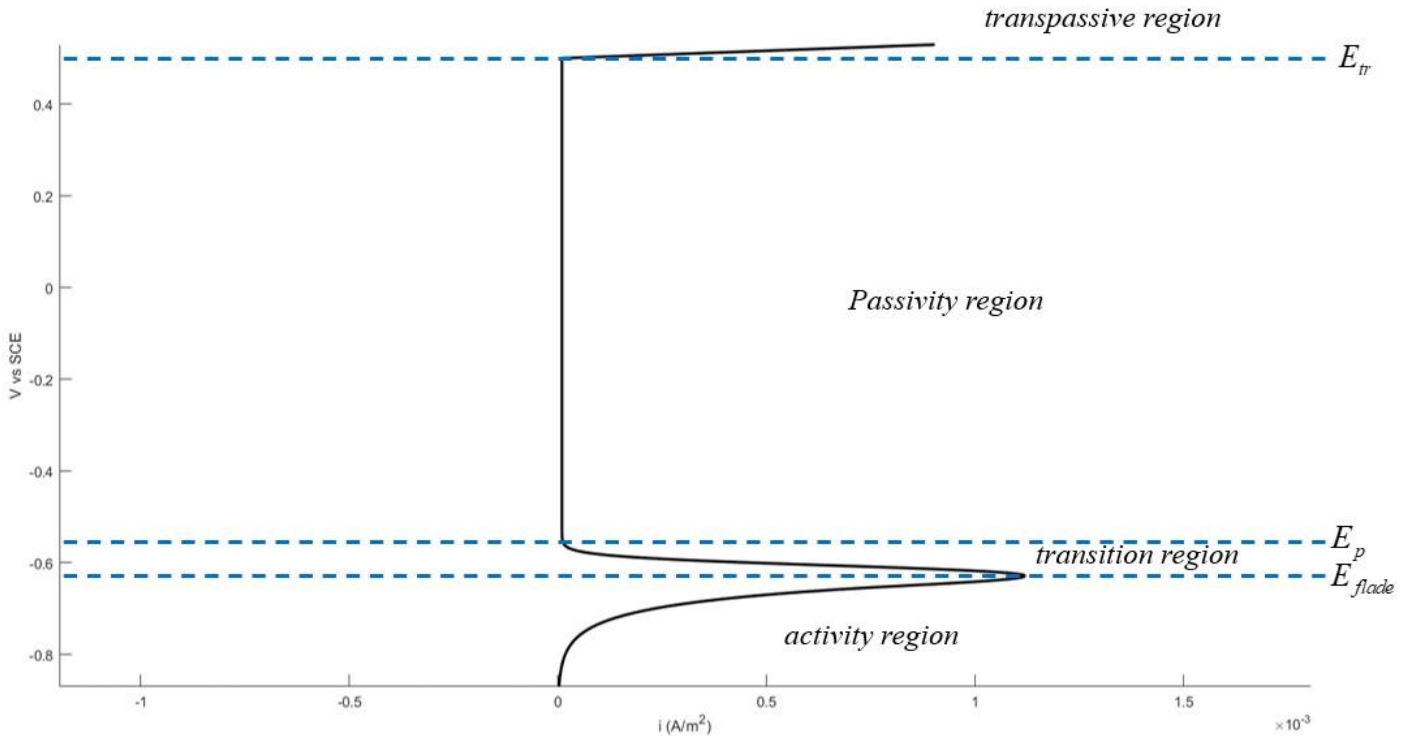

Rate of steel dissolution

$$i_a = i_{Fe}^0 e^{\frac{\varphi - \varphi_{eq,Fe}}{b_a}}$$

$$b_a = \frac{RT}{(1-a)zF}$$

$$i_{Fe}^0 = f\left([Fe]\right)$$

Iron equilibrium potential is constant for pH < 10

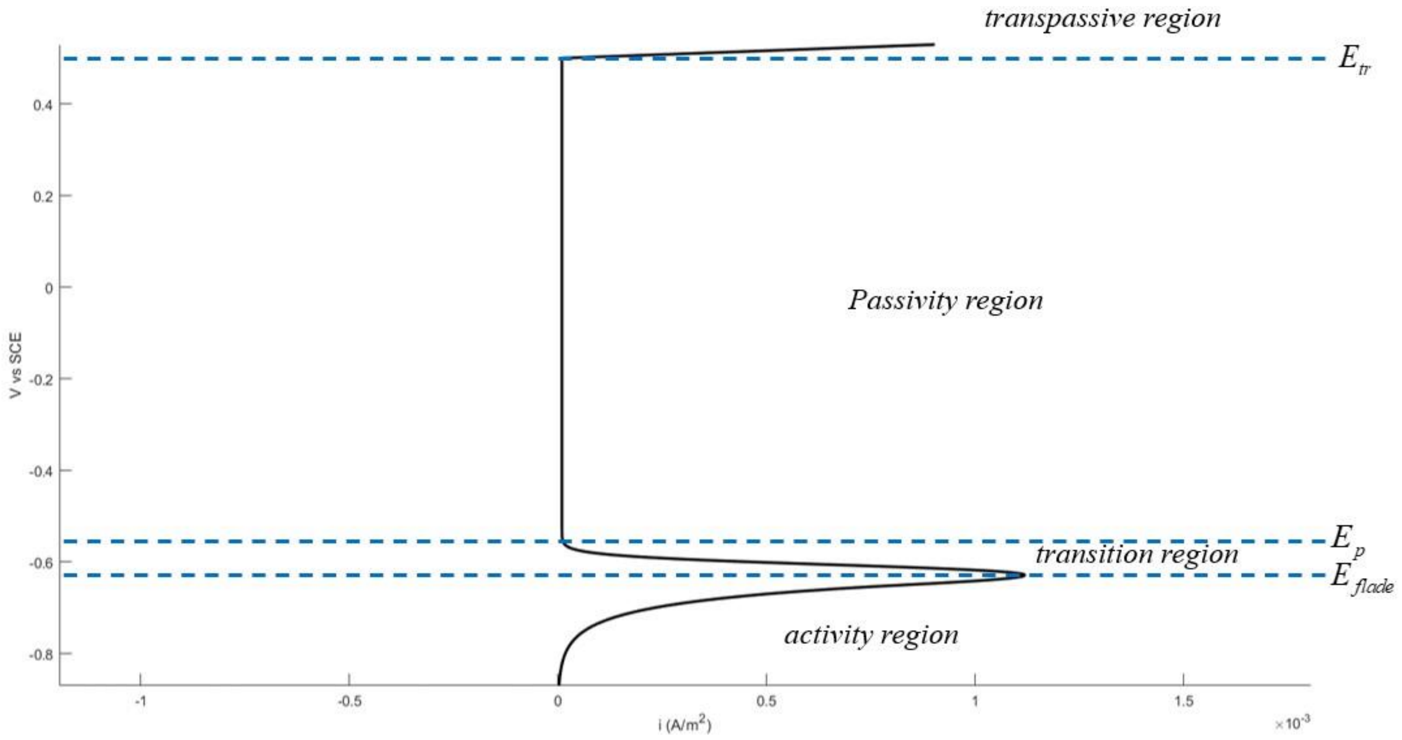

Rates of the cathodic partial reactions

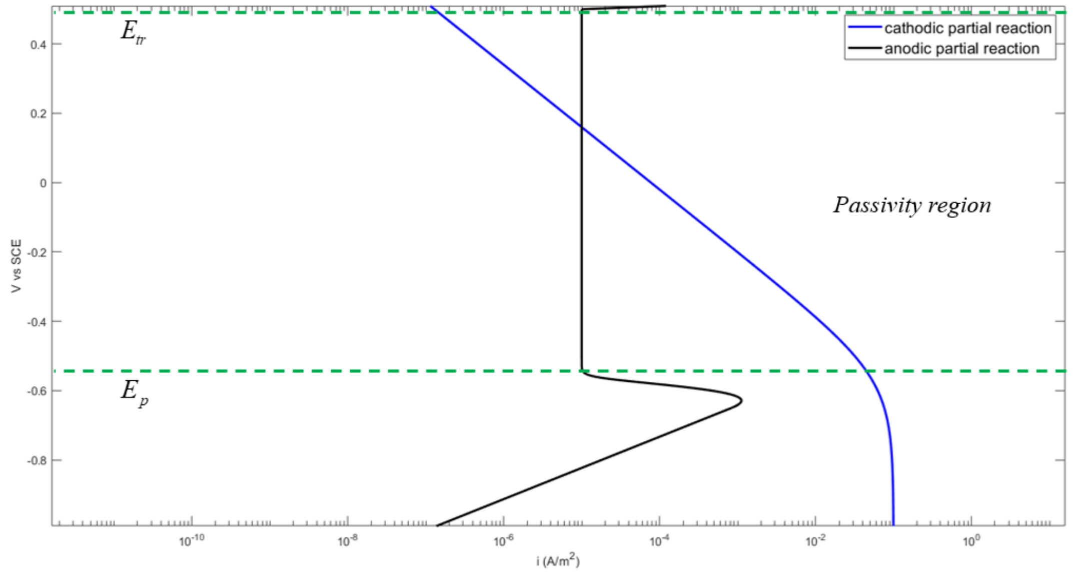

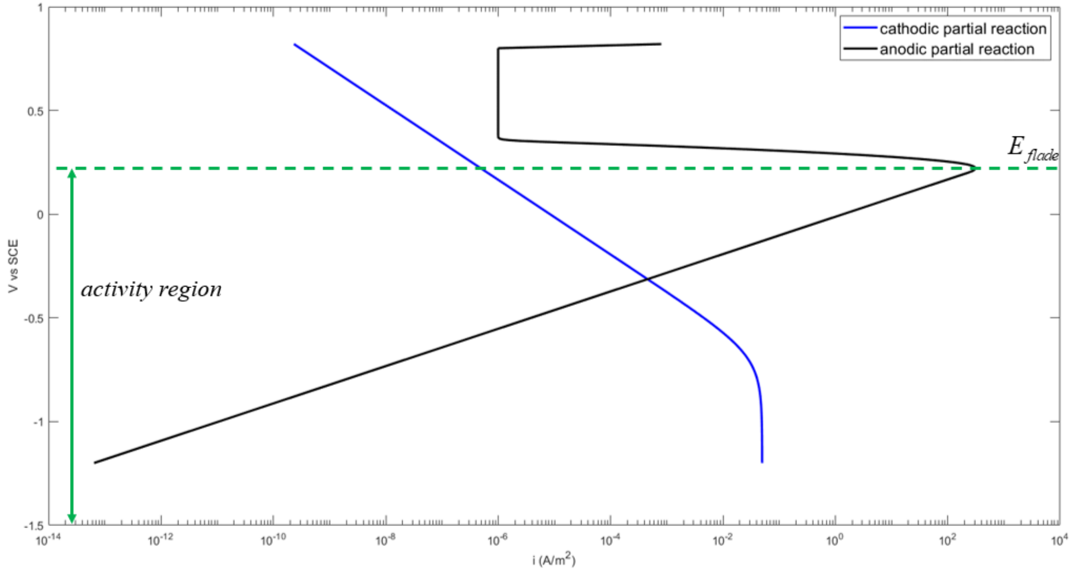

$$i_c = \frac{c_O}{c_O^b} i_O^0 e^{\frac{\varphi - \varphi_{eq,O}}{b_c}} \qquad b_c = -\frac{RT}{azF} \qquad i_O^0 = f([O])$$

$$\varphi_{eq,O_2} = \varphi_{O_2}^0 + 2.303\frac{RT}{zF}\log\left(\frac{P_{O_2}}{a_{OH^-}^4}\right) =$$

$$0.401 + 2.303\frac{RT}{4F}\log P_{O_2} - 2.303\frac{RT}{F}(14 - pH) \text{ , V vs SHE}$$

$$\varphi_{eq,H_2} = \varphi_{H_2}^0 + 2.303\frac{RT}{zF}\log\left(\frac{a_{H^+}^2}{P_{H_2}}\right) =$$

$$0.0 - 2.303\frac{RT}{2F}\log P_{H_2} - 2.303\frac{RT}{F}pH \text{ , V vs SHE}$$

Types of Corrosion

1. *Galvanic corrosion*
2. *Atmospheric corrosion*
3. *Pitting corrosion*
4. *Crevice corrosion*
5. *Stray-Current induced corrosion*
6. *Corrosion Fatigue*
7. *Hydrogen induced cracking*

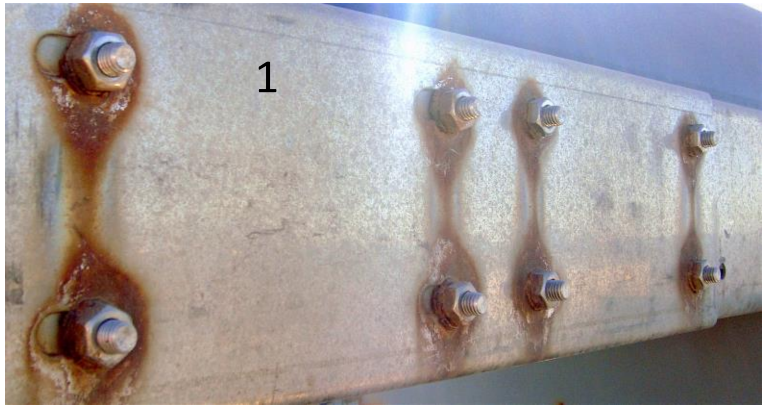

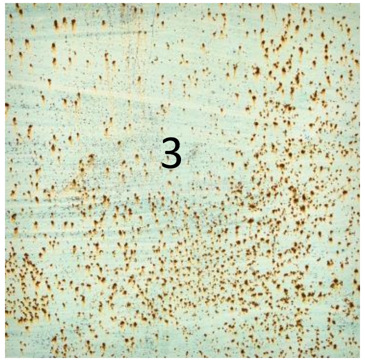

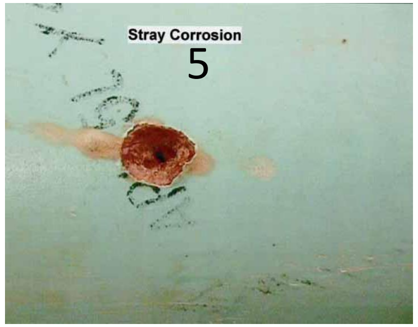

Stray Current Induced Corrosion

- *stray currents originate from any power source, such as electrified railway, transit and trolley bus systems, equipment at industrial sites, welding machines, CP rectifiers etc.*
- *stray current discharging is local, resulting in localized corrosion.*
- *the stray current-induced corrosion is one of the most severe types of corrosion*

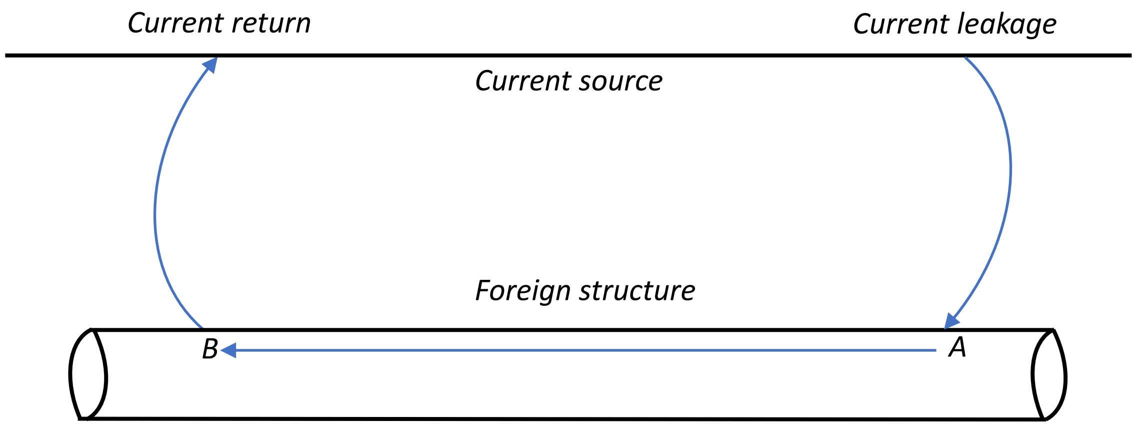

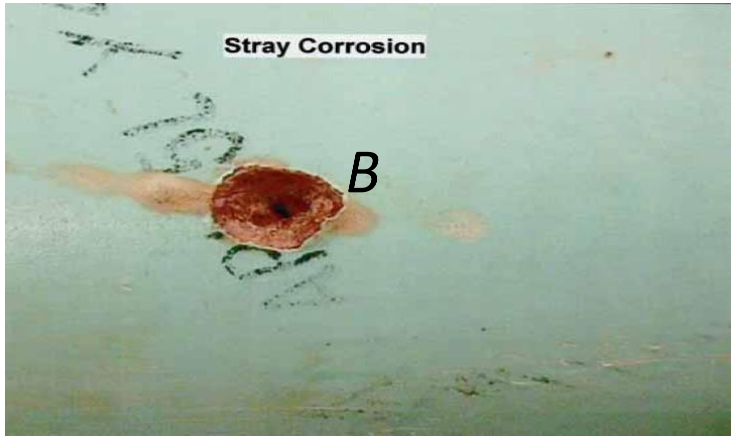

Galvanic Corrosion

The **potential difference** established when two metals (alloys) are **electrically connected** in a **conducting medium** produces electron flow and causes:

- the metal (alloy) with more negative potential to preferentially corrode (**anode**)
- the more positive metal (alloy) becomes a **cathode** and is protected by the negative metal (alloy)

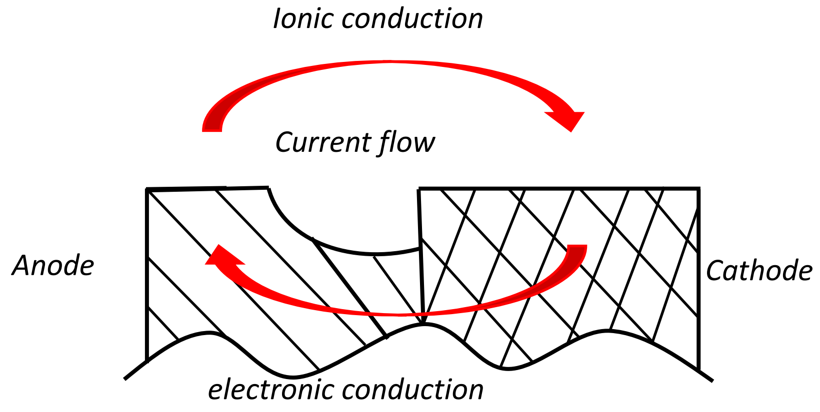

Galvanic Corrosion

- *Galvanic corrosion also occurs when the **same metal** is in contact with an electrolyte at two **different concentrations** or with **different aeration** levels (differential aeration cell).*

- *Soil with varying salinity or pH, in contact with a buried structure, creates galvanic cells.*

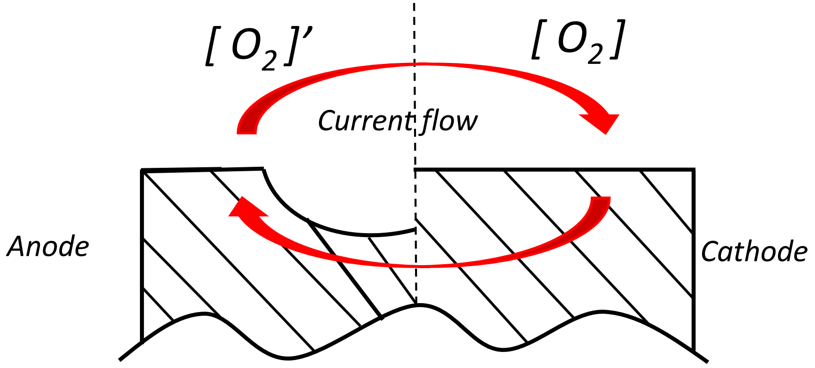

Galvanic Corrosion

- *Approximately constant temperature and pH for depth < 200m*

*other **parameters** that influence corrosion are*

- *calcareous deposits*
- *the* presence or activity (or both) of microorganisms in the steel surface.

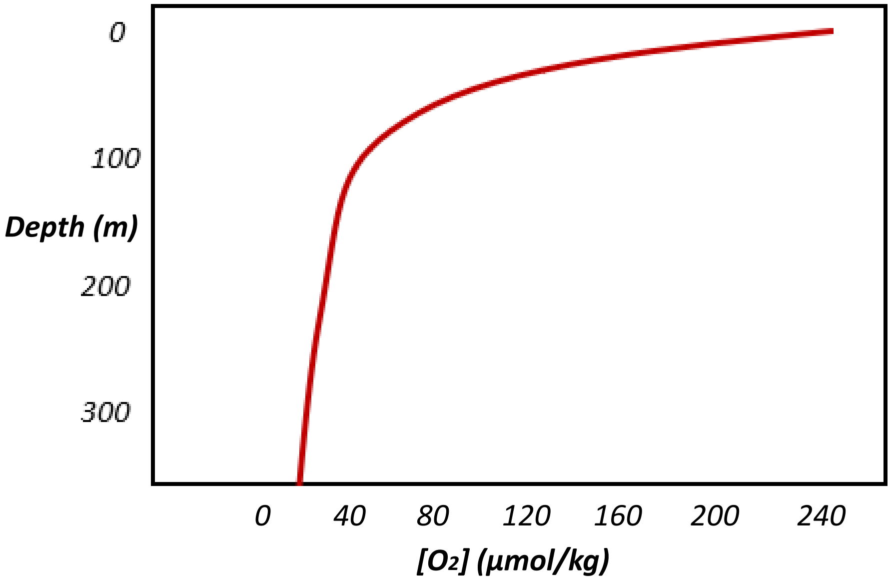

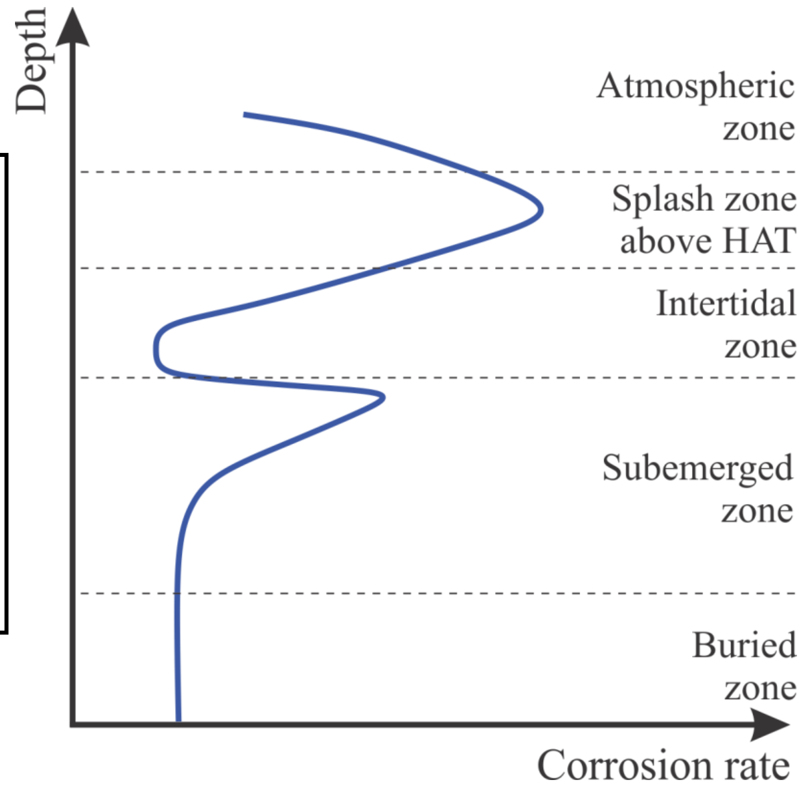

Atmospheric corrosion

- *Atmospheric corrosion is a special case of galvanic corrosion.*
- *Occurs in the presence of a thin aqueous layer on the oxidized metal in the atmosphere and its pollutants.*
- *Oxygen from the atmosphere is provided to the thin film electrolyte.*
- *It can be both dry and wet.*

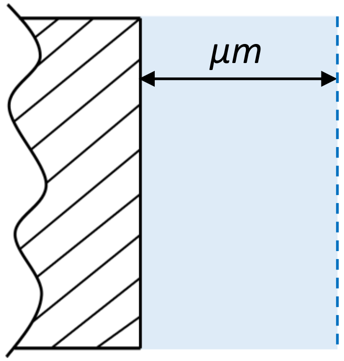

Wet conditions

- *The surface degradation process occurs when chloride particles deposit on the steel surface.*
- *The passive film is dissolved, the corrosion starts under a thin aqueous layer.*
- *Localized corrosion can develop when the chloride ion concentration of the solution is high enough.*

Dry conditions

When the atmospheric conditions become drier, rust will form around the corroded areas because dissolved species such as ferric cation (Fe^{3+}) will be deposited, leading to further surface degradation.

Atmospheric corrosion: blocking effect

- *The main sources of contamination of steel surfaces are airborne salts and pollution.*
- *The main contaminants contained in the atmosphere include chloride ions (Cl^-), sulphate ion (SO_4^-), nitrate (NO_3^-) and sulphur dioxide (SO_2).*
- *The presence of surface contaminants or dust deposits can block the supply of oxygen from the atmosphere and form a crevice.*
- *Also, corrosion inhibition due to the contaminants has been observed.*
- *For example, an inhibitor effect for nitrate was found under magnesium salt droplets.*

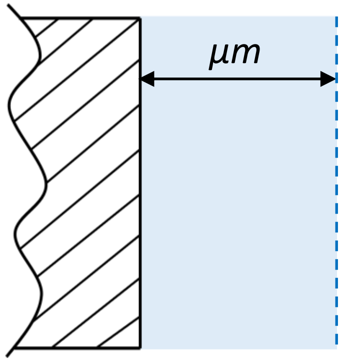

Atmospheric corrosion: exposure conditions

- *The effect of different exposure conditions such as temperature and relative humidity should be considered as a conductive electrolyte is needed for atmospheric corrosion to occur.*

- *High humidity and high temperature create favorable conditions for the occurrence of atmospheric corrosion.*

- *High humidity generates a film of moisture on the steel surface that dissolves salt deposits and creates a corrosive electrolyte .*

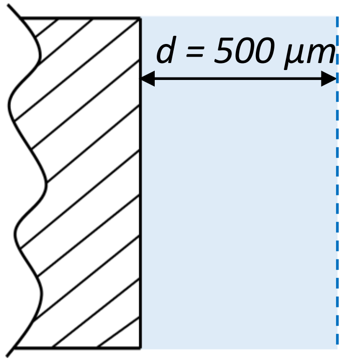

Pitting corrosion

- *Pitting represents an extremely localized attack that produces holes in the metals or alloys.*
- *It is one of the most destructive, localized forms of corrosion.*
- *The pits are small cavities or holes with a depth greater than or equal to its surface diameter.*
- *They penetrate the metal, causing equipment failure due to preformation with minimal weight loss.*

Pitting corrosion: initiation

- *In the presence of chloride ions, the passive film is removed by its reaction with chloride ions to form salt islands.*

$$FeOOH + Cl^{-} \rightarrow FeOCl + OH^{-}$$

- *the reaction of salts islands with water produce ferritic ions.*

$$FeOCl + H_2O \rightarrow Fe^{3+} + Cl^{-} + 2OH^{-}$$

- *Small surface area anodes are formed on the metal surface, which are in contact with the large surface area of the passive film cathodes.*

- *The active-passive cell potential (0.5 V) triggers a high anodic current density due to the much smaller electroactive surface areas of the anodes.*

- *Metal cations hydrolysis, due to metal dissolution results in a local pH decrease and, also the chloride concentration increases at the* ***pitting initiation*** *site.*

$$Fe^{2+} + 2H_2O + Cl^{-} \rightarrow Fe(OH)_2$$

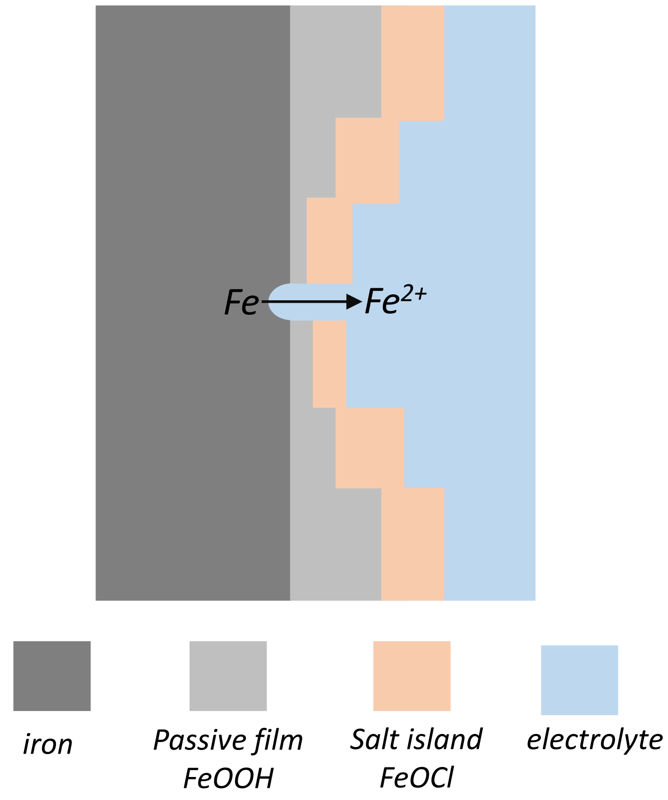

Pitting corrosion: propagation

- *Oxygen reduction occurs at the passive region and ferrous ions formed at the anode beneath the hydrated oxide film.*
- *Potential gradient established at the pit interface drives chloride electromigration due to voltage drop between the pit interior and cathodic sites of passive film*
- *Positively charged ferrous ions attract negatively charged chloride ions from the bulk solution and accumulate on the initial pitting site.*
- *Oxygen also diffuses through the rust membrane and oxidizes ferrous ions that diffuse from the acidic pit bottom to the pit mouth, where it produces Fe(OH)3 as a corrosion product at the insoluble porous rust cap.*
- *During pitting, the pit is acidified, enriched with chlorides and metal cations, while oxygen is depleted from the pit interior.*
- *Oxygen reduction occurs on the passive film, while the anodic reaction takes place at the interior of the pit, as result, the acidity developed in the pit is not neutralized.*
- *Low pH, aggressive chloride, and oxidizing agents in the pit interior promote pit growth in most metals.*

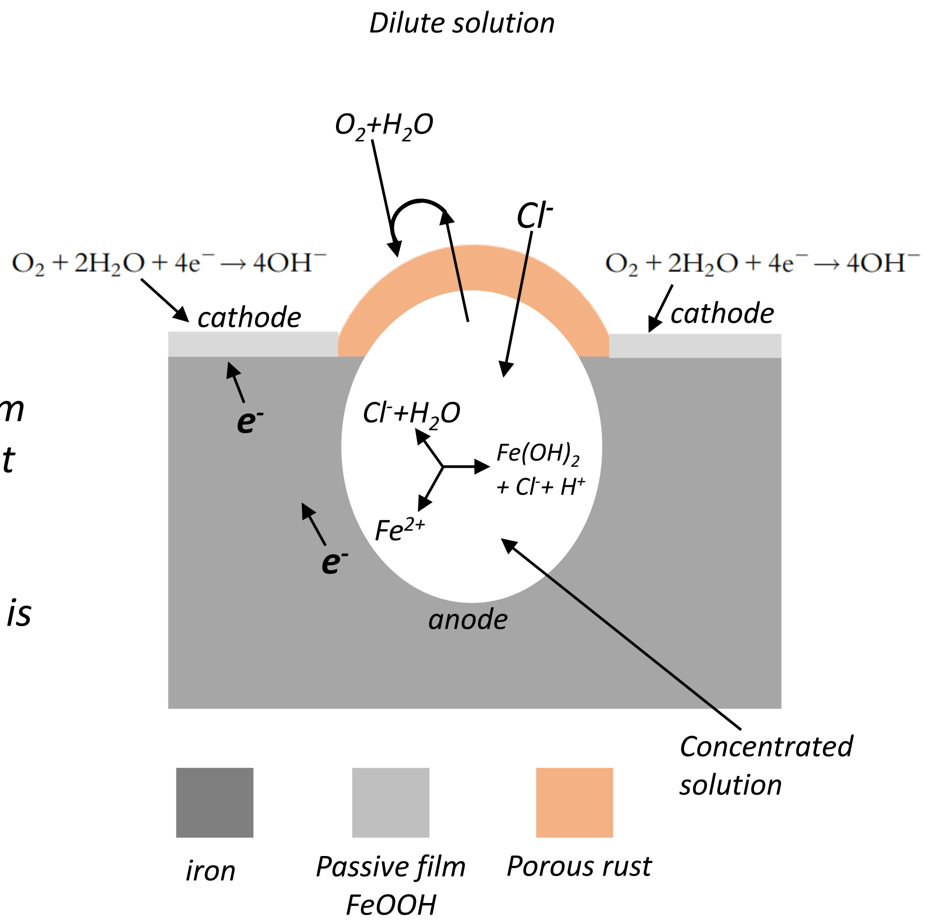

Pitting corrosion: pit arrest

- *As pit depth increases with time the local pit potential decreases.*

- *The local pit potential decrease cause a decrease in pit current density and, consequently, a decrease in metal dissolution rate.*

- *If at some point the outer surface potential is higher than the dissolving pit wall potential, the chloride ions will transport out of the pit.*

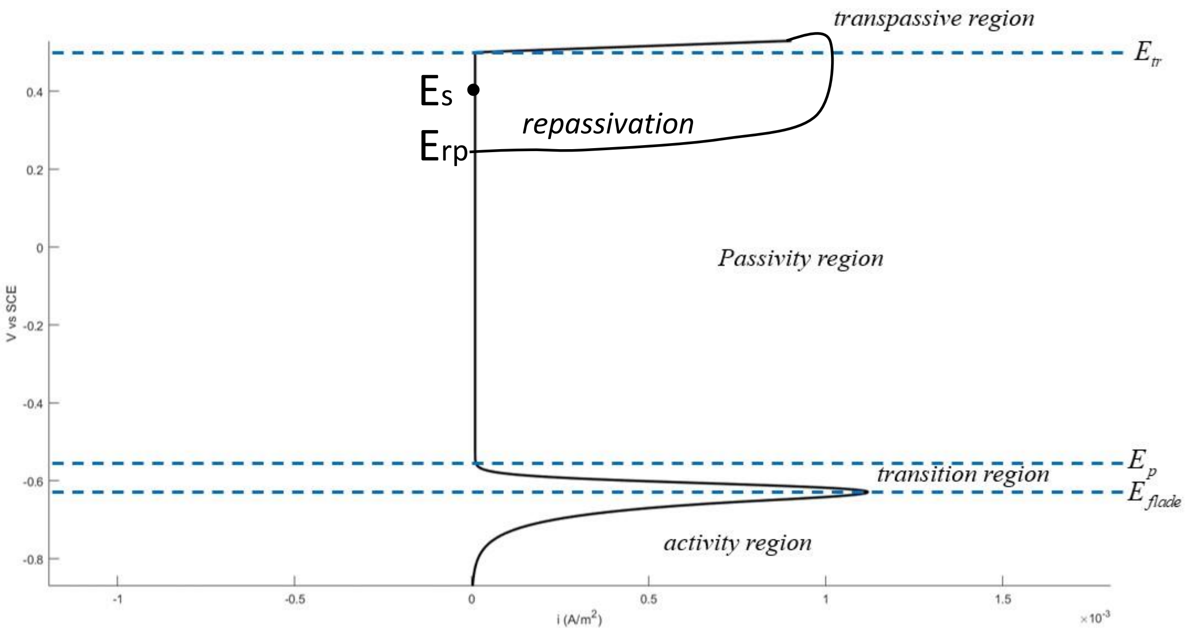

Crevice corrosion

- *Crevice corrosion is initiated by small solution volumes captured under bolt gasket rivets or surface deposits.*

- *It destroys the integrity of mechanical joints in engineering structures constructed from stainless steel, aluminum, titanium, and copper.*

- *For crevice corrosion to occur, the crevice must allow the entry of the aggressive solution and be sufficiently narrow to keep the corrosion products inside the crevice.*

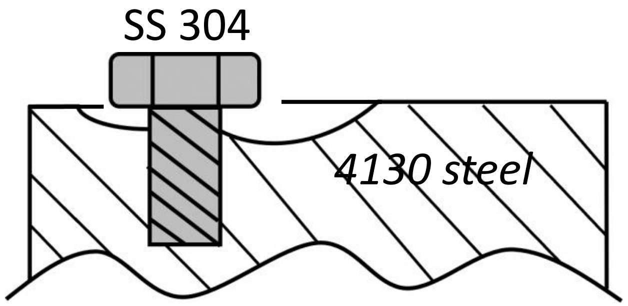

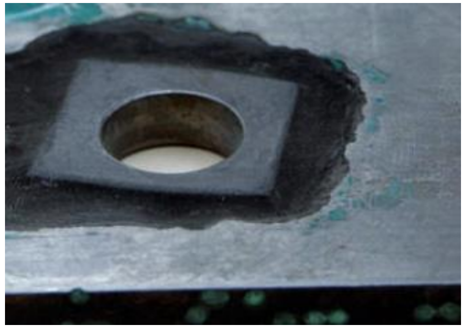

Crevice corrosion

- *The crevice corrosion reaction involves oxygen reduction and metal dissolution:*

$$2Fe \rightarrow 2Fe^{2+} + 4e^{-}$$

$$O_2 + 2H_2O + 4e^{-} \rightarrow 4OH^{-}$$

- *Active-passive short circuits are formed between the aggressive solution in the crevice, which becomes depleted in oxygen (anode) and the external metal surface (cathode).*

- *The short-circuit current between anode and cathode results in electrolytic chloride migration that initiates pit formation in the crevice.*

- *As discussed in pitting corrosion, metal dissolution in a crevice is followed by electrolyte hydrolysis and acidification at the pit interior.*

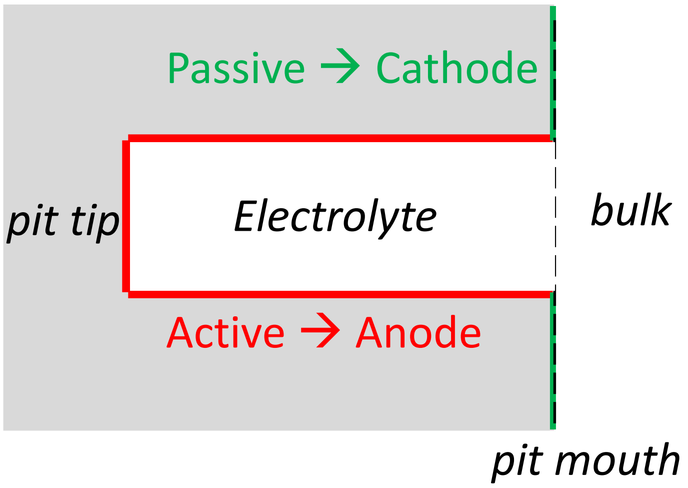

Corrosion Fatigue

Corrosion fatigue is fatigue in a corrosive environment. It is the mechanical degradation of a material under the joint action of corrosion and cyclic loading.

- The strength of metals and alloys, under cycling loading, decreases in corrosive environments.
- Fatigue-crack-growth rate is enhanced by corrosion
- Fractures are initiated in pits.

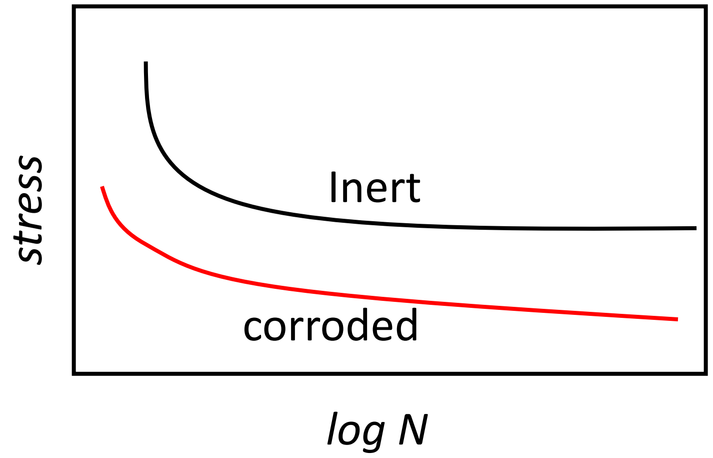

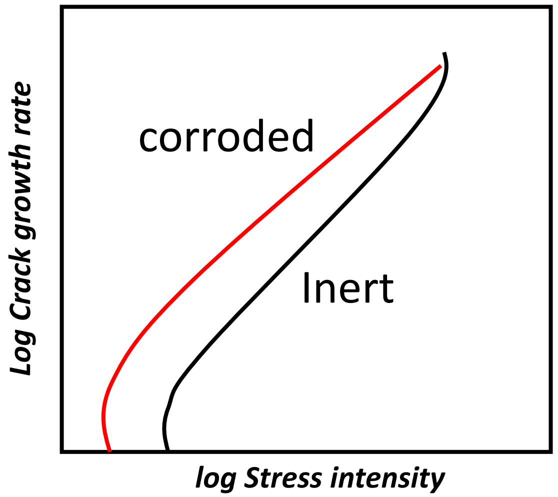

Hydrogen induced cracking

A second cathodic process, which plays no part in the free corrosion reaction, becomes energetically viable at more negative potentials than the iron equilibrium potential. The electrolysis of water:

$$2H_2O + 2e^- \rightarrow H_2 + 2OH^-$$

- *Hydrogen is evolved during processes such as electroplating, corrosion, and cathodic protection.*
- *HIC is a major problem in the gas and oil industries, causing severe equipment failure.*
- *Hydrogen-induced damage results in internal cracks caused by hydrogen recombination into gaseous molecules in bulk steel.*

Hydrogen induced cracking

- **Hydrogen diffusion** is via the drifting of hydrogen atoms between normal interstitial lattice sites (NILS) in metals.
- Besides the NILS, there is another group of sites which hydrogen resides, the trapping sites

mechanisms

Hydrogen enhanced localized plasticity (HELP)

sufficiently concentrated hydrogen at the crack tip will promote whatever deformation processes that the microstructure allowed.

the HELP mechanism only affects the yield condition of the material

Hydrogen enhanced decohesion (HEDE)

The presence of hydrogen in metals will reduce the bonding energy between metal atoms.

- reduction of cohesive strength along the grain boundary
- transition of the fracture mechanism from ductile to brittle.

Hydrogen Embrittlement

Hydrogen embrittlement results from alloy exposure to hydrogen in processes such as welding, casting, or ***cathodic protection****.*

During electrochemical reactions, some evolved atomic hydrogen is adsorbed on the metallic surface, the extent of which depends on surface adsorption kinetics.

Damage occurs when hydrogen accumulates in interstitial defects (hollow spaces) of the lattice.

In areas of high concentration of hydrogen, adsorbed hydrogen recombines to form molecular hydrogen, causing high localized pressures.

Irreversible hydrogen accumulation within the metal lattice leads to the mechanical property deterioration, steels lose ductility, resulting in hydrogen embrittlement.

Some adsorbed hydrogen diffuses into the crystalline substrate lattice where it reacts with metal atoms to form brittle metal hydrides, causing the structure to fail far below the yield strength.

High-strength steels have the highest susceptibility to hydrogen embrittlement. The atomic hydrogen and metallic atomic structure interaction inhibits the ability to stretch under load, causing steel to become brittle.

Cracking due to hydrogen embrittlement is caused by hydrogen evolution at the interface and increases with increasing cathodic current

Hydrogen Embrittlement

HIC numerical modeling is a research field that has recently started to develop.

Although from the electrode kinetics it is found that for electric potential values more negative than -0.73 V vs Ag/AgCl seawater (Equilibrium potential of HER) the rate of the HER is increasing. Thus, the more hydrogen ions migrate towards the metals surface.

Wang et.al. (2022) predicted the probability of hydrogen embrittlement to occur in X60 buried pipelines, under CP and DC stray current.

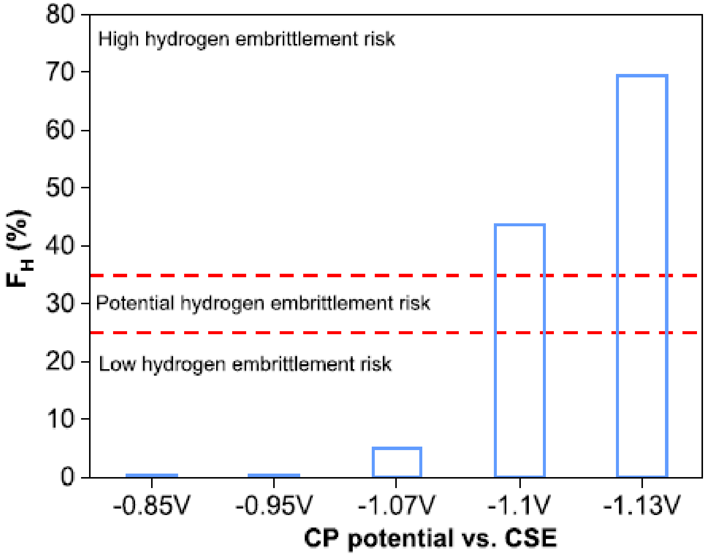

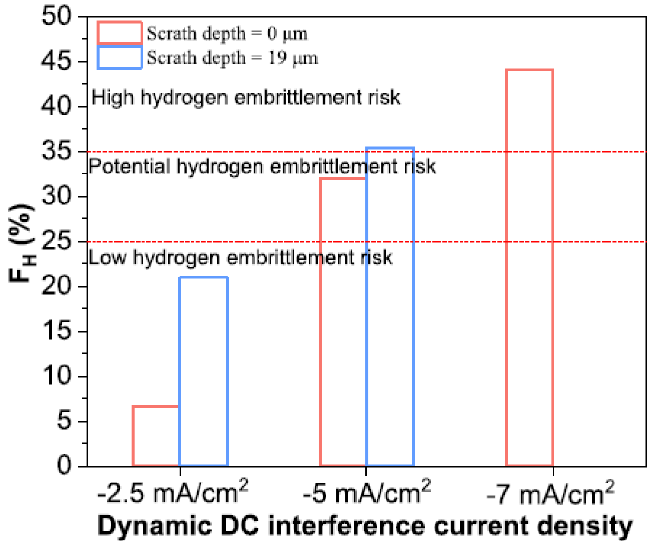

Wang, X., Wang, Y., Wang, B., Xing, Y., Lu, M., Qiao, L., & Zhang, L. (2022). Effect of scratches on hydrogen embrittlement sensitivity of carbon steel in cathodic protection and dynamic DC stray current interference environments. International Journal of Pressure Vessels and Piping, 199, 104712

Numerical Modeling of Corrosion

- Governing Equations
- Numerical Methods

Transport of reactive species in dilute solutions

diffusion

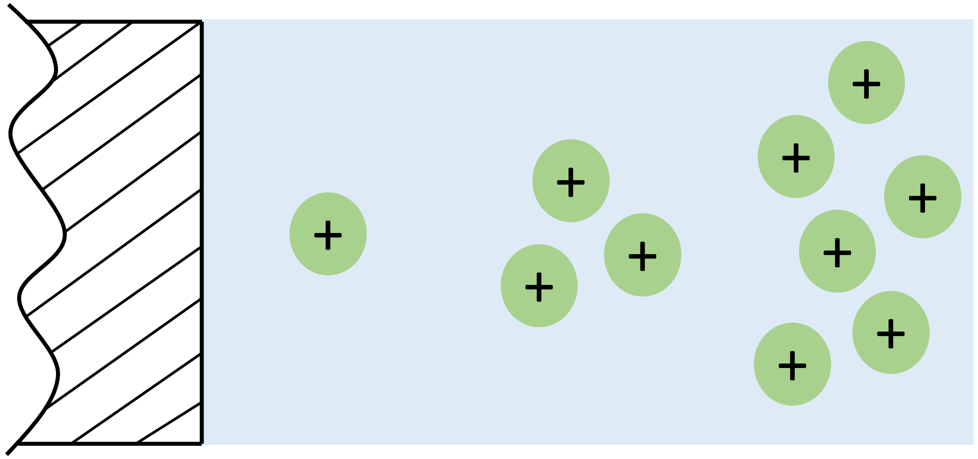

Increasing concentration of positive ions

Increasing diffusion of positive ions

migration

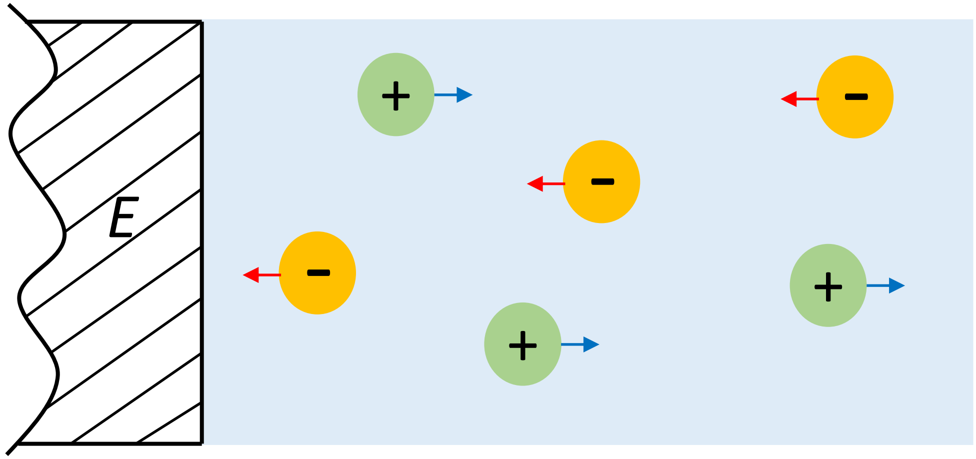

Increasing electrostatic potential φ

Direction of electric field $-\nabla\varphi$

Governing Equations

Reactive species transport

$$\frac{\partial c_i}{\partial t} + \mathbf{v} \cdot \nabla c_i = \underbrace{z_i F \nabla \cdot \left(u_i c_i \nabla \varphi \right)}_{\text{migration}} + \underbrace{\nabla \cdot \left(D_i \nabla c_i \right)}_{\text{diffusion}} + A_i$$

$$\nabla^2 \varphi = -\frac{1}{\varepsilon} F \sum z_i c_i$$

$$\mathbf{J} = -F \sum z_i D_i \nabla c_i - \sigma \nabla \varphi$$

$$\sigma = F^2 \sum z_i^2 u_i c_i$$

Electrolyte flow

$$\nabla \cdot \mathbf{v} = 0$$

$$\rho \left(\frac{\partial \mathbf{v}}{\partial t} + \mathbf{v} \cdot \nabla \mathbf{v} \right) = \mu \nabla^2 \mathbf{v} - \nabla p - \rho \mathbf{g}$$

Production Rate

$$\underbrace{Fe + 2HCl}_{\textit{reactants}} \overset{\pm ne}{\rightleftarrows} \underbrace{FeCl_2 + H_2}_{\textit{products}}$$

$\longrightarrow$ *forward*

$\longleftarrow$ *backward*

- The rate of a homogeneous reaction *i* can be generalized as :

$$r^i = -k_f^i \prod c_r^i + k_b^i \prod c_p^i$$

- The rate of production or consumption of chemical species, j, due to a homogeneous reaction *i* can be generalized as :

$$A_j = \sum_i \lambda_{ij} r_i$$

$$\lambda_{ij} = \begin{cases} \text{-1 , when j species is reactant at reaction i} \\ \text{1, when j species is product at reaction i} \\ \text{0 , when j species is neither rectant nor} \\ \quad \text{product at reaction i} \end{cases}$$

Double Layer Structure

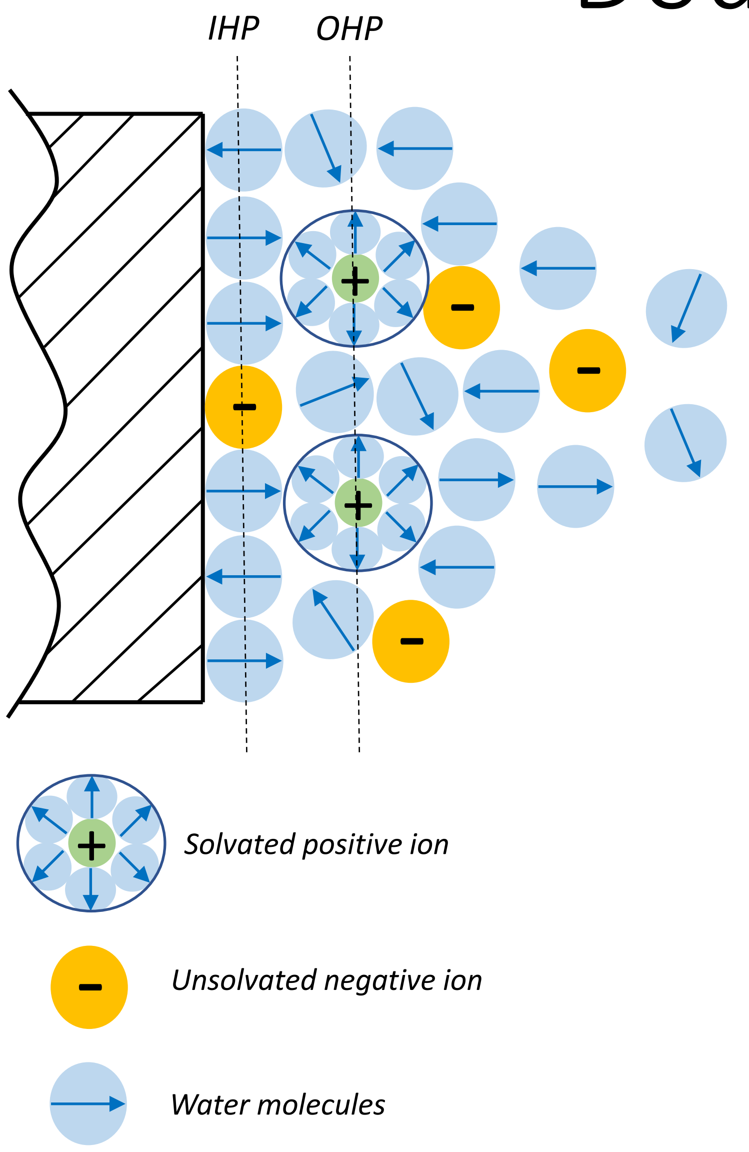

The movement of ions is due to forces from ion-ion interaction

The Nernst-Planck equations for dilute solutions do not hold!

Implementation of dilute solutions theory

- The outer boundary of the geometrical model is the OHP.

- A robin boundary condition is assigned → the polarization curve.

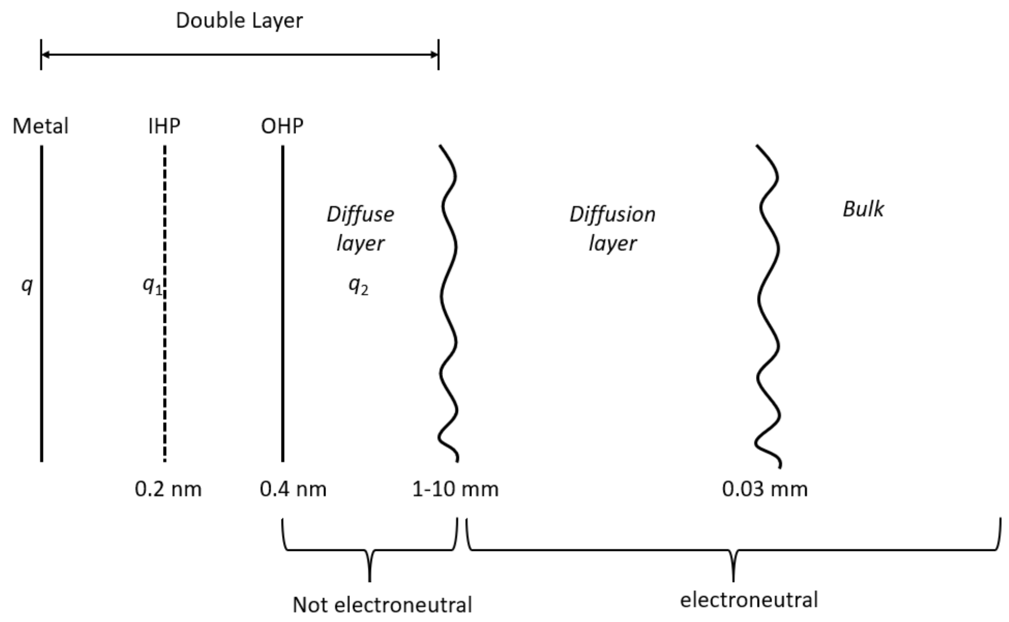

Electroneutrality

$$\boxed{\sum z_i c_i = 0}$$

$$\mathbf{J} = -F\sum z_i D_i \nabla c_i - \sigma \nabla \varphi$$

The conservation of charge can be expressed starting from the mass balance of the dissolved species multiplying mass conservation equation by zF and summation of all species:

$$\frac{\partial}{\partial t}\left(F\sum z_i c_i\right) = -\nabla\cdot\left(F\sum z_i \mathbf{N}_i\right) + F\sum z_i A_i$$

Electrically balanced reactions: $\sum z_i A_i = 0$

$$\Rightarrow \nabla\cdot\left(F\sum z_i \mathbf{N}_i\right) = 0 \Rightarrow \boxed{\nabla\cdot\mathbf{J} = 0}$$

Implementation of dilute solutions theory

Diffusion Layer

$$\frac{\partial c_i}{\partial t} + \mathbf{v} \cdot \nabla c_i = (F z_i u_i \nabla \varphi) \nabla c_i + D_i \nabla^2 c_i + A_i$$

$$\nabla^2 \varphi = 0$$

$$\sum z_i c_i = 0$$

Bulk

$$\nabla^2 \varphi = 0$$

$$\nabla^2 c_i + A_i = 0$$

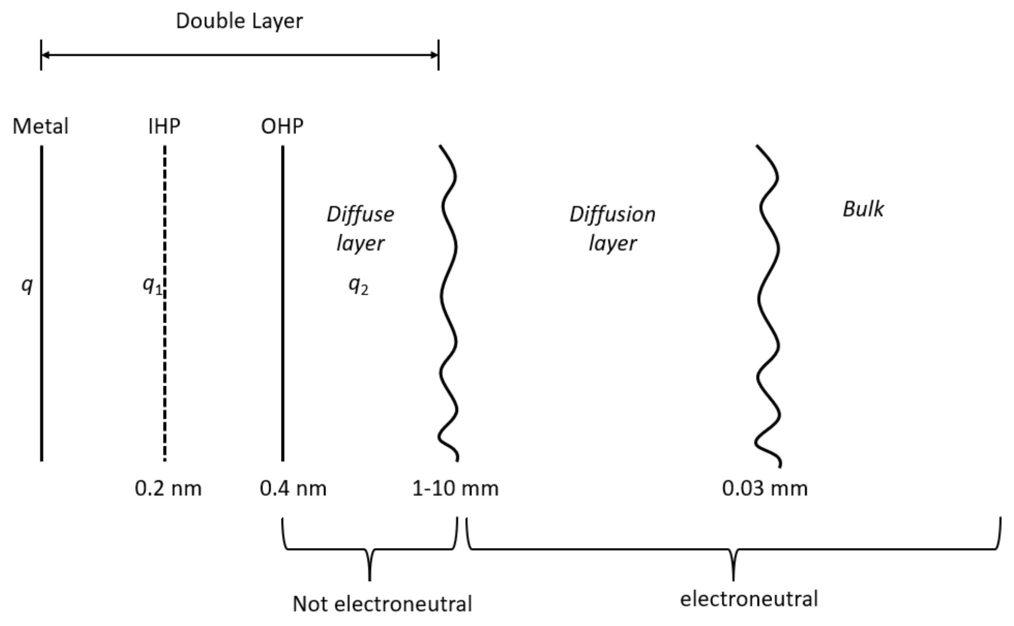

Robin Boundary conditions assignment

Poisson / Laplace equation

$$i = -\sigma \mathbf{n} \cdot \nabla \varphi = \sum f_k(c_k, \varphi) = g(\varphi)$$

Nernst-Planck equations

$$i = \sum_k \left(-F z_k D_k \mathbf{n} \cdot \nabla c_k - F^2 z_k^2 u_k c_k \mathbf{n} \cdot \nabla \varphi \right) = \sum f_k(c_k, \varphi) = \sum g_k(c_k)$$

For all species k that participate in the electrode reaction

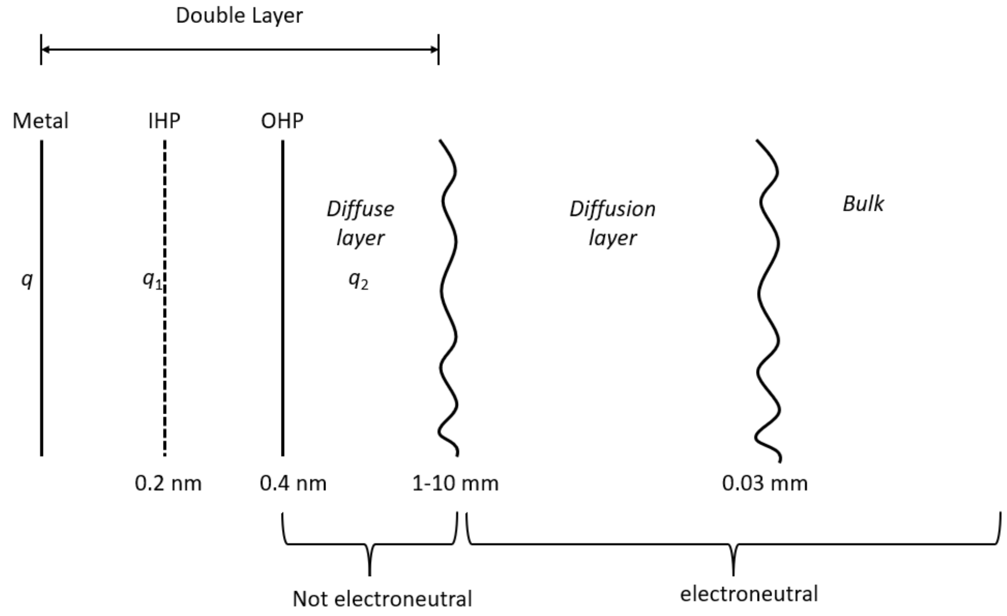

Boundary conditions assignment

Nernst-Planck equations

$$c_k = c_k^b \text{ or}$$
$$\mathbf{n} \cdot \nabla c_k = p_k \text{ or}$$
$$\mathbf{n} \cdot \nabla c_k = h_k(\mathbf{x}, t)$$

$$\mathbf{n} \cdot \nabla c_k = 0$$

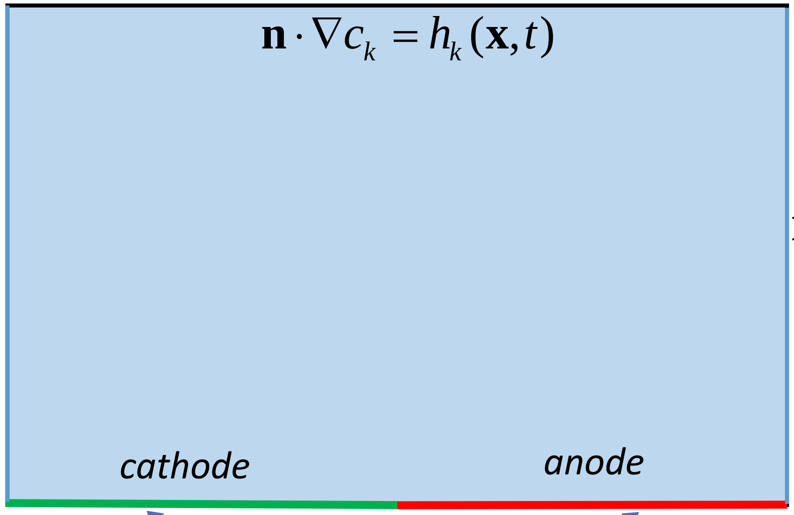

$$\mathbf{n} \cdot \nabla c_k = 0$$

$$\sum_k \left(-F z_k D_k \mathbf{n} \cdot \nabla c_k - F^2 z_k^2 u_k c_k \mathbf{n} \cdot \nabla \varphi\right) = f_k(c_k, \varphi)$$

$$\sum_k \left(-F z_k D_k \mathbf{n} \cdot \nabla c_k - F^2 z_k^2 u_k c_k \mathbf{n} \cdot \nabla \varphi\right) = g_k(c_k, \varphi)$$

Poisson / Laplace equation

$$-\sigma \mathbf{n} \cdot \nabla \varphi = 0$$

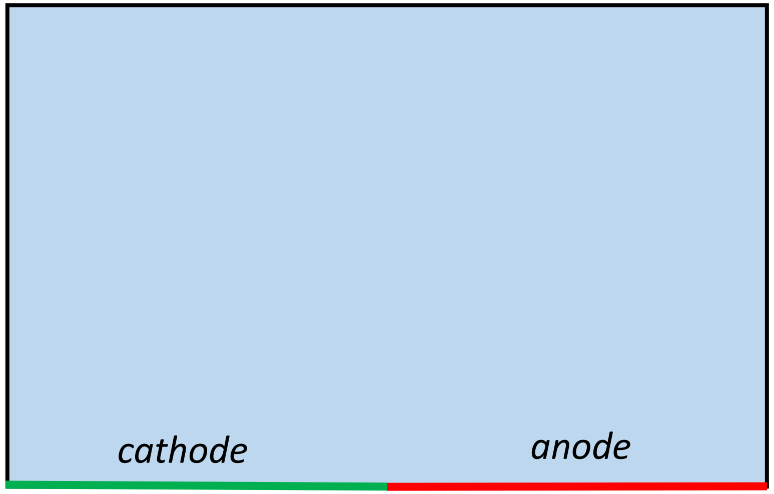

$$-\sigma \mathbf{n} \cdot \nabla \varphi = f(\varphi)$$

$$-\sigma \mathbf{n} \cdot \nabla \varphi = g(\varphi)$$

DAAD Deutscher Akademischer Austausch Dienst German Academic Exchange Service

KIT Karlsruhe Institute of Technology

UNIVERSITY OF PATRAS

Double Layer unknown fields calculation

- *The exact ion distribution in the EDL at an arbitrarily charged surface or ionic strength of the electrolyte solution can be obtained by molecular-scale simulation.*

- *Therefore, the statistic information obtained by the molecular-scale simulation can be used to calculate the excess chemical potential in the DL . Then, the* following modified N-P for the EDL region can be derived:

$$\boxed{\frac{\partial c_i}{\partial t} + \mathbf{v} \cdot \nabla c_i = z_i F \nabla \cdot \left(u_i c_i \nabla \varphi \right) + \nabla \cdot \left(D_i \nabla c_i \right) + \nabla \mu_i + A_i}$$

- *The last 80 years numerous continuous-scale theoretical models were developed to calculate the excess chemical potential in the Stern layer, to avoid the MD simulations, but each theory has its limitations. Although (*Giera et.al, 2015) work, is promising as they proposed a constitutional equation, for the excess chemical potential in the EDL, exhibiting excellent agreement with the MD simulation results.

- The Strong ion−ion interactions in the EDL are predominantly steric in nature rather than electrostatic, according to *(*Giera et.al, 2015) :

$$\boxed{\mu_i^{exc} = f\left(c_i, d_i\right)}$$

d_i is the ions diameter
f is a polynomial function.

Calculation of the change of the electrode shape

Dissolution and/or deposition is always assumed to occur in the normal direction to an electrode boundary.

The amount of material dissolved or deposited is governed by the Faraday law.

$$\mathbf{n}\cdot\frac{\partial \mathbf{x}}{\partial t}=\frac{dh}{dt}=u_{dc}=\frac{M}{\rho}\frac{1}{zF}i_{loc}$$

Where M the molar mass and ρ the density.

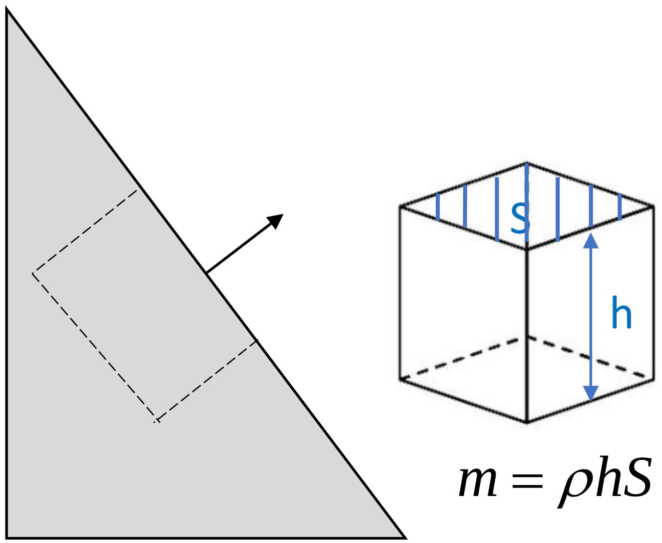

$$m=\rho hS$$

Reliability of numerical models for simulating galvanic corrosion processes

$$j_y = \mathbf{n}\cdot\mathbf{J} = -F\sum z_i D_i \mathbf{n}\cdot\nabla c_i - \sigma\mathbf{n}\cdot\nabla\varphi$$

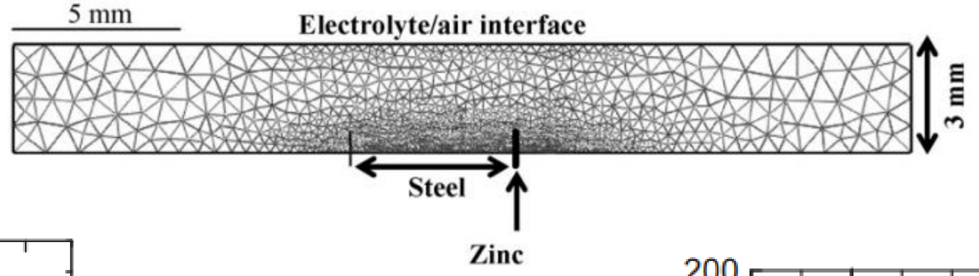

circles: experimental profile
solid line: numerical profile

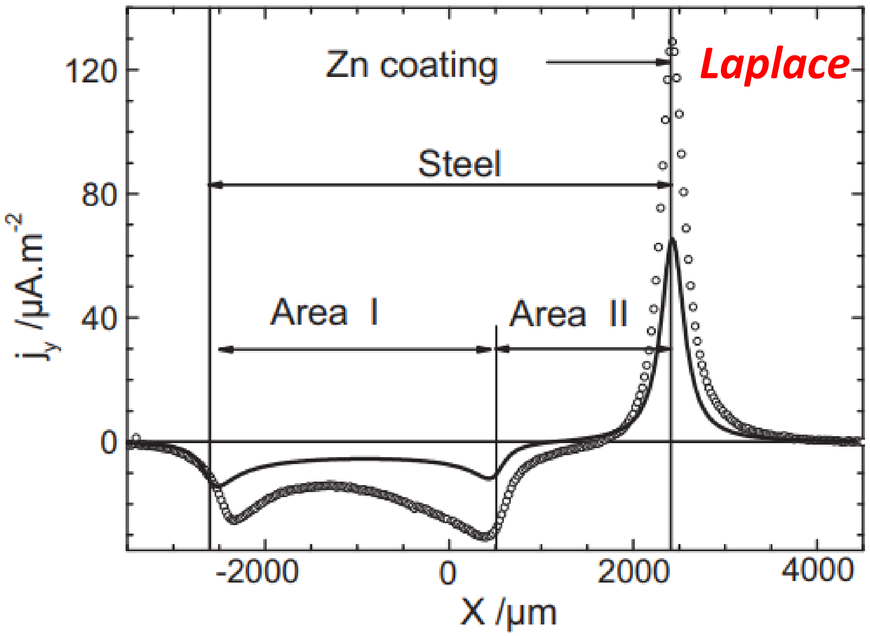

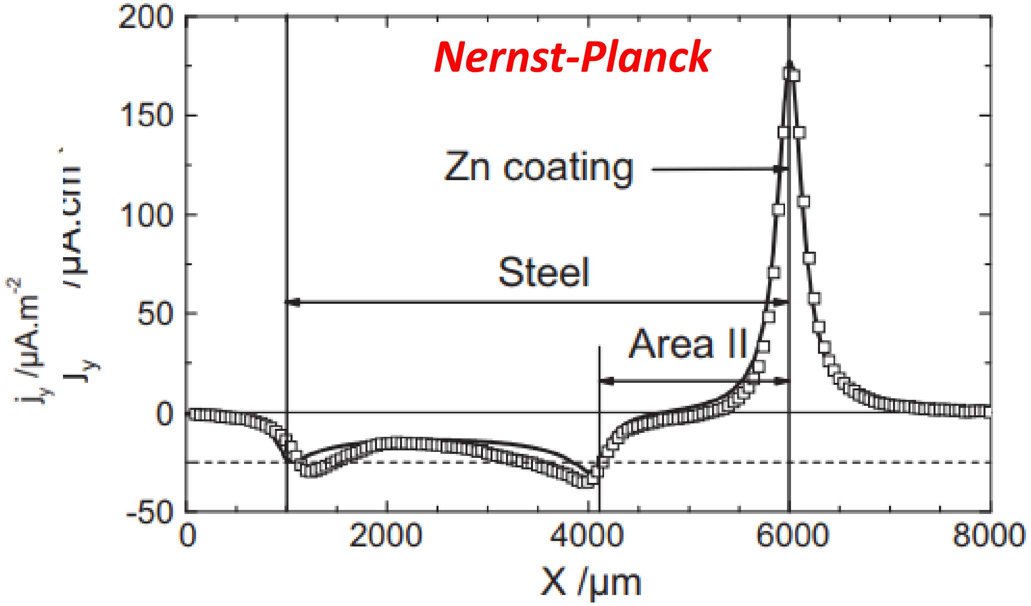

Thébault, F., Vuillemin, B., Oltra, R., Allely, C., & Ogle, K. (2012). Reliability of numerical models for simulating galvanic corrosion processes. Electrochimica Acta, 82, 349–355

Numerical Methods

- FEM → stabilization Techniques
- FVM → handling of the robin boundary conditions
- ✓ LD-BEM

FEM

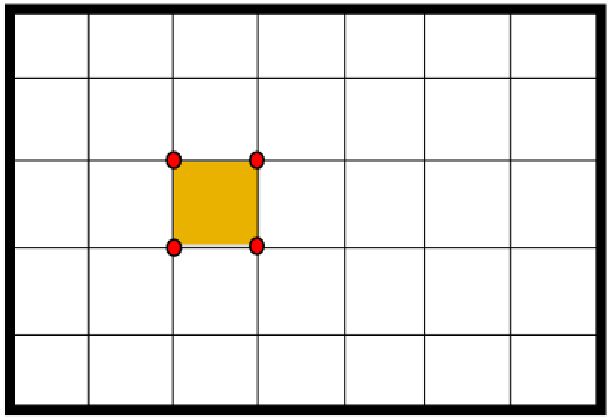

FVM

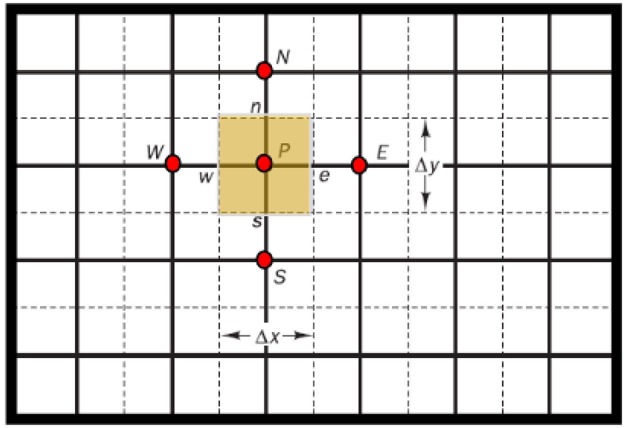

LD-BEM

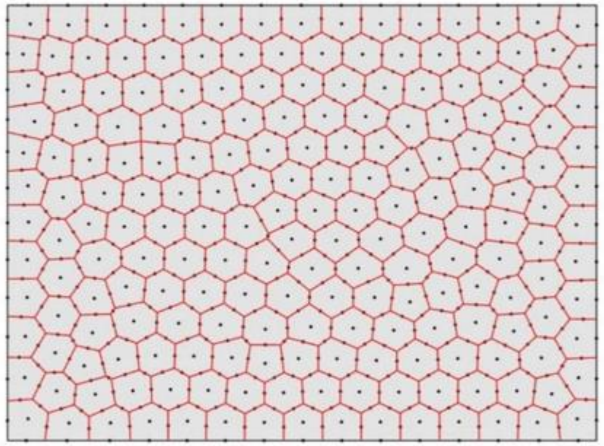

Reactive species transport utilizing FEM

$$\left.\begin{aligned} \mathbf{v}_T \cdot \nabla c_i - D_i \nabla^2 c_i = 0 \\ \sum z_i c_i = 0 \\ \nabla^2 \varphi = 0 \\ \mathbf{v}_T = \mathbf{v} + \mathbf{v}_M \\ \mathbf{v}_M = -F z_i u_i \nabla \varphi \end{aligned}\right\}$$

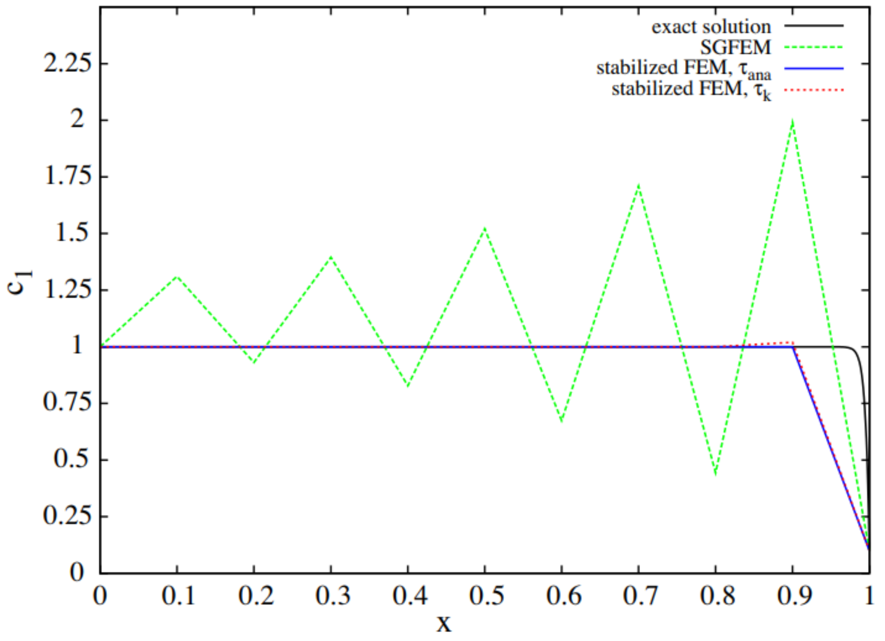

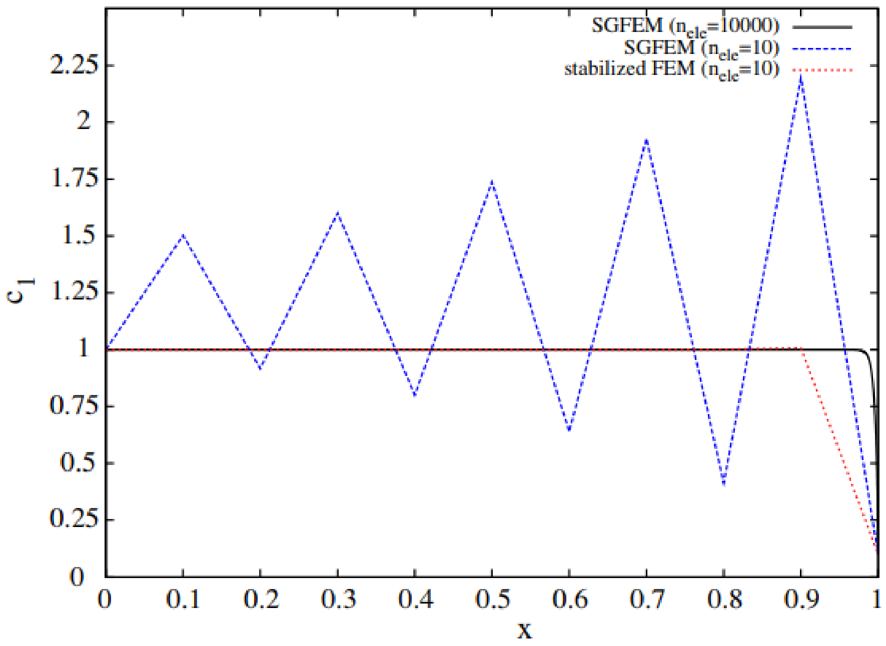

Bauer, G., Gravemeier, V., & Wall, W. A. (2012). A stabilized finite element method for the numerical simulation of multi-ion transport in electrochemical systems. Computer Methods in Applied Mechanics and Engineering, 223–224, 199–210.

FVM: handling of the robin boundary conditions

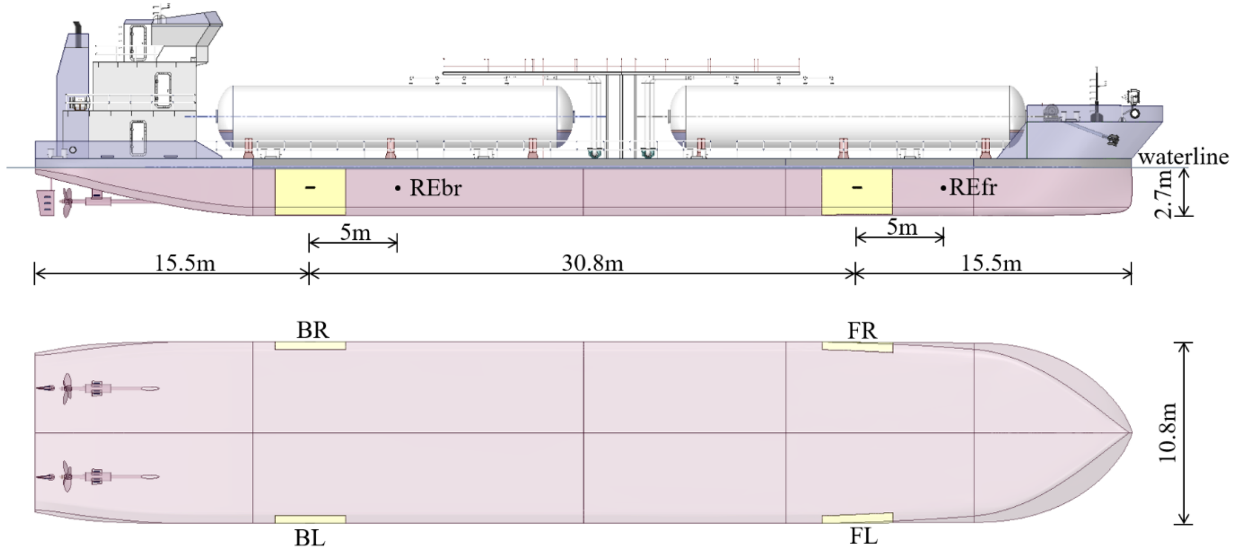

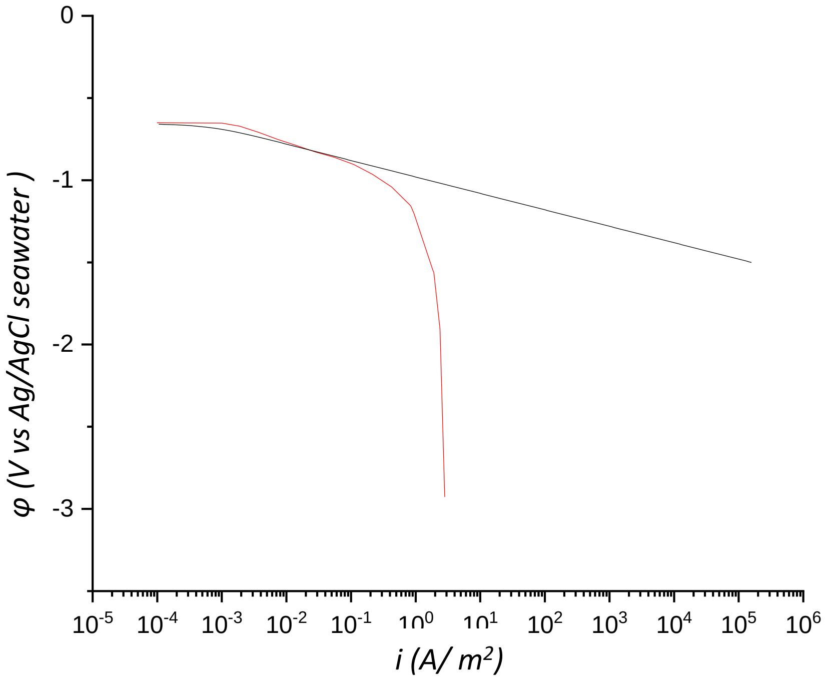

Case	*Steel polarization curve*
I	*Black*
II	*Red*

FVM: handling of the robin boundary conditions

Case I

BEM

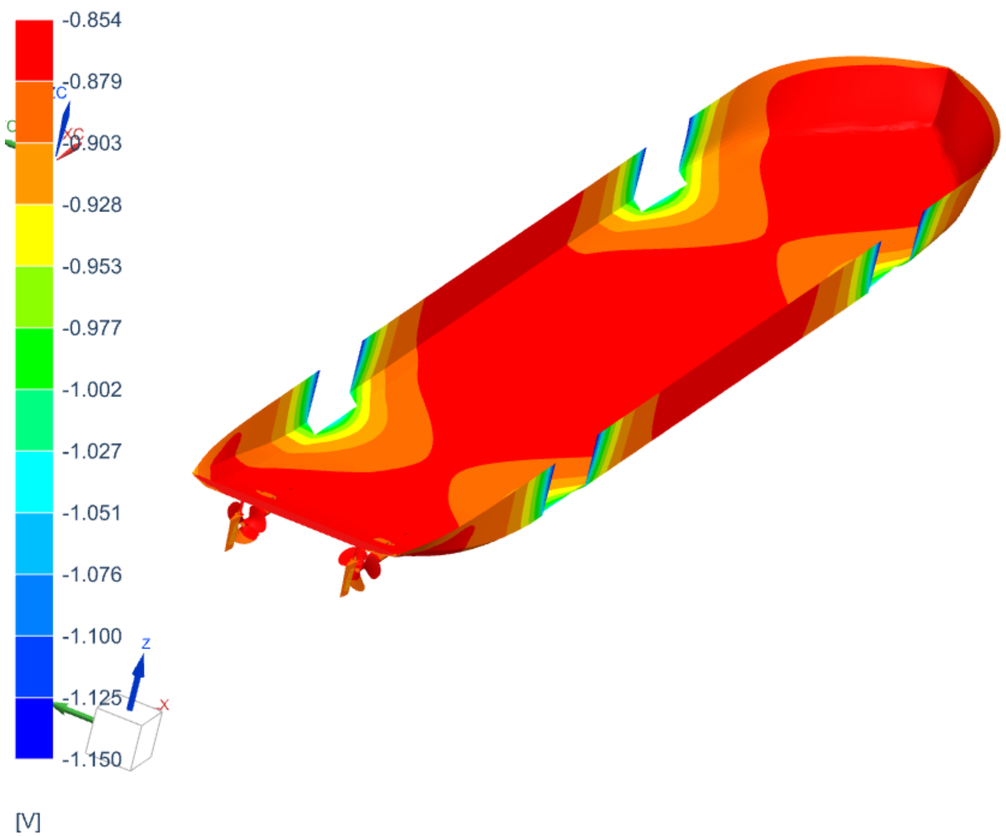

FVM

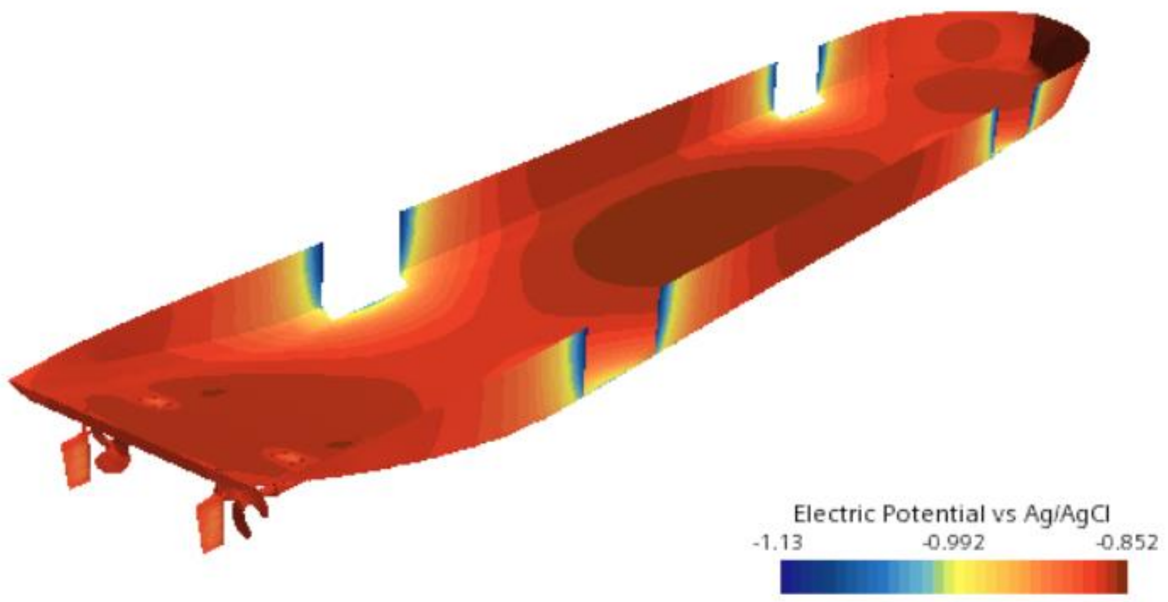

FVM: handling of the robin boundary conditions

Case II

BEM

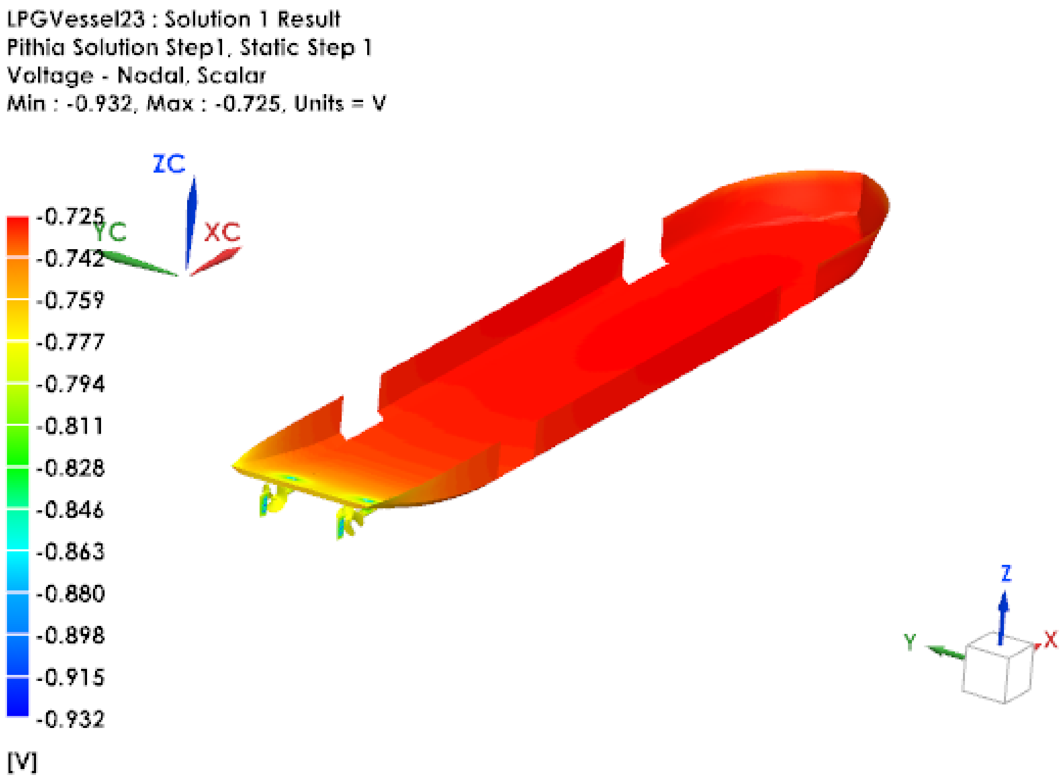

FVM

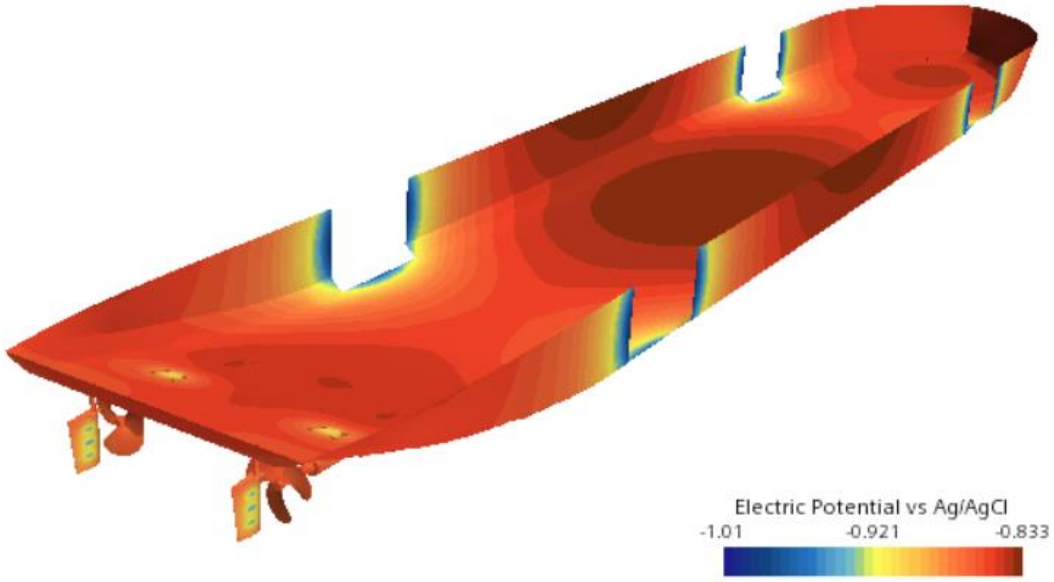

Local Domain BEM

$$\frac{\partial c_i}{\partial t} + \mathbf{v} \cdot \nabla c_i - D_i \nabla^2 c_i = 0$$

Pe=25

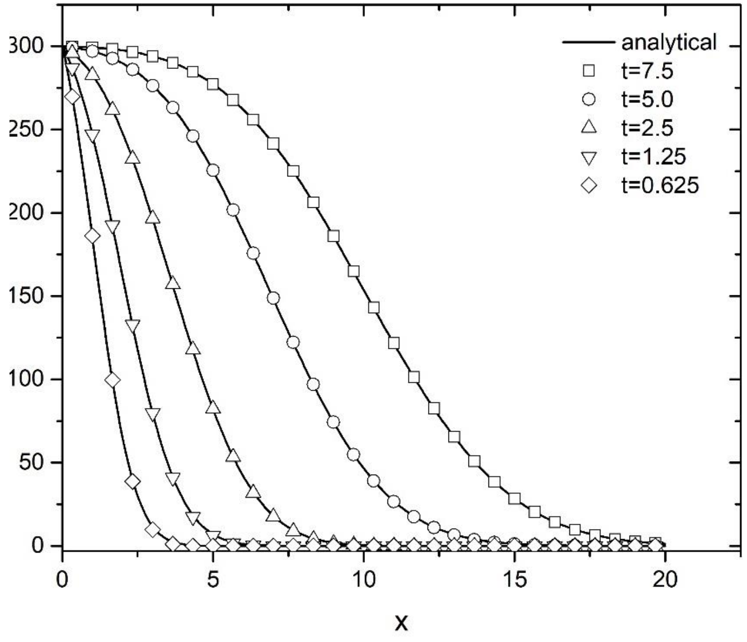

Pe=50

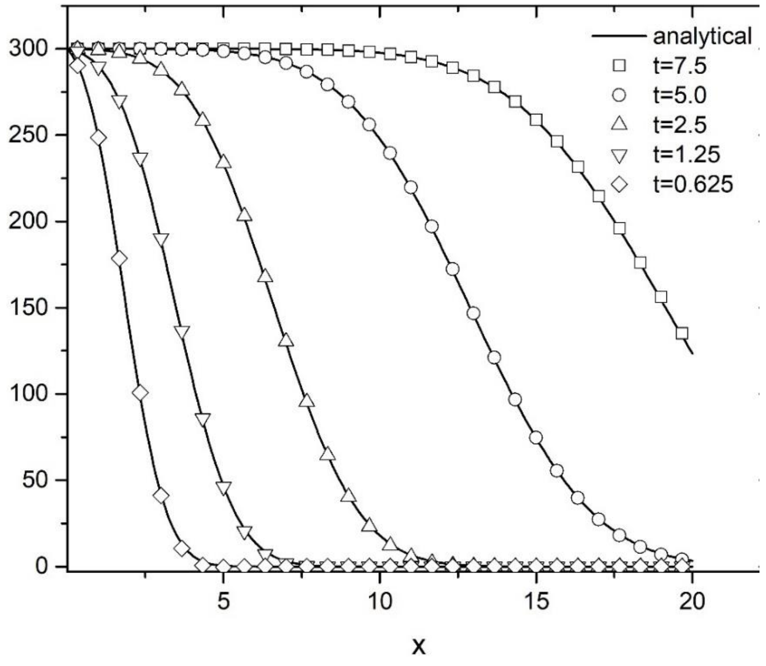

Pe=100

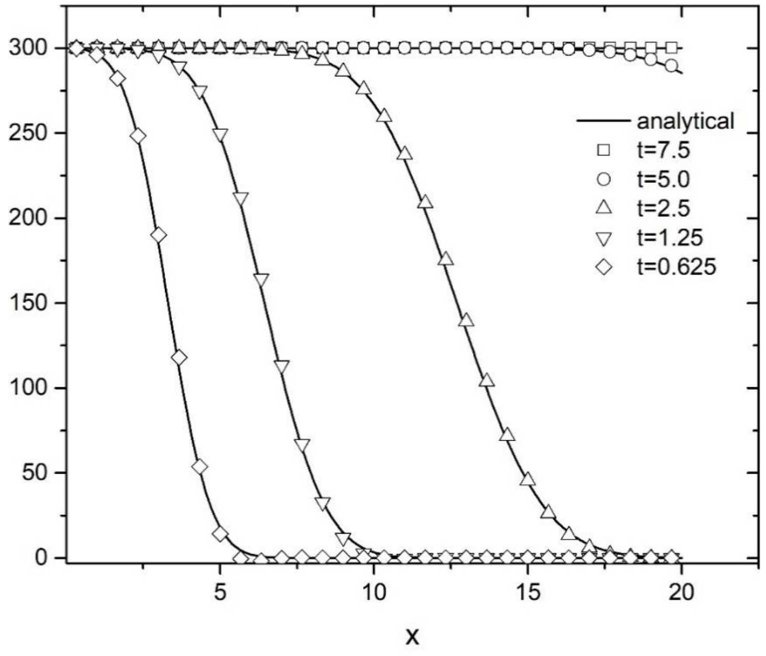

Gortsas, T. v, & Tsinopoulos, S. v. (2022). A local domain BEM for solving transient convection-diffusion-reaction problems. International Journal of Heat and Mass Transfer, 194, 123029.

Numerical Simulation of Corrosion of W/Ts

- Galvanic Corrosion
- Atmospheric Corrosion
- Pitting Corrosion
- Crevice Corrosion
- Stay Current Induced Corrosion
- Corrosion Fatigue

Galvanic Corrosion

- *Neutral solution*

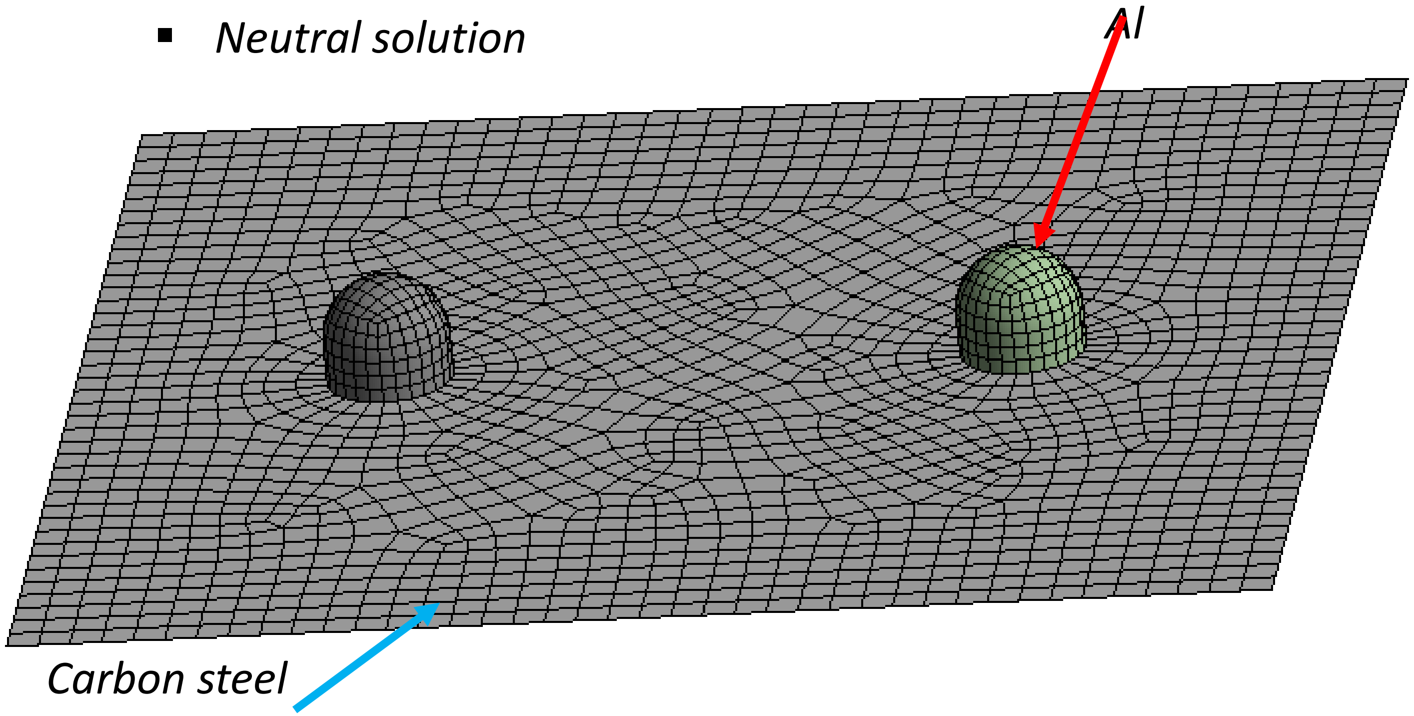

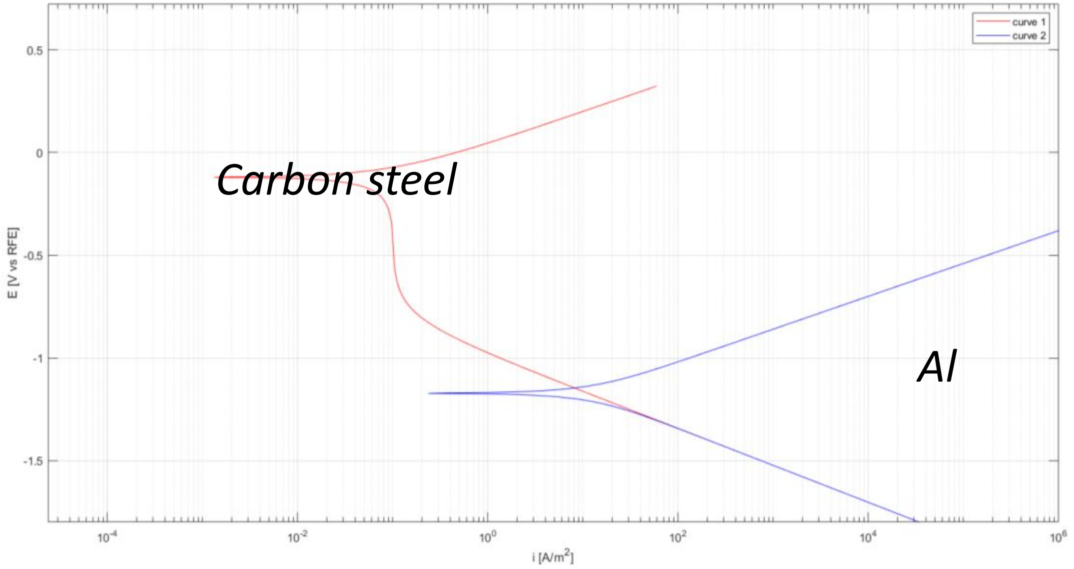

<u>*Partial Reactions*</u>

$$O_2 + 2H_2O + 4e^- \rightarrow 4OH^-$$

$$Fe \rightarrow Fe^{2+} + 2e^-$$

$$Al \rightarrow Al^{3+} + 3e^-$$

ACA/BEM analysis utilizing PITHIA CP

Galvanic Corrosion

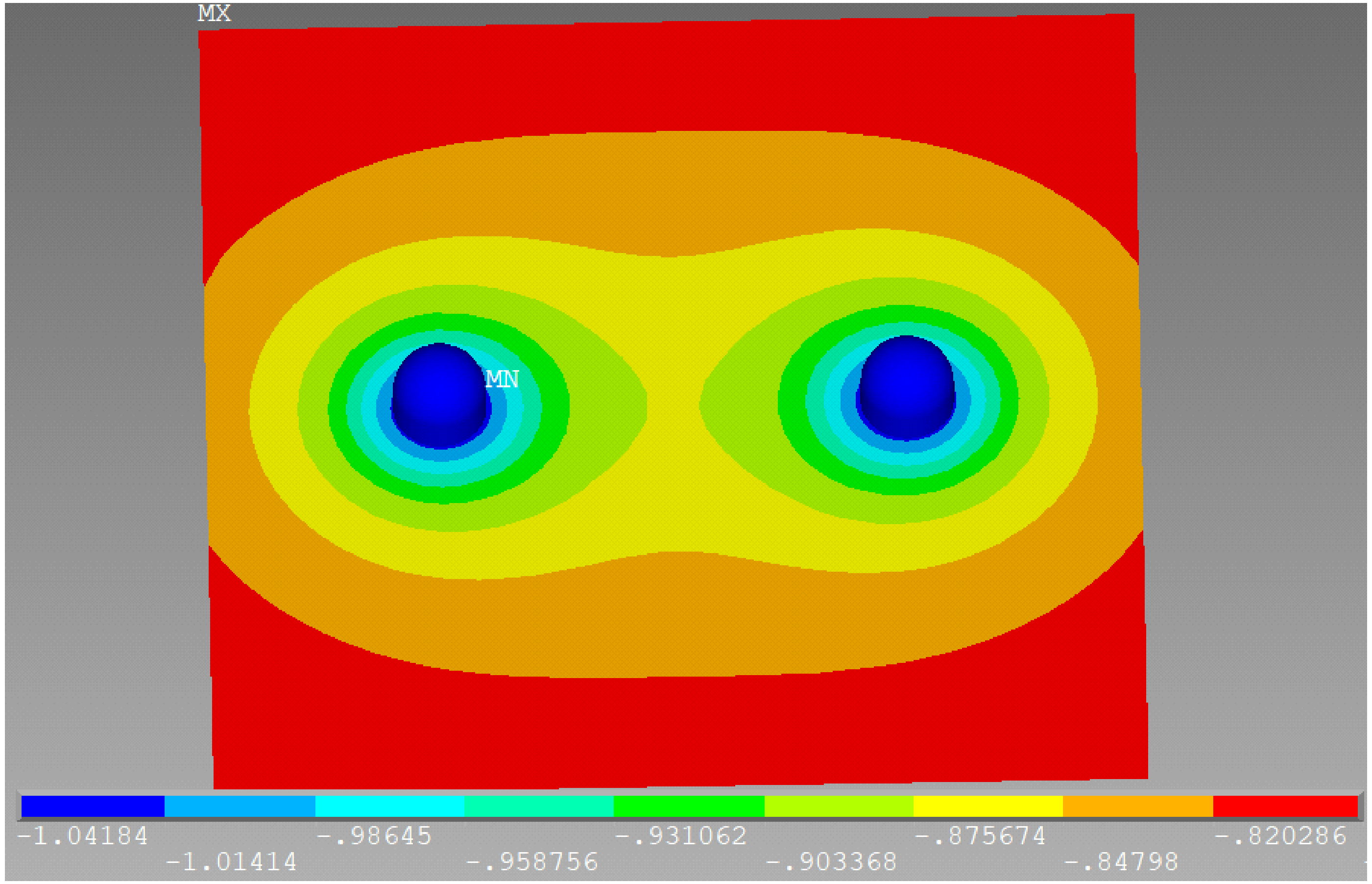

Electric Potential Distribution in V vs Ag/AgCl seawater

Galvanic Corrosion

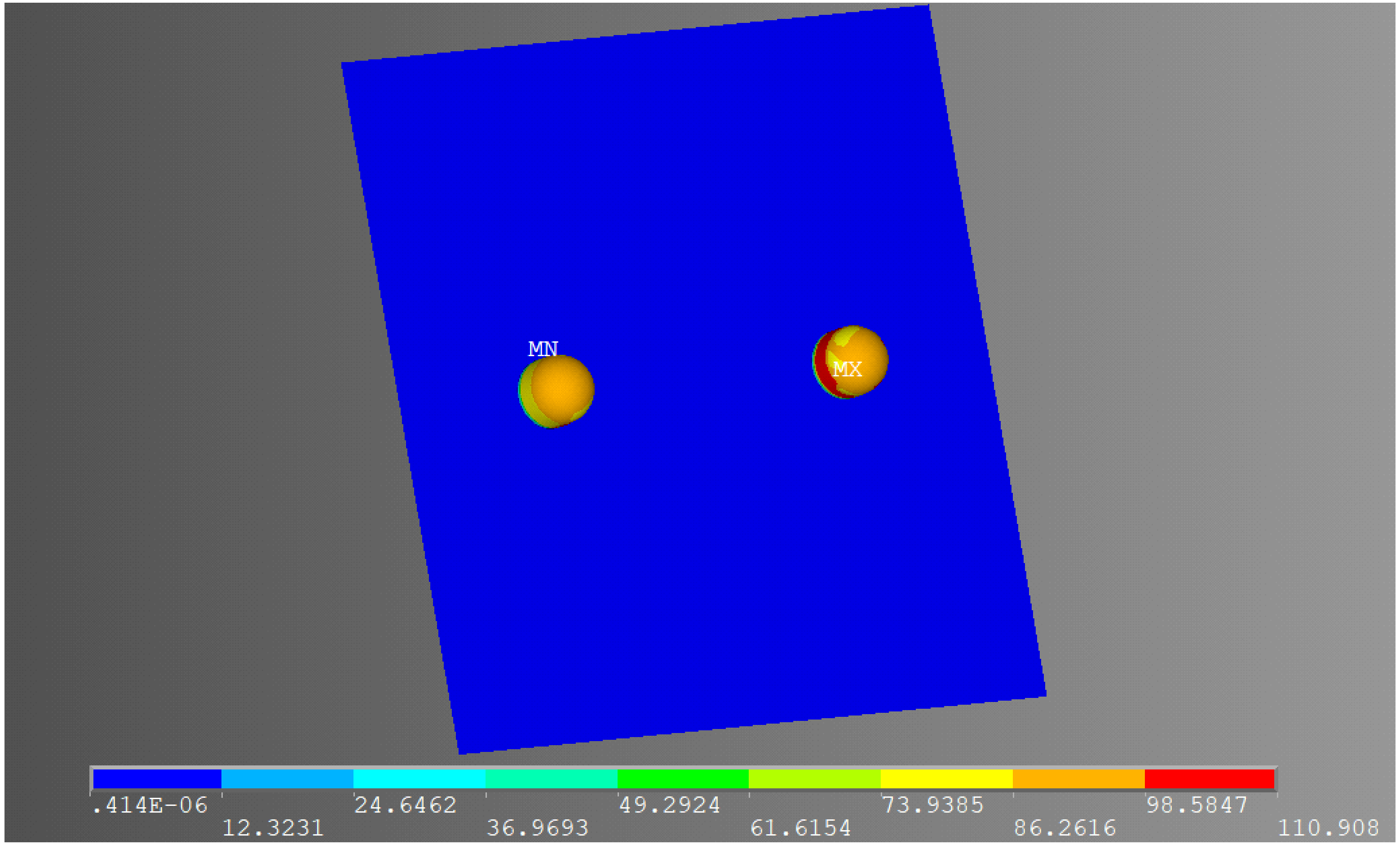

Corrosion rate distribution in mm/yr.

ACA/BEM analysis utilizing PITHIA CP

Galvanic Corrosion

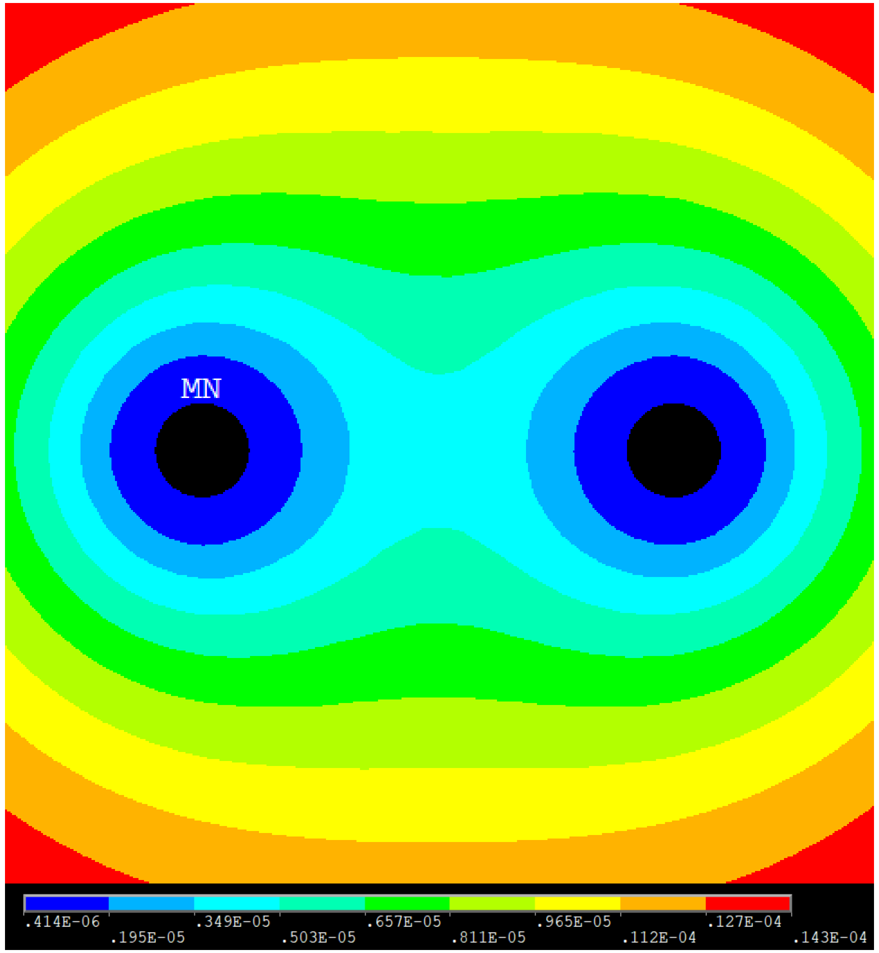

Corrosion rate distribution in mm/yr.

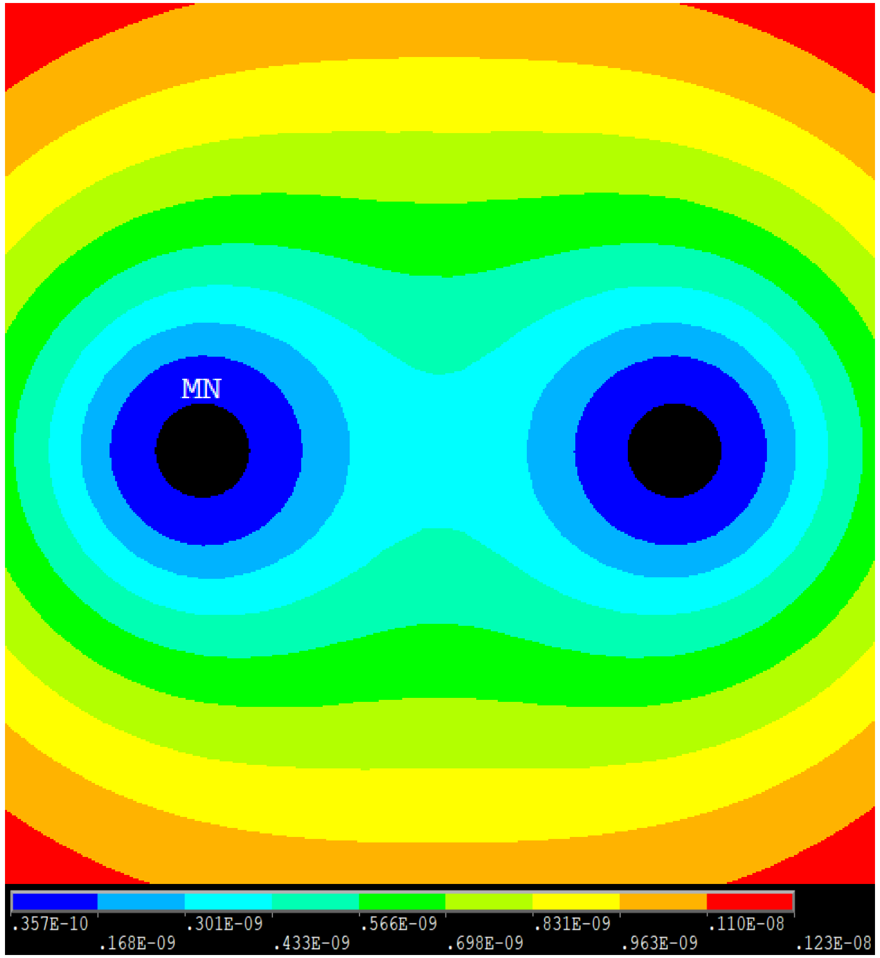

Local current density in A/cm^2

Galvanic Corrosion

- *Neutral solution*

Stainless steel

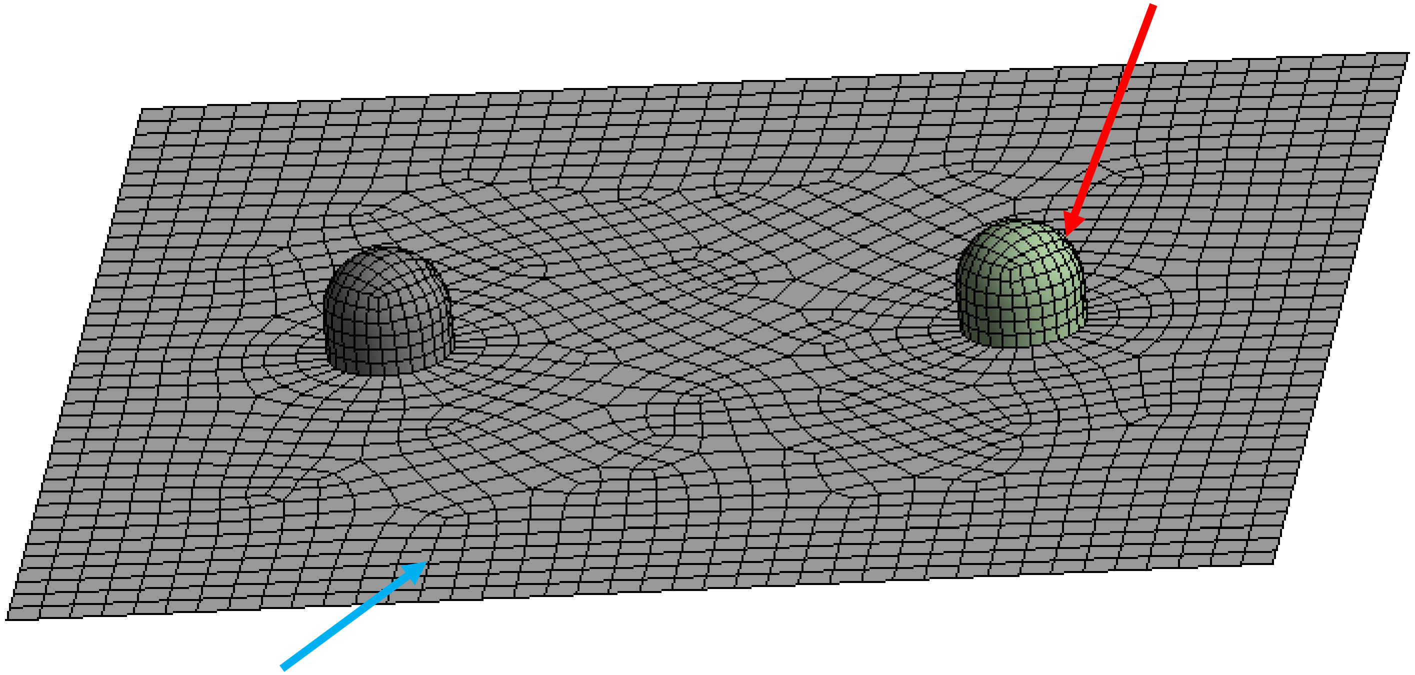

Carbon steel

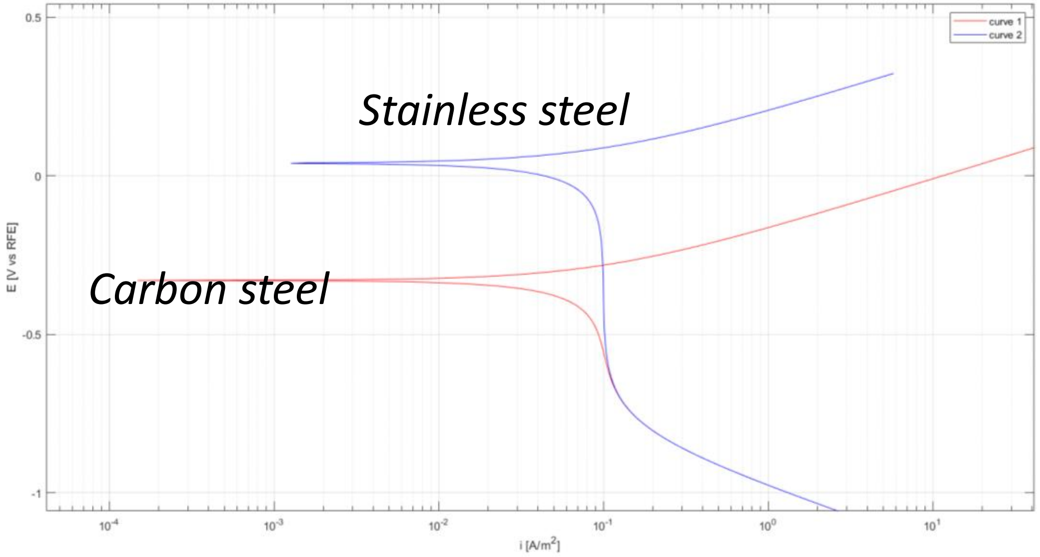

Partial Reactions

$$O_2 + 2H_2O + 4e^- \rightarrow 4OH^-$$

$$Fe \rightarrow Fe^{2+} + 2e^-$$

Galvanic Corrosion

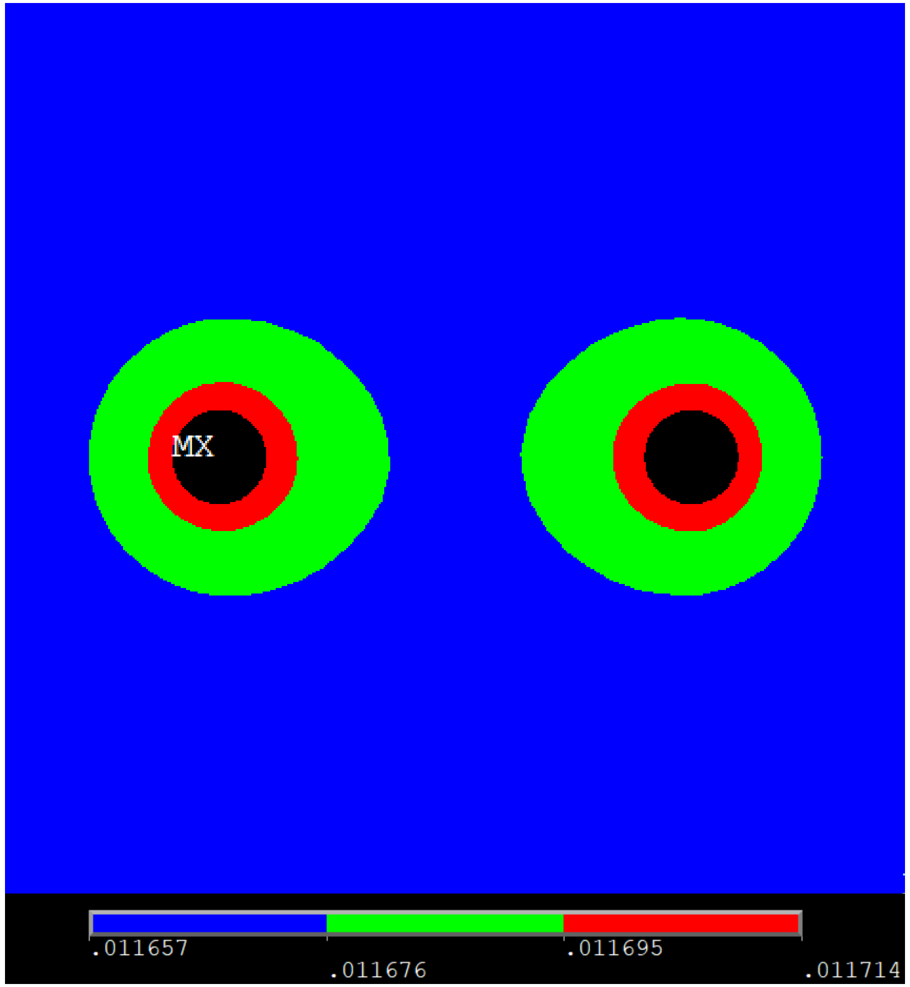

Corrosion rate distribution in mm/yr.

ACA/BEM analysis utilizing PITHIA CP

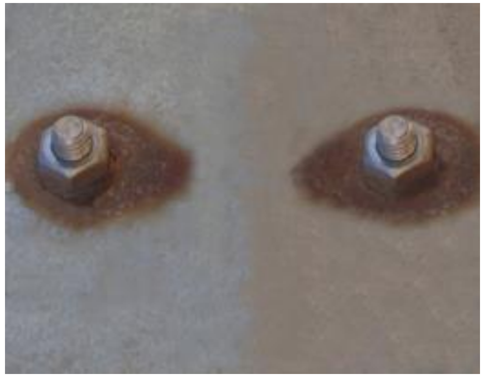

Corrosion rate distribution in mm/yr.

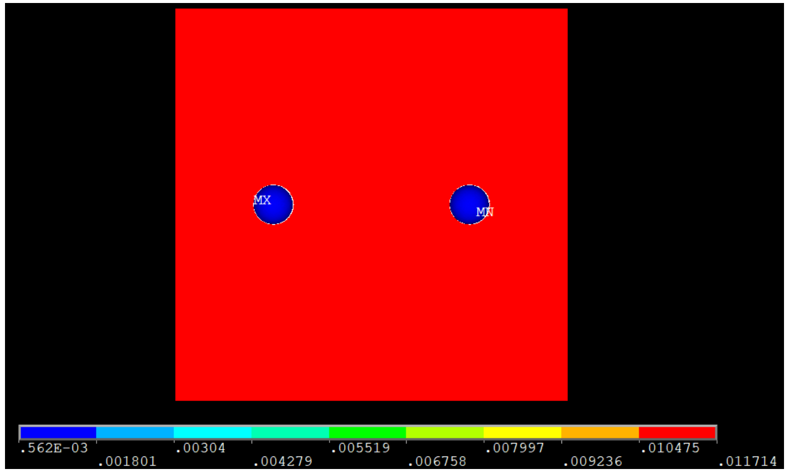

Comparison of Al/Carbon steel and Stainless Steel/Carbon Steel galvanic couples

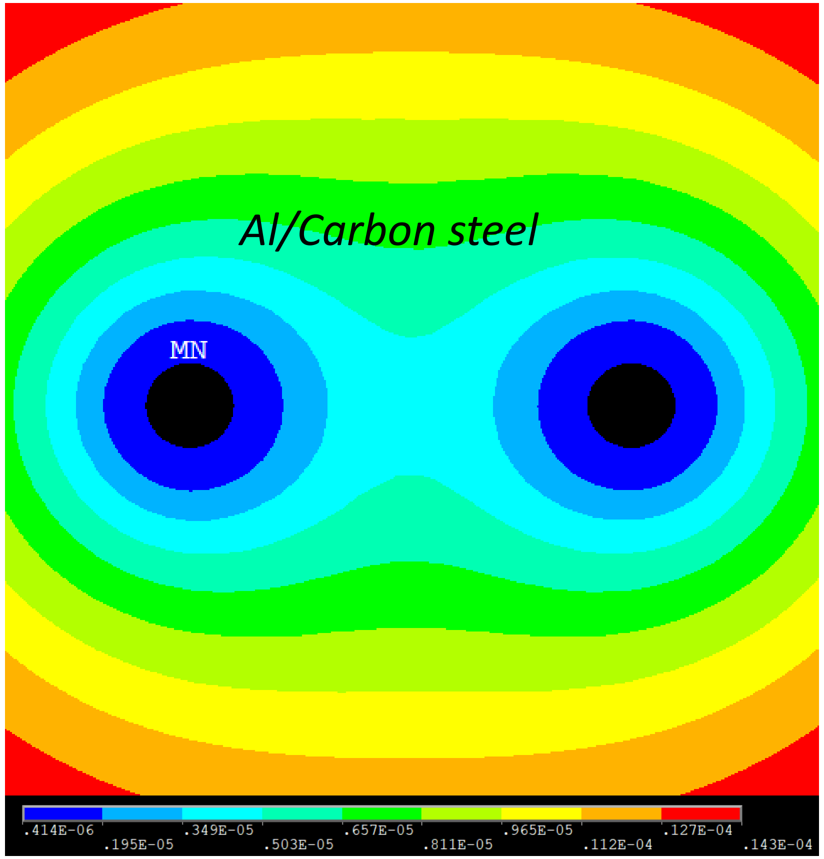

Corrosion rate distribution in mm/yr.

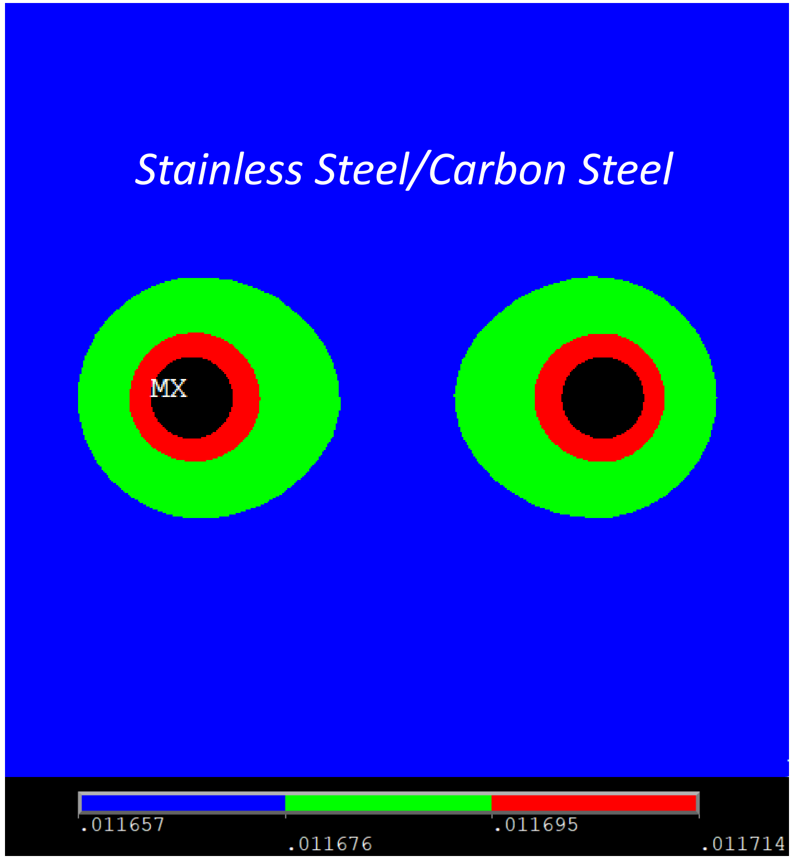

Galvanic Corrosion

- *Neutral solution*

Partial Reactions

$$O_2 + 2H_2O + 4e^- \rightarrow 4OH^-$$

$$Fe \rightarrow Fe^{2+} + 2e^-$$

$$Mg \rightarrow Mg^{2+} + 2e^-$$

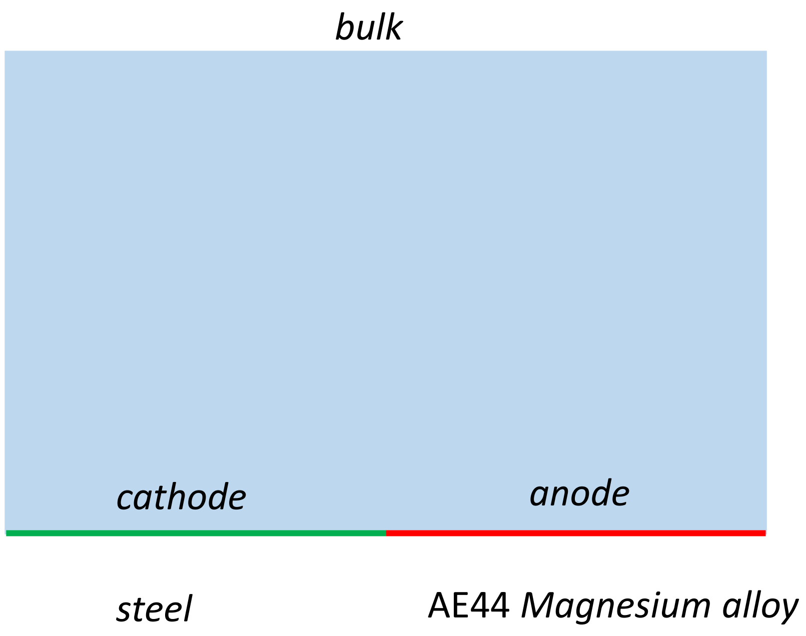

Galvanic Corrosion

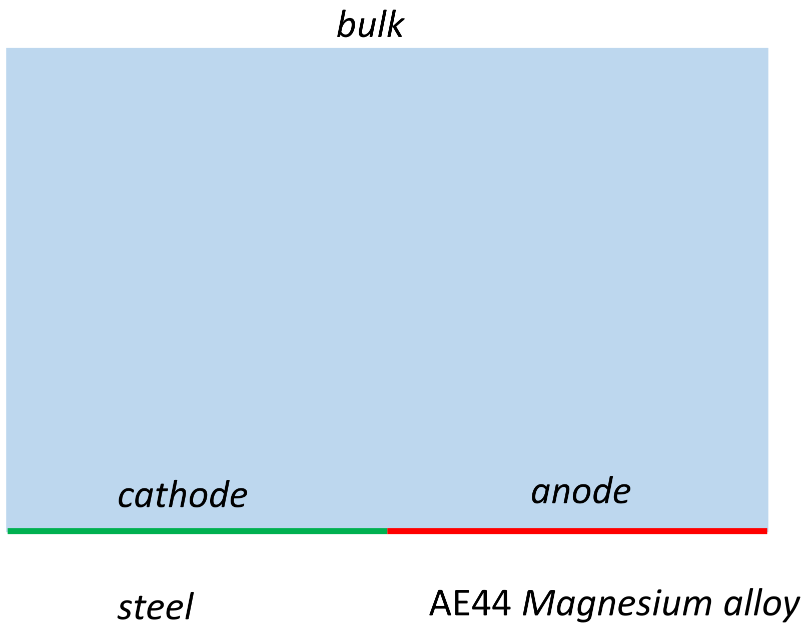

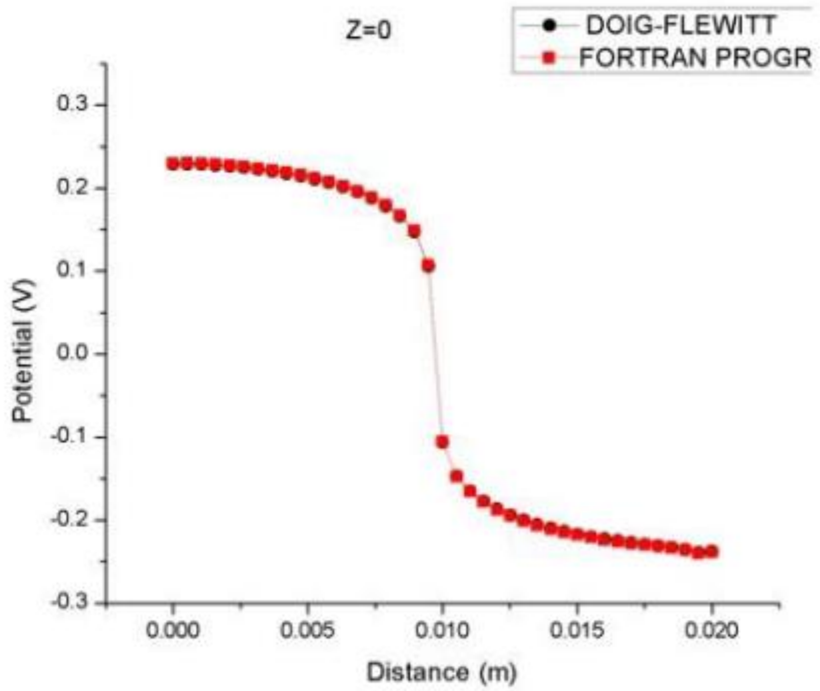

Galvanic Corrosion

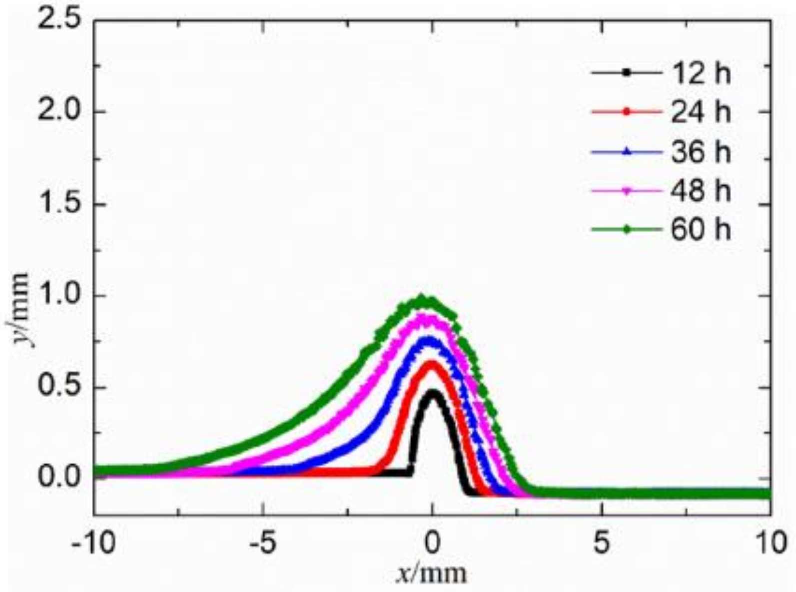

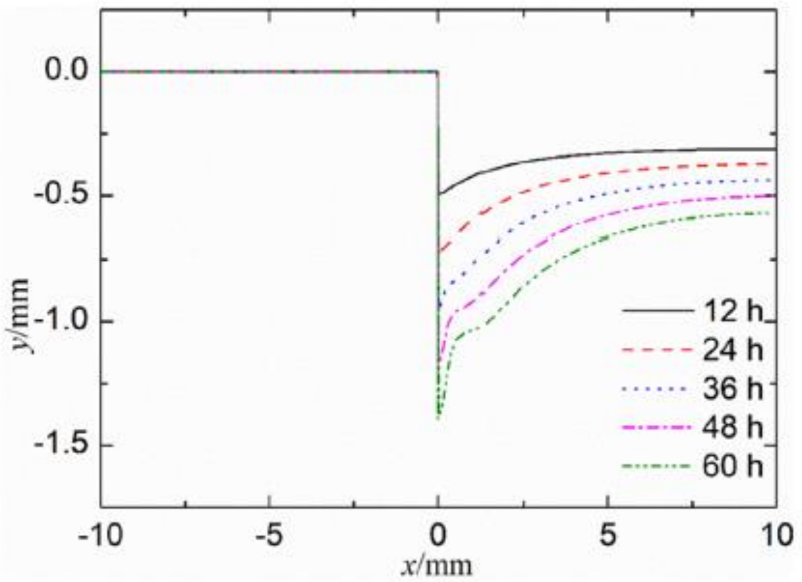

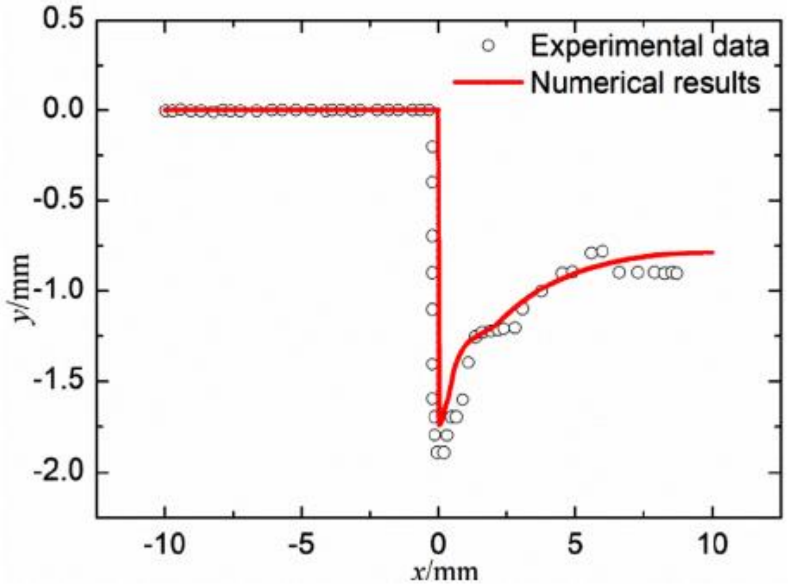

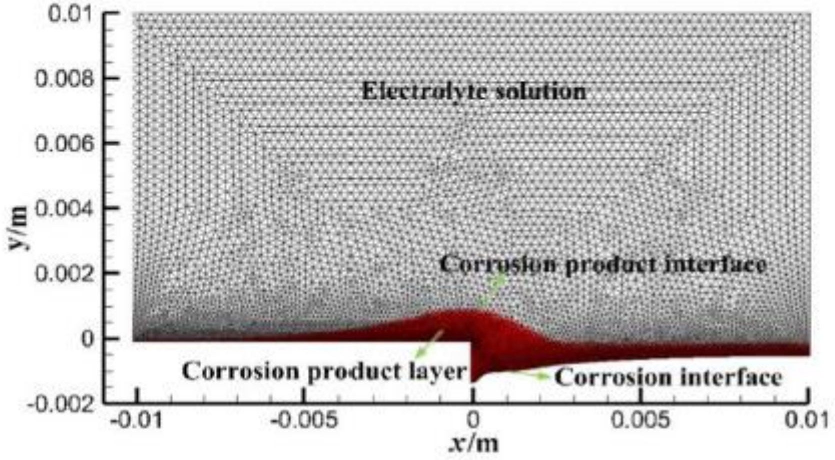

Wang, K., Li, C., Li, Y., Lu, J., Wang, Y., & Luo, X. (2021). Multi-physics analysis of the galvanic corrosion of Mg-steel couple under the influence of time-dependent anisotropic deposition film. Journal of Magnesium and Alloys, 9(3), 866–882

Galvanic Corrosion

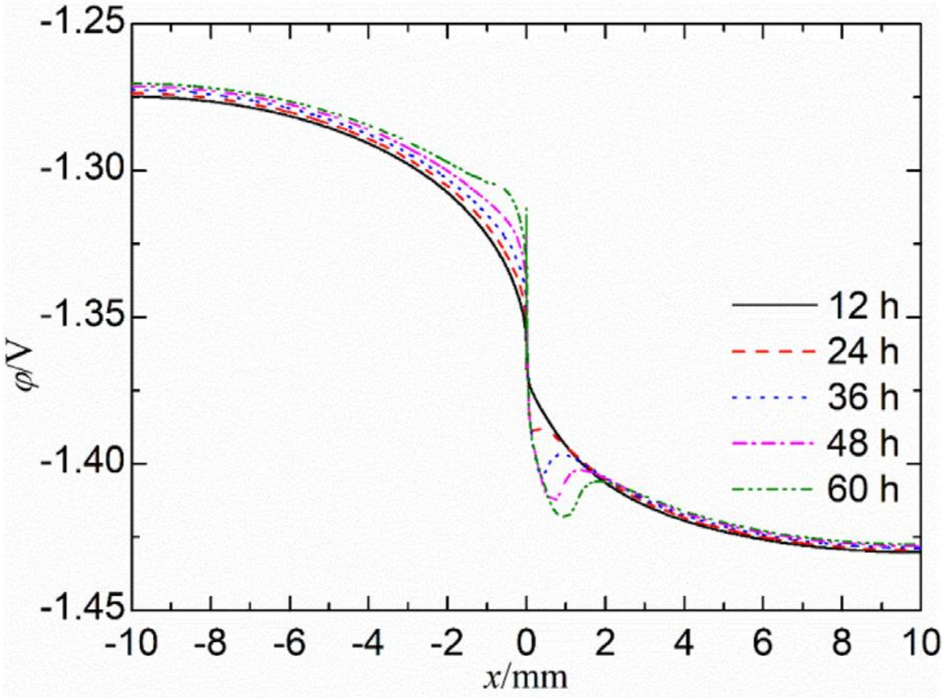

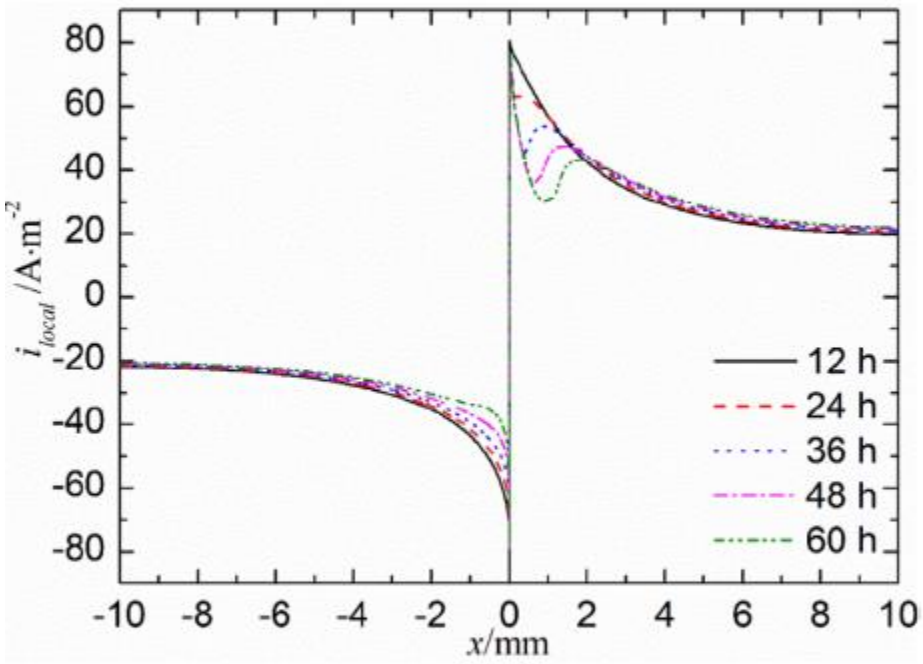

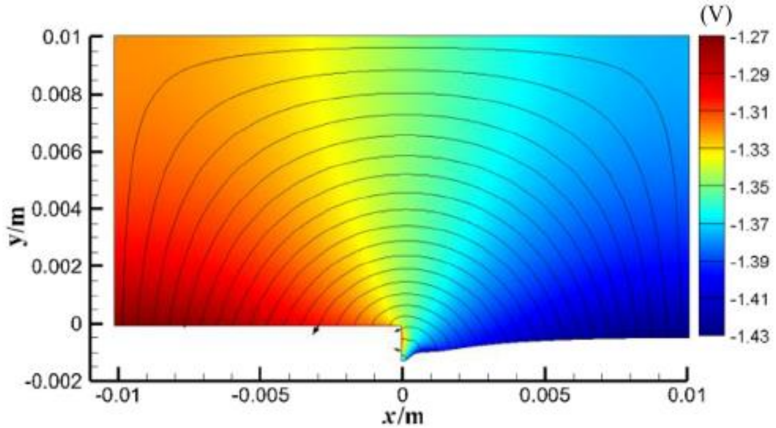

Wang, K., Li, C., Li, Y., Lu, J., Wang, Y., & Luo, X. (2021). Multi-physics analysis of the galvanic corrosion of Mg-steel couple under the influence of time-dependent anisotropic deposition film. Journal of Magnesium and Alloys, 9(3), 866–882

Atmospheric corrosion

- *Neutral solution*

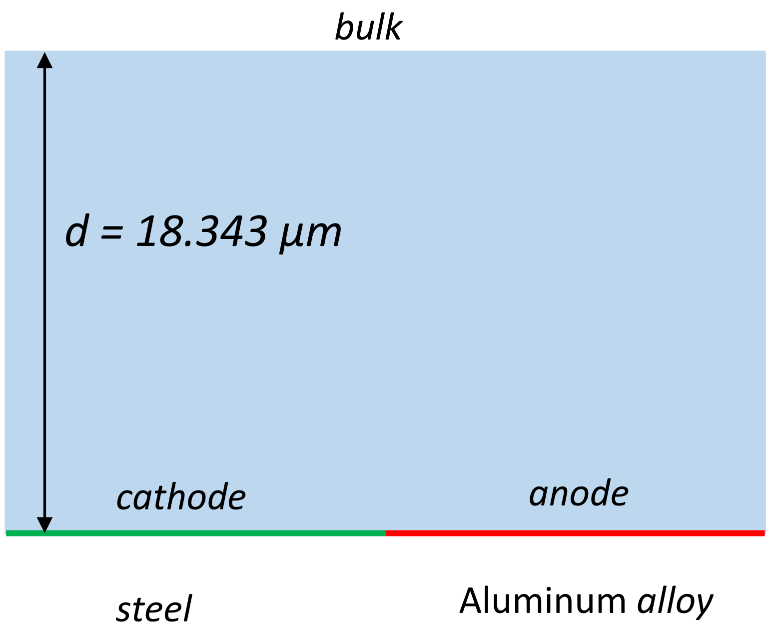

Partial Reactions

$$H_2O \rightarrow H^+ + OH^-$$

$$Al^{3+} + OH^- \rightarrow AlOH^{2+}$$

$$AlOH^{2+} + OH^- \rightarrow Al(OH)_2^+$$

$$Al(OH)_2^+ + OH^- \rightarrow Al(OH)_3$$

$$Al^{3+} + Cl^- \rightarrow AlCl^{2+}$$

$$AlOH^{2+} + Cl^- \rightarrow AlHCl^+$$

Atmospheric corrosion

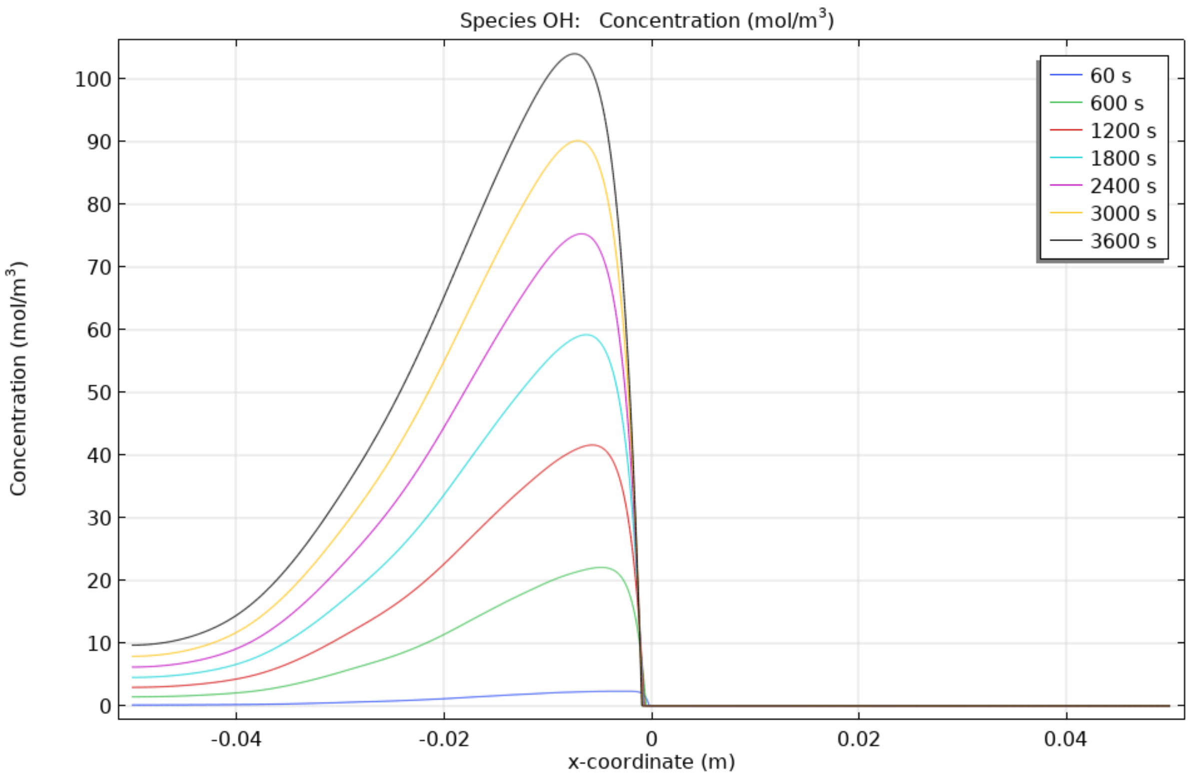

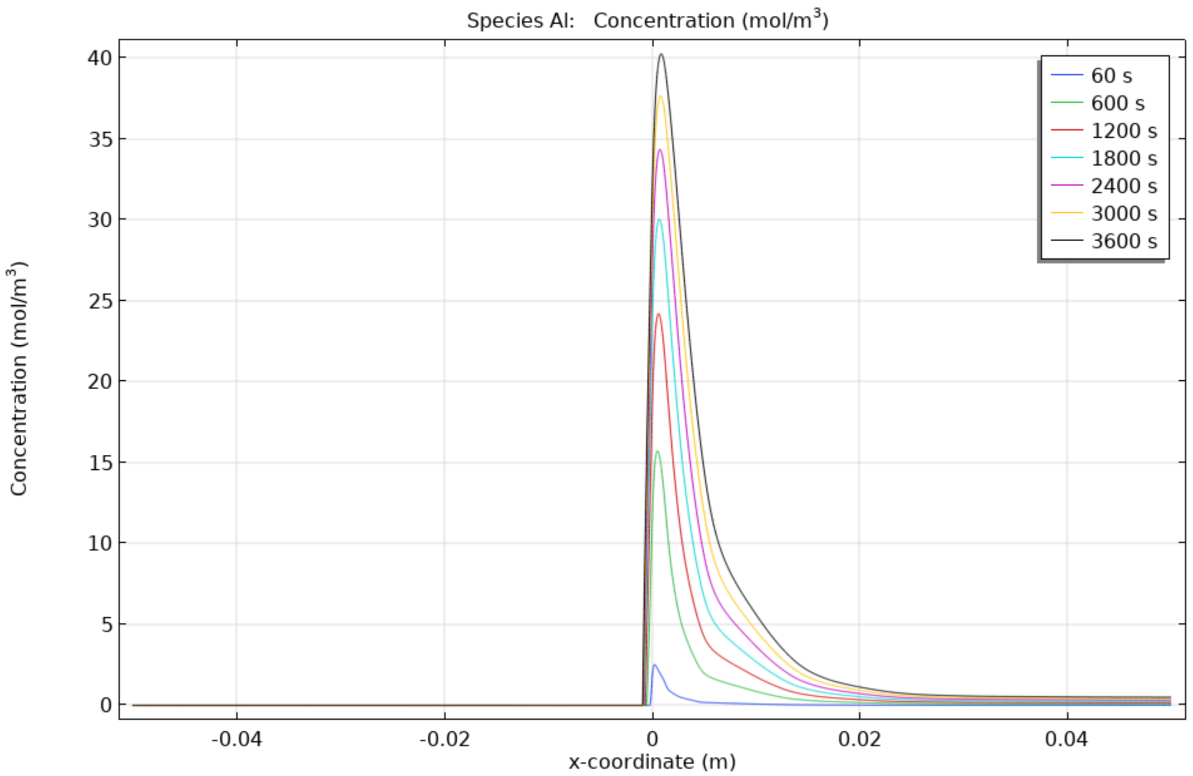

Atmospheric corrosion

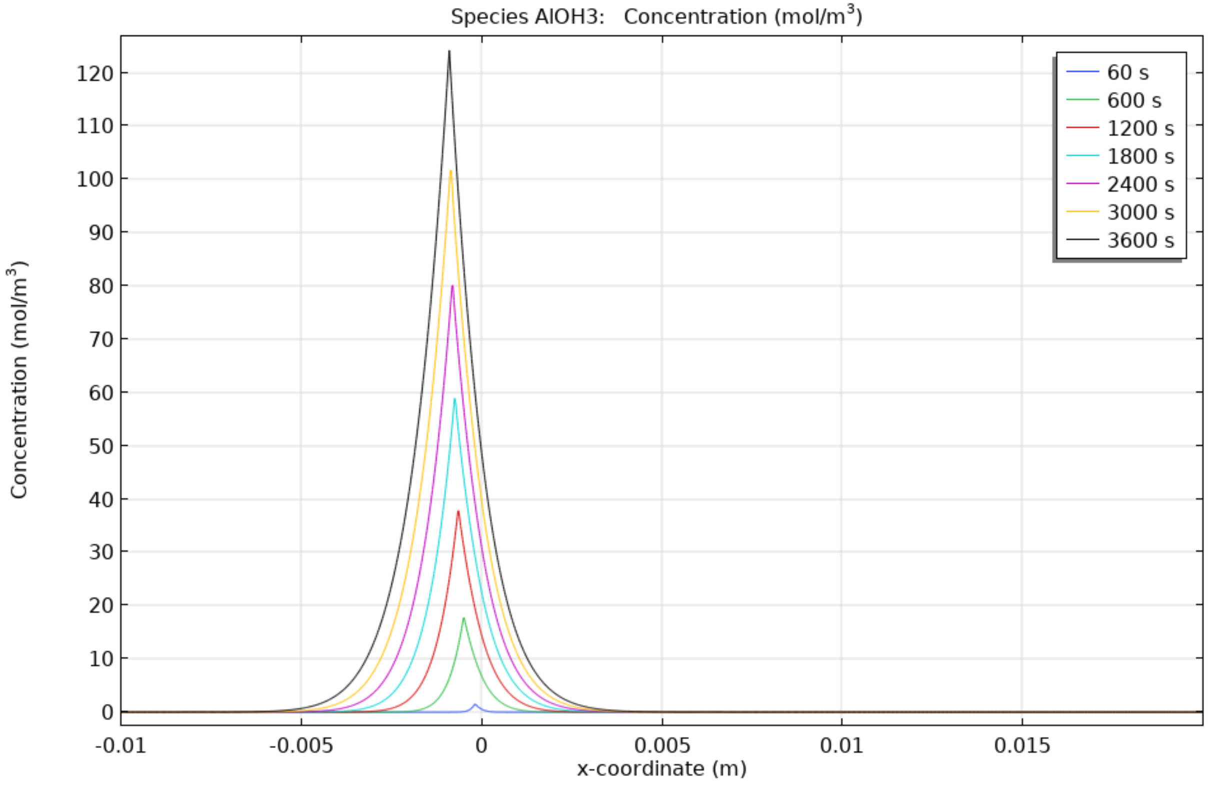

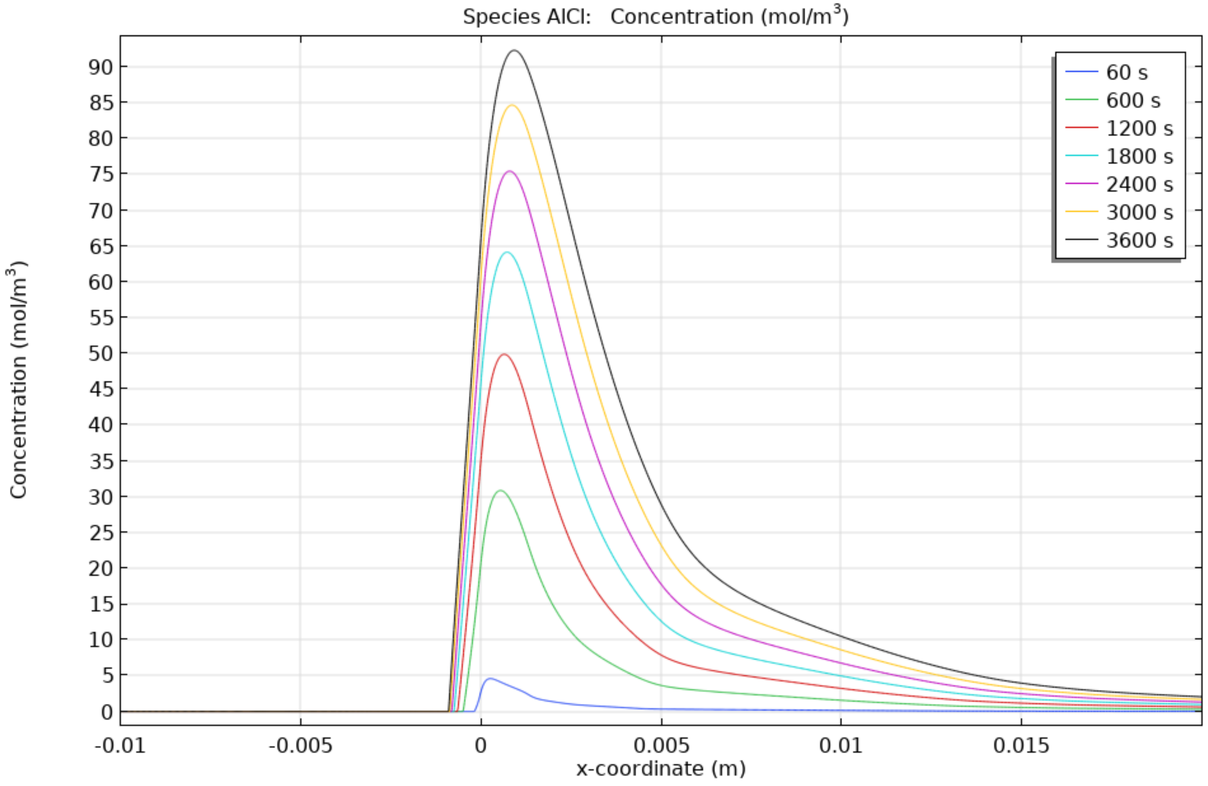

Pitting corrosion

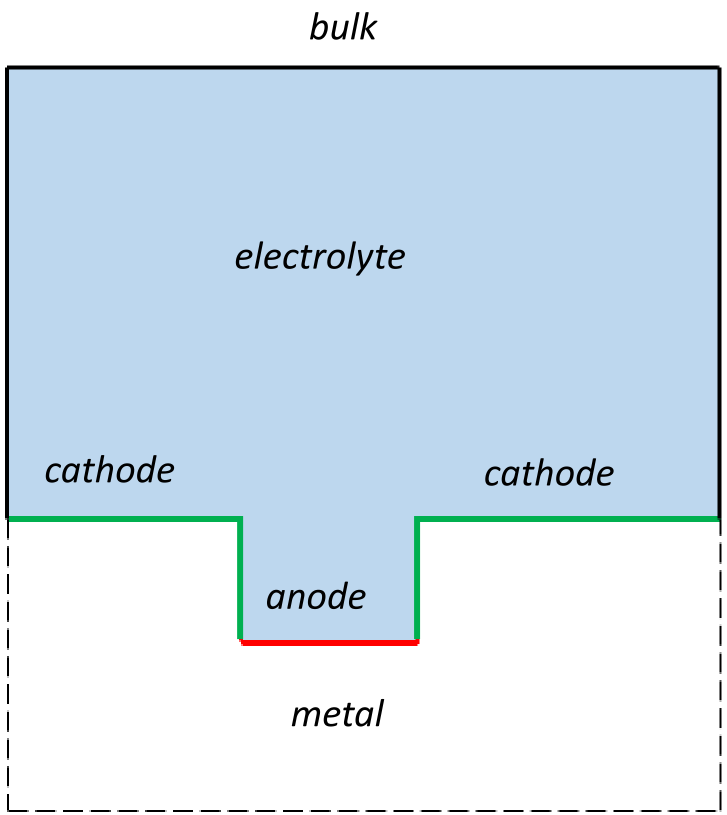

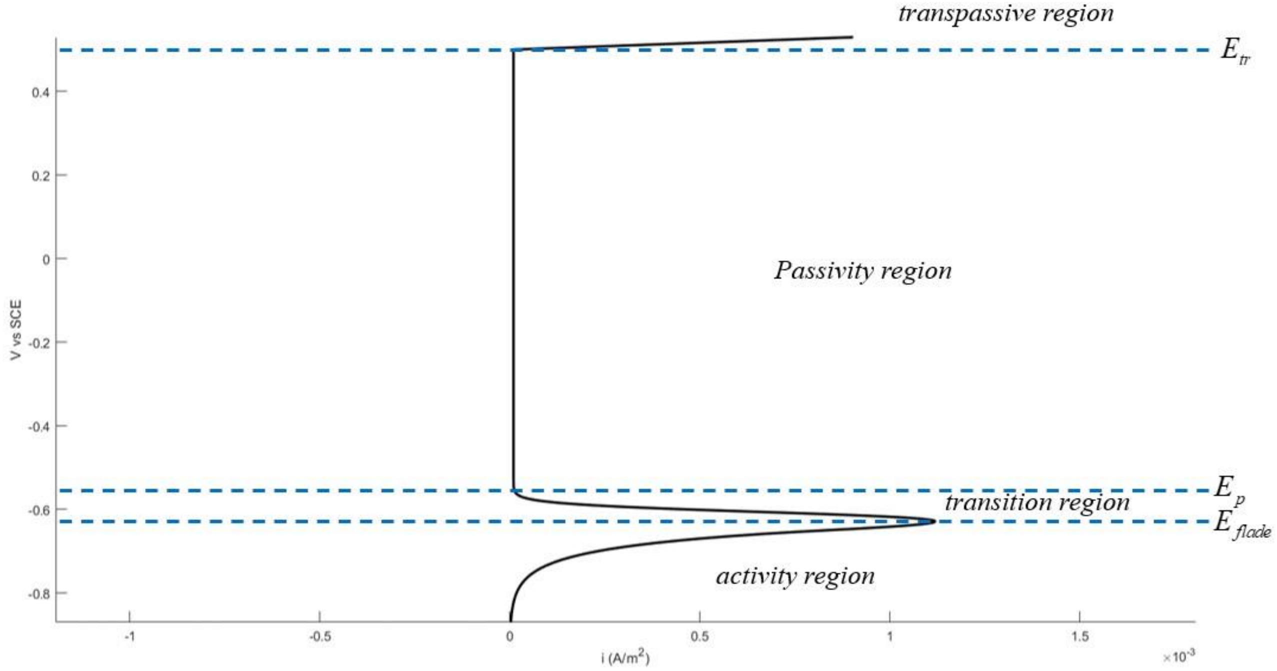

The boundaries of the problem are denoted with solid lines

Pitting corrosion

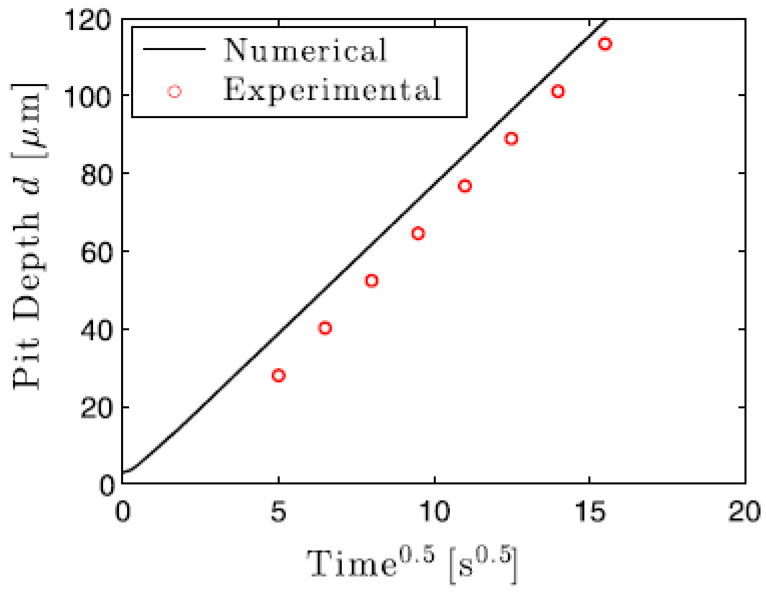

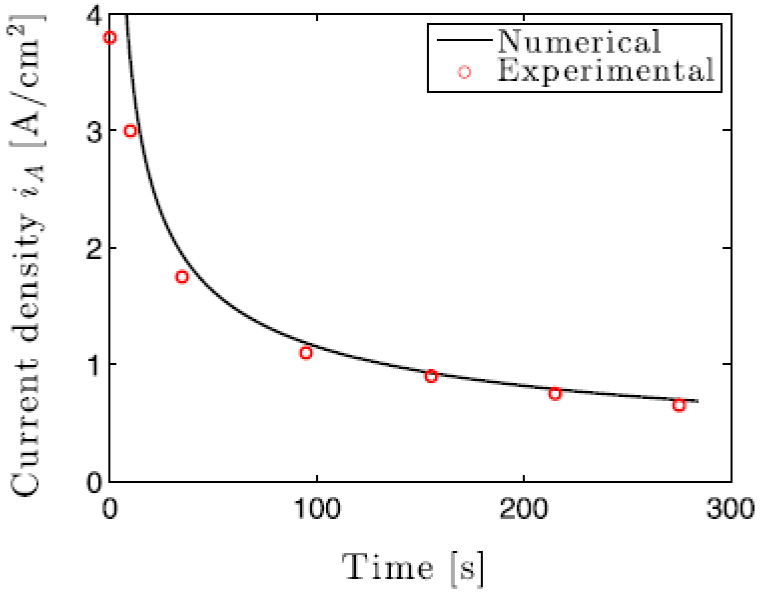

Duddu, R. (2014). Numerical modeling of corrosion pit propagation using the combined extended finite element and level set method. Computational Mechanics, 54(3), 613–627.

Pitting corrosion

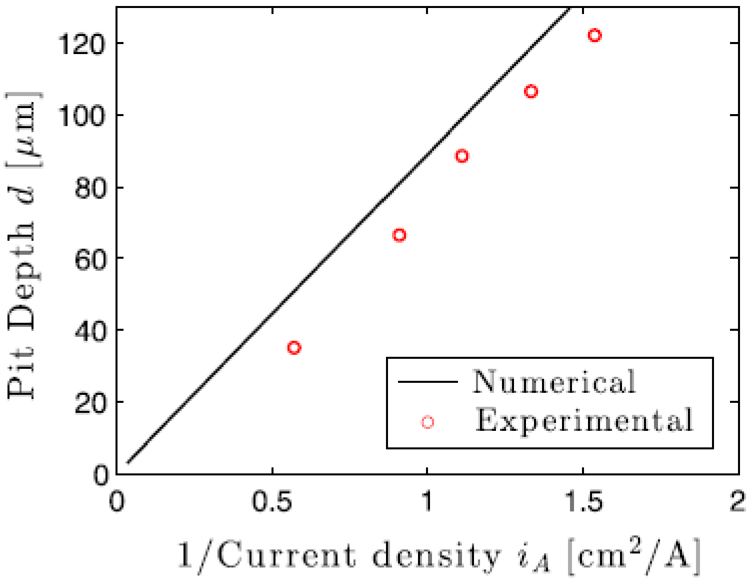

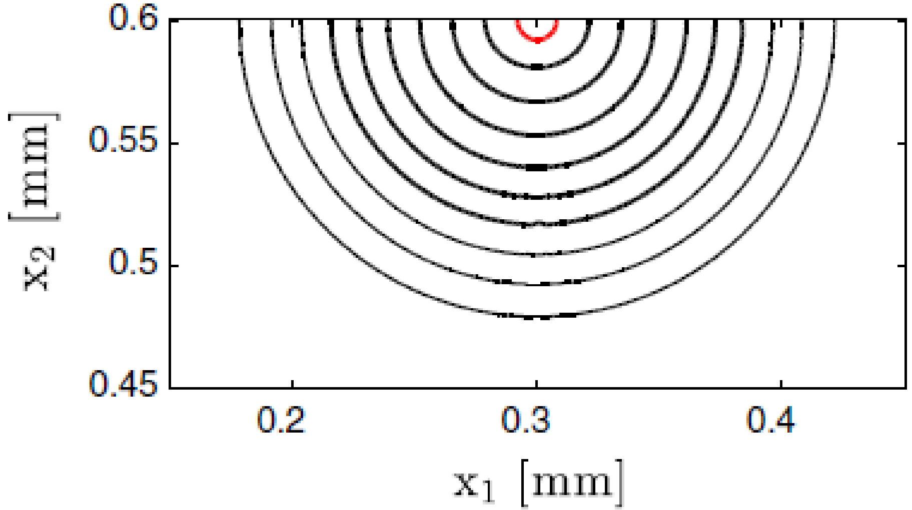

Duddu, R. (2014). Numerical modeling of corrosion pit propagation using the combined extended finite element and level set method. Computational Mechanics, 54(3), 613–627.

Pitting corrosion

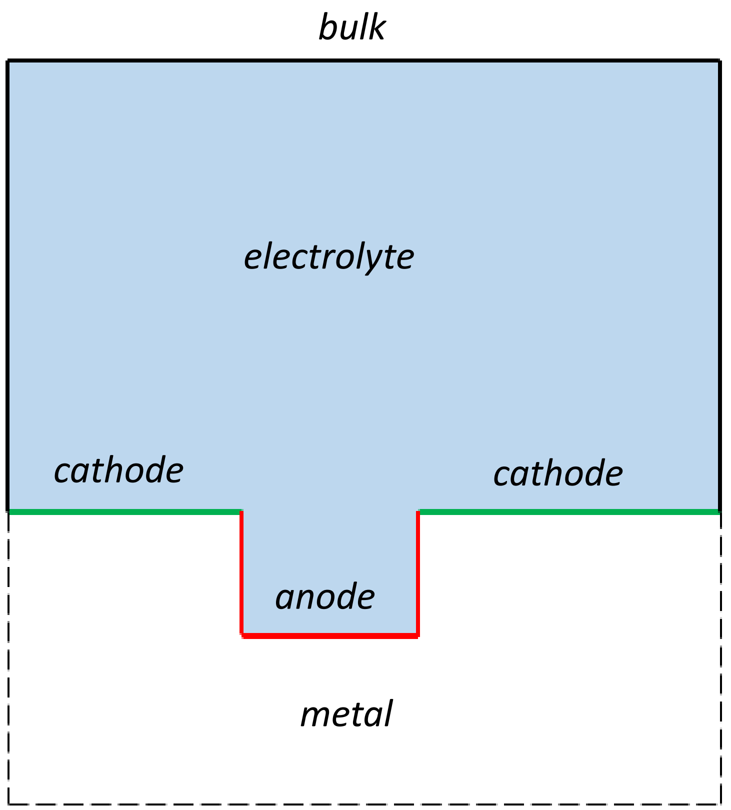

The boundaries of the problem are denoted with solid lines

- On the non-isolated pit (Duddu, R. ,2014) FEM-LSM formulation failed to provide an accurate approximation of the solution, compared to the experimental ones.
- In fact, the (Duddu, R. ,2014) FEM-LSM, considerably underestimated the resulting pit depth with time.

Pitting corrosion: Acidification of the solution inside the pit

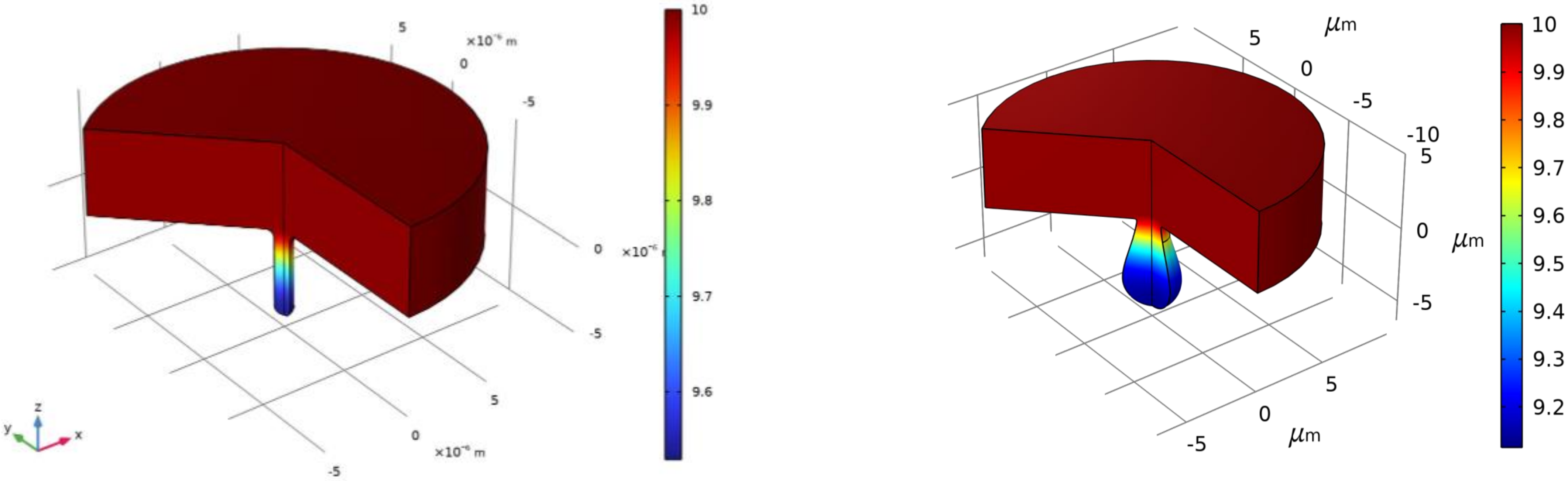

t=0

t=30 days

Crevice corrosion

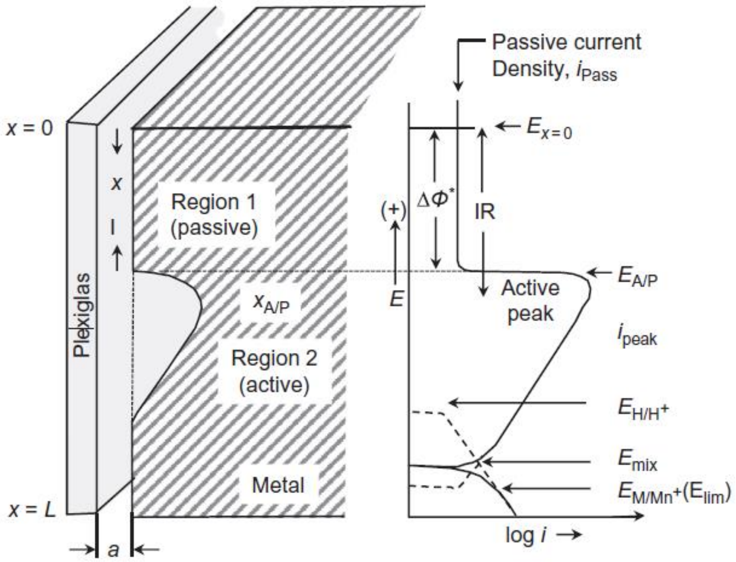

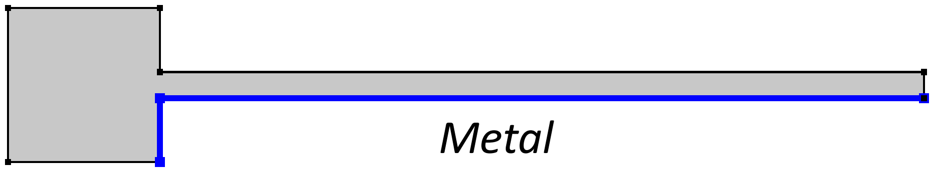

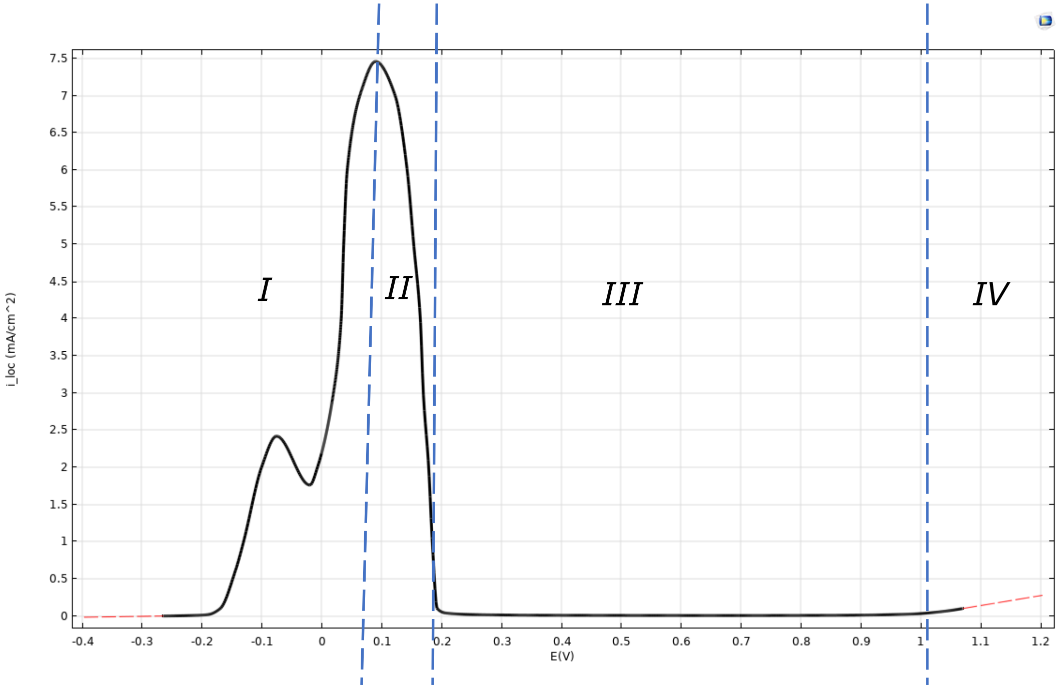

I Active region
II transition region
III passive region
IV transpassive region

Crevice corrosion

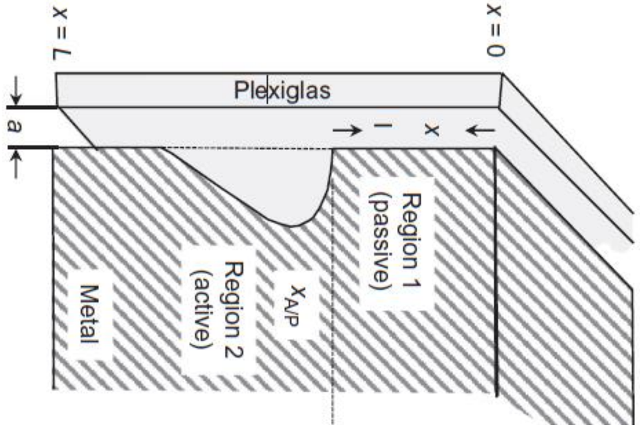

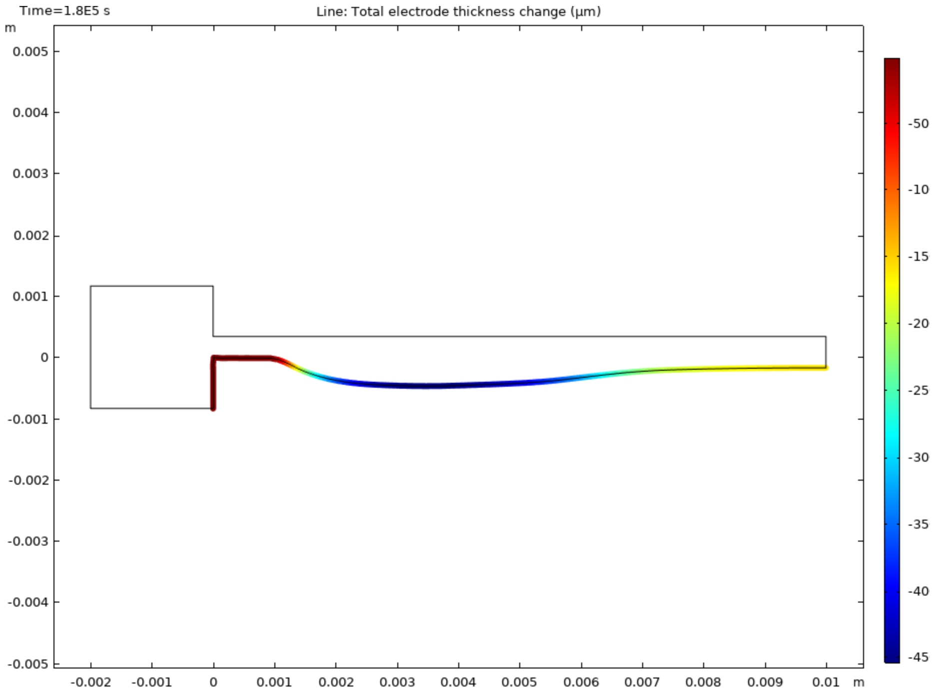

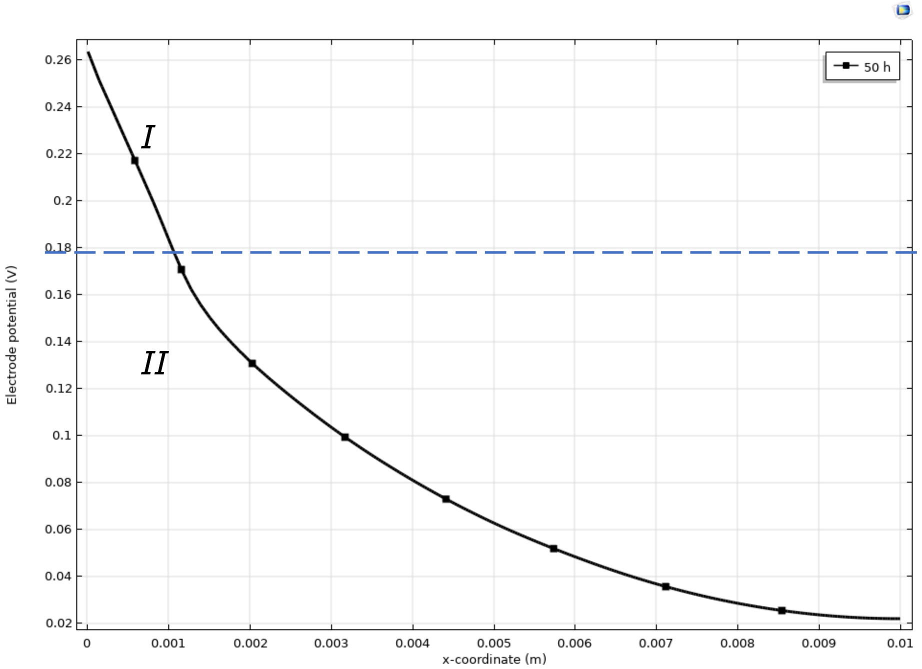

Crevice corrosion

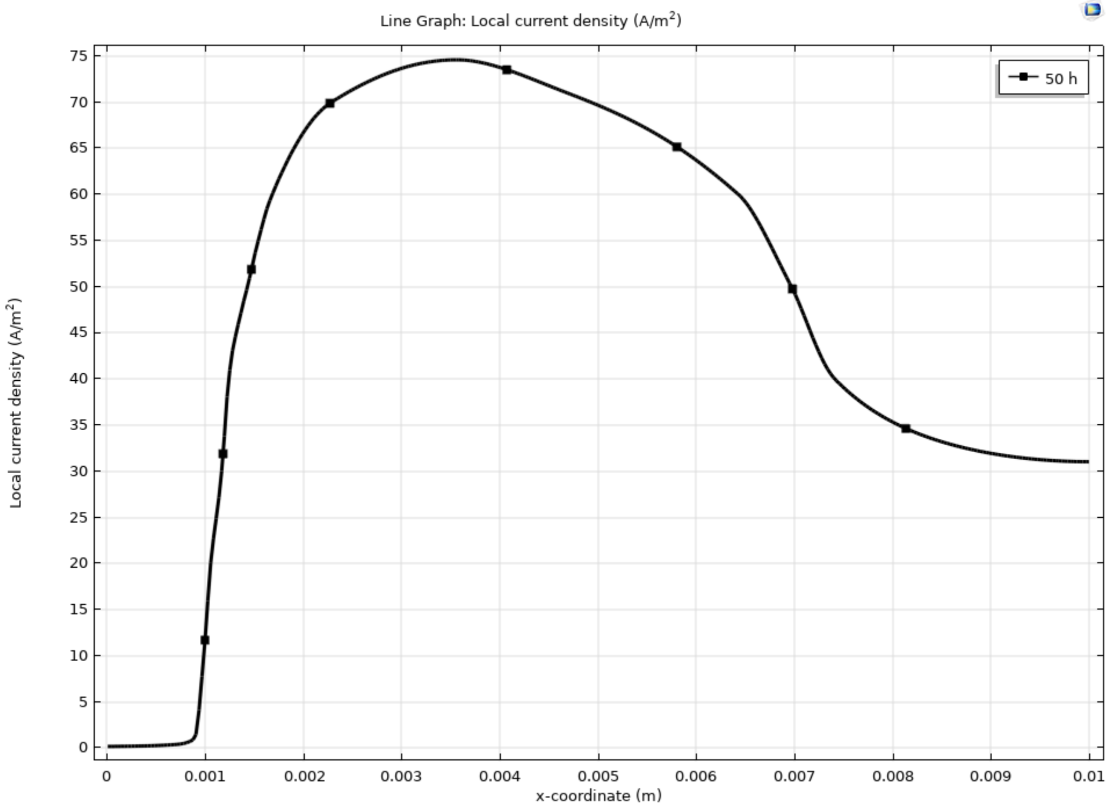

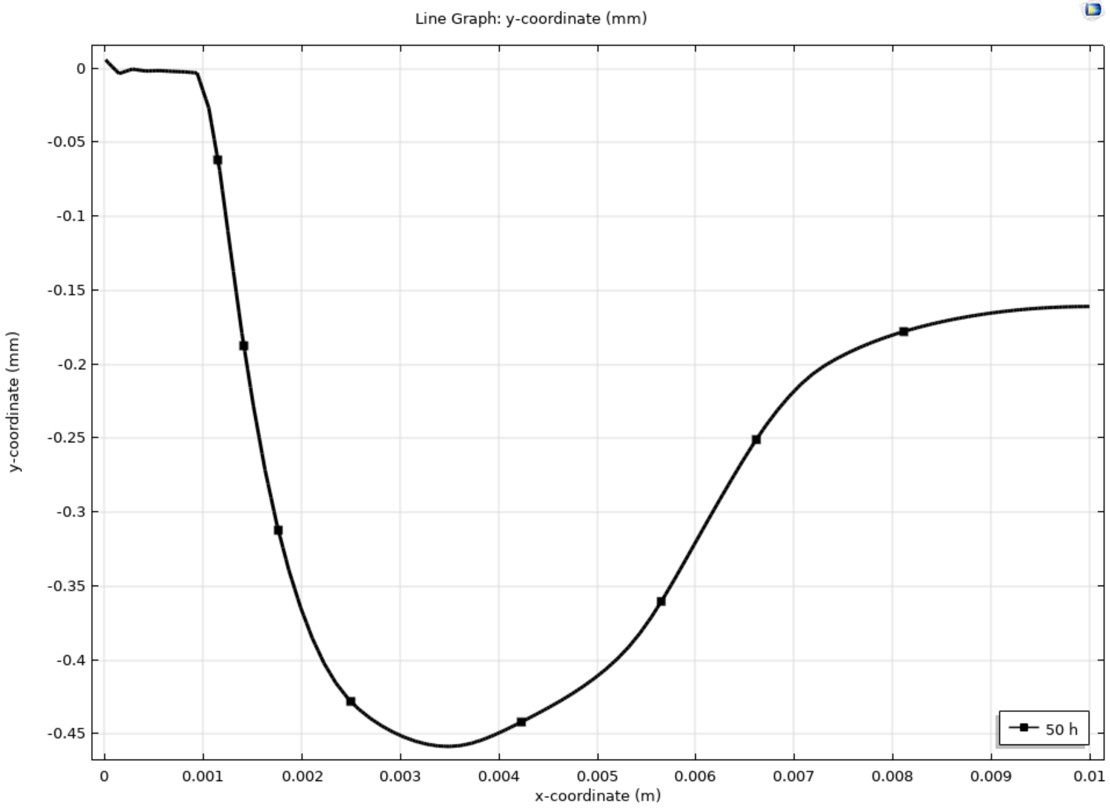

Crevice corrosion

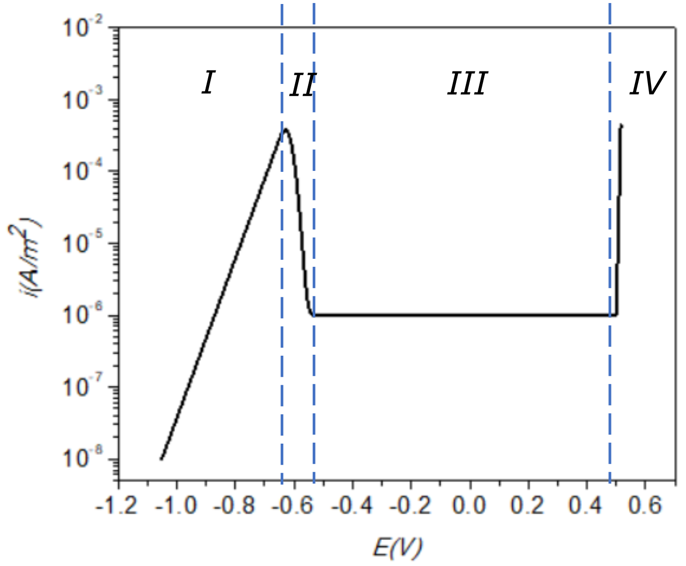

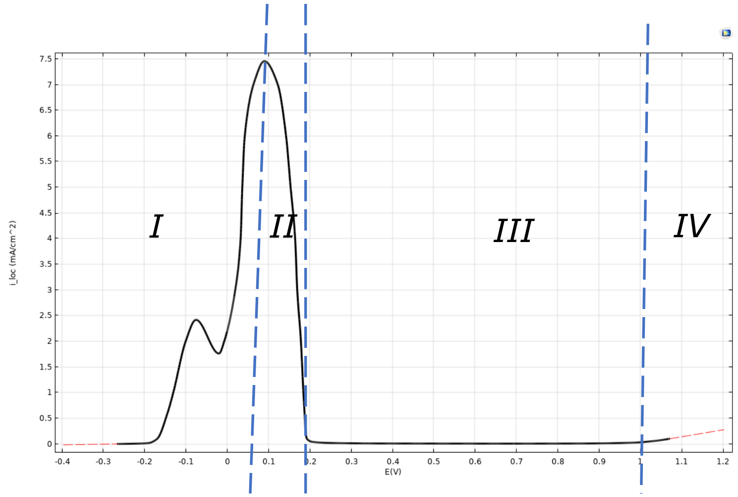

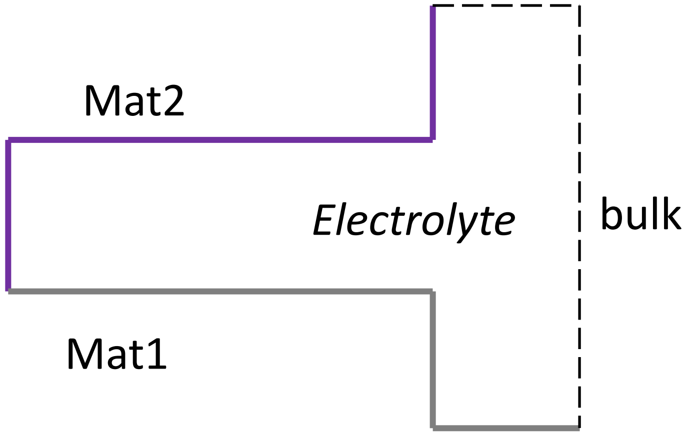

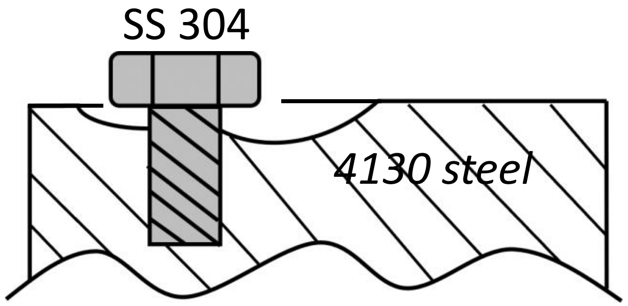

I Active region
II transition region
III passive region
IV transpassive region

Crevice corrosion

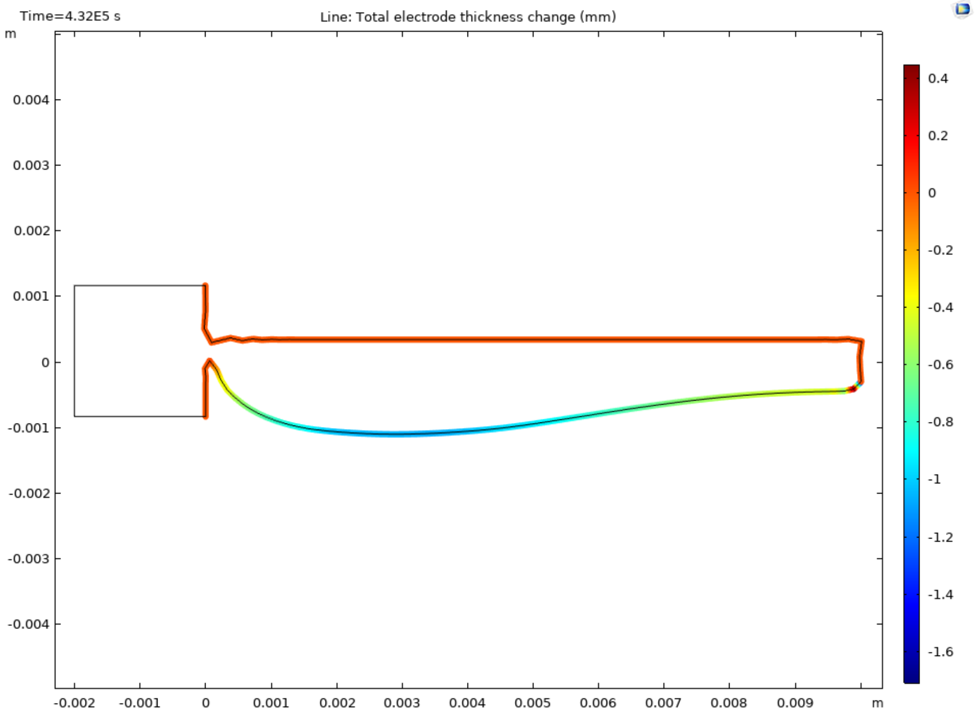

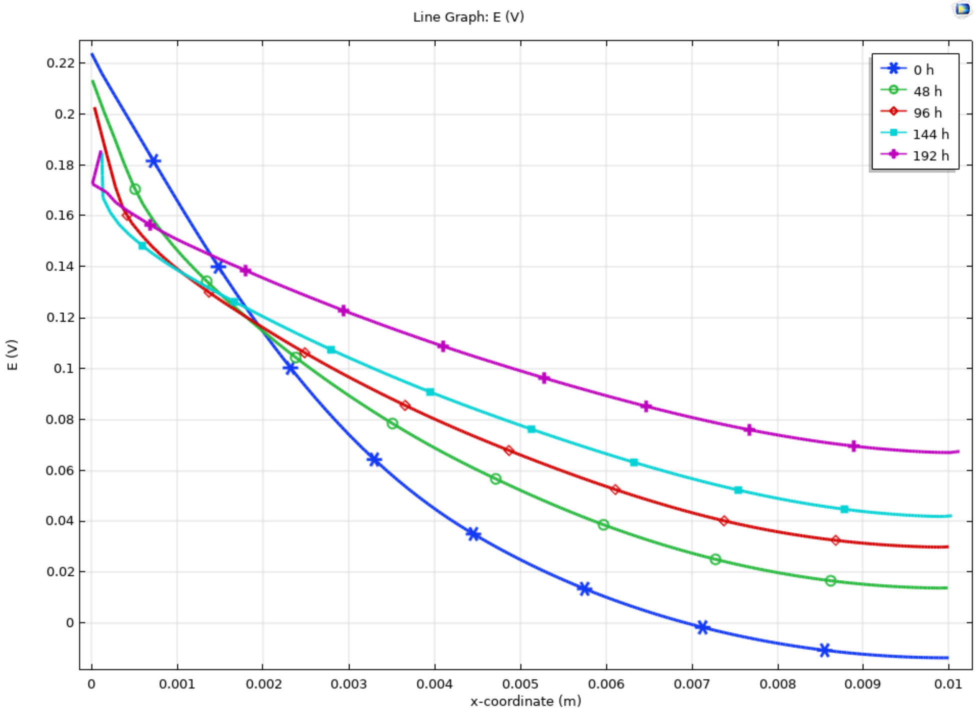

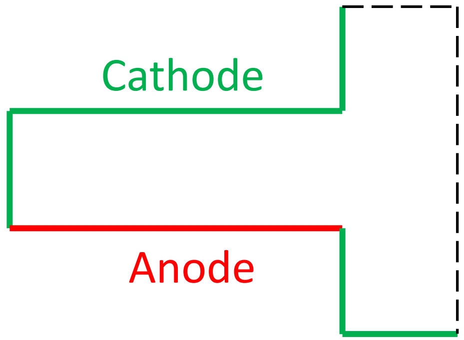

Crevice corrosion

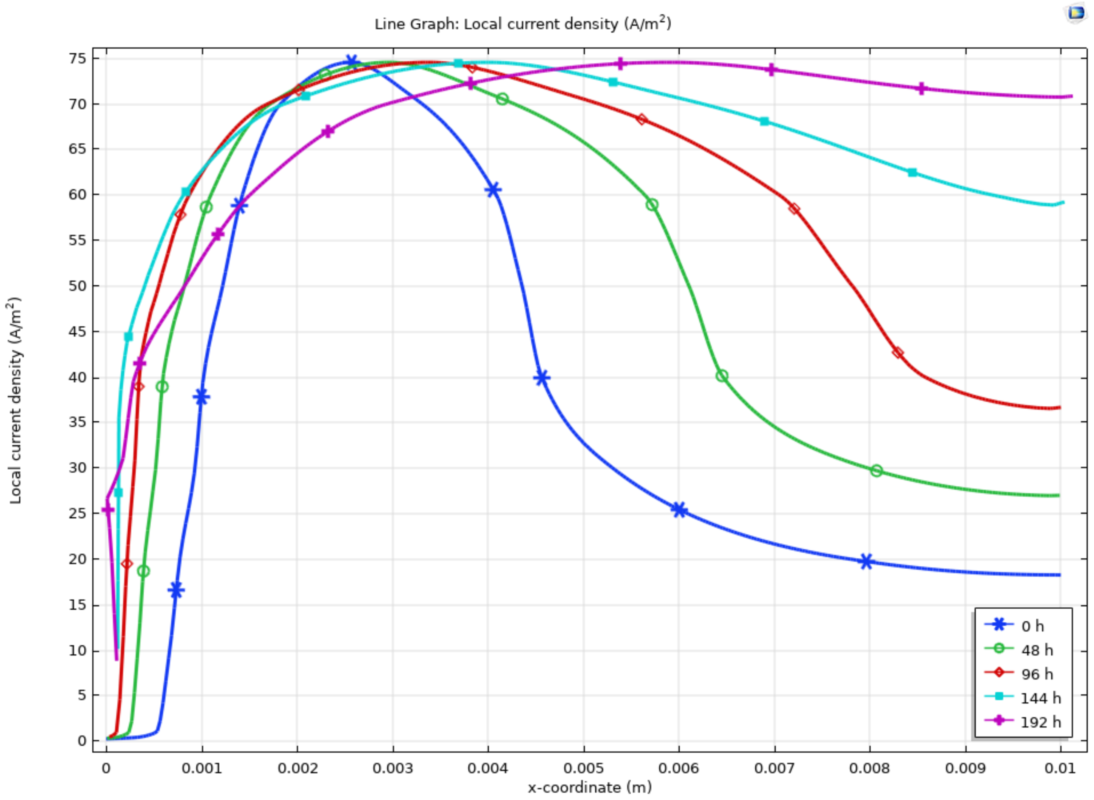

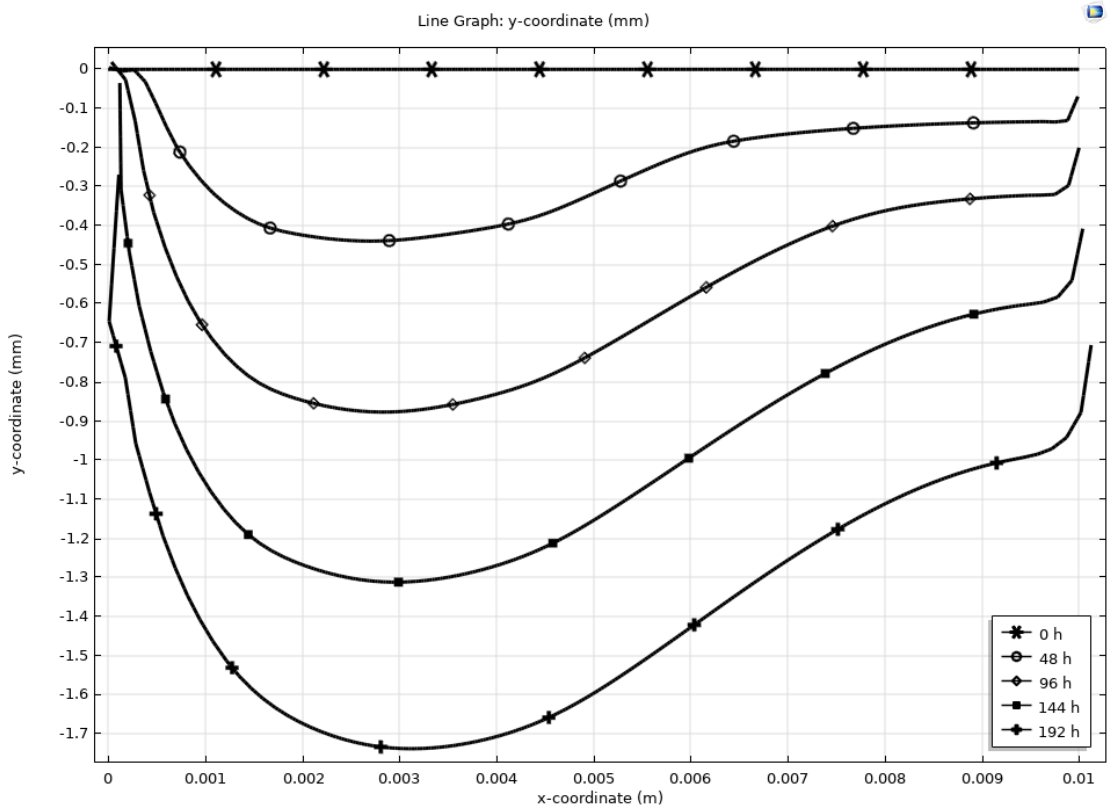

Stray Current Induced Corrosion

Governing Equations

$$\nabla \cdot \mathbf{i} = 0$$

$$\nabla^2 \varphi = 0$$

$$i = \mathbf{n} \cdot \mathbf{i} = -\sigma \, \mathbf{n} \cdot \nabla \varphi = -\sigma \, \partial_n \varphi$$

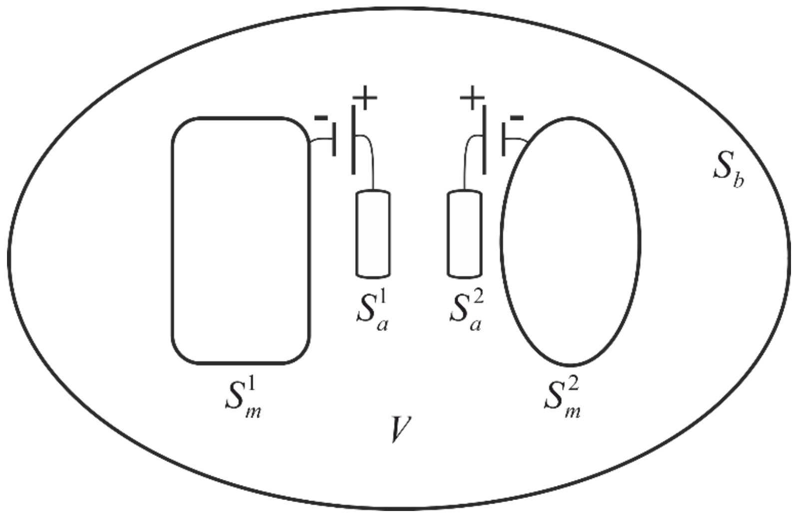

$$I_{\mathrm{CP}_1}^{\mathrm{net}} = \int_{S_m^1 \cup S_a^1} i \, ds = 0 \qquad I_{\mathrm{CP}_2}^{\mathrm{net}} = \int_{S_m^2 \cup S_a^2} i \, ds = 0$$

$$\int_V \nabla \cdot \mathbf{i} \, dV = 0 \text{ or } \int_{S_m^1 \cup S_a^1} i \, ds + \int_{S_m^2 \cup S_a^2} i \, ds + \int_{S_b} i \, ds = 0 \text{ or } I_{\mathrm{CP}_1}^{\mathrm{net}} + I_{\mathrm{CP}_2}^{\mathrm{net}} + \int_{S_b} i \, ds = 0$$

Stray Current Induced Corrosion

BEM formulation

$$c(\mathbf{x})\varphi(\mathbf{x})+\int_{S_m^1\cup S_a^1\cup S_m^2\cup S_a^2}\partial_n G(\mathbf{x},\mathbf{y})\varphi(\mathbf{y})\,dS+\frac{1}{\sigma}\int_{S_m^1\cup S_a^1\cup S_m^2\cup S_a^2}G(\mathbf{x},\mathbf{y})i(\mathbf{y})\,dS-\varphi_\infty^1=0\ ,\ \mathbf{x}\in S_m^1\cup S_a^1$$

$$c(\mathbf{x})\varphi(\mathbf{x})+\int_{S_m^1\cup S_a^1\cup S_m^2\cup S_a^2}\partial_n G(\mathbf{x},\mathbf{y})\varphi(\mathbf{y})\,dS+\frac{1}{\sigma}\int_{S_m^1\cup S_a^1\cup S_m^2\cup S_a^2}G(\mathbf{x},\mathbf{y})i(\mathbf{y})\,dS-\varphi_\infty^2=0\ ,\ \mathbf{x}\in S_m^2\cup S_a^2$$

$$\begin{bmatrix}\mathbf{H}_{11} & \mathbf{H}_{12} & \mathbf{I}_1 & \mathbf{0}\\ \mathbf{H}_{21} & \mathbf{H}_{22} & \mathbf{0} & \mathbf{I}_2\\ \mathbf{0} & \mathbf{0} & 0 & 0\\ \mathbf{0} & \mathbf{0} & 0 & 0\end{bmatrix}\cdot\begin{Bmatrix}\boldsymbol{\varphi}_{\mathrm{cp}_1}\\ \boldsymbol{\varphi}_{\mathrm{cp}_2}\\ \varphi_\infty^1\\ \varphi_\infty^2\end{Bmatrix}=\begin{bmatrix}\mathbf{G}_{11} & \mathbf{G}_{12}\\ \mathbf{G}_{21} & \mathbf{G}_{22}\\ \mathbf{C}_1 & \mathbf{0}\\ \mathbf{0} & \mathbf{C}_2\end{bmatrix}\cdot\begin{Bmatrix}\mathbf{i}_{\mathrm{cp}_1}\\ \mathbf{i}_{\mathrm{cp}_2}\end{Bmatrix}$$

ACA/BEM analysis utilizing PITHIA CP

Stray Current Induced Corrosion

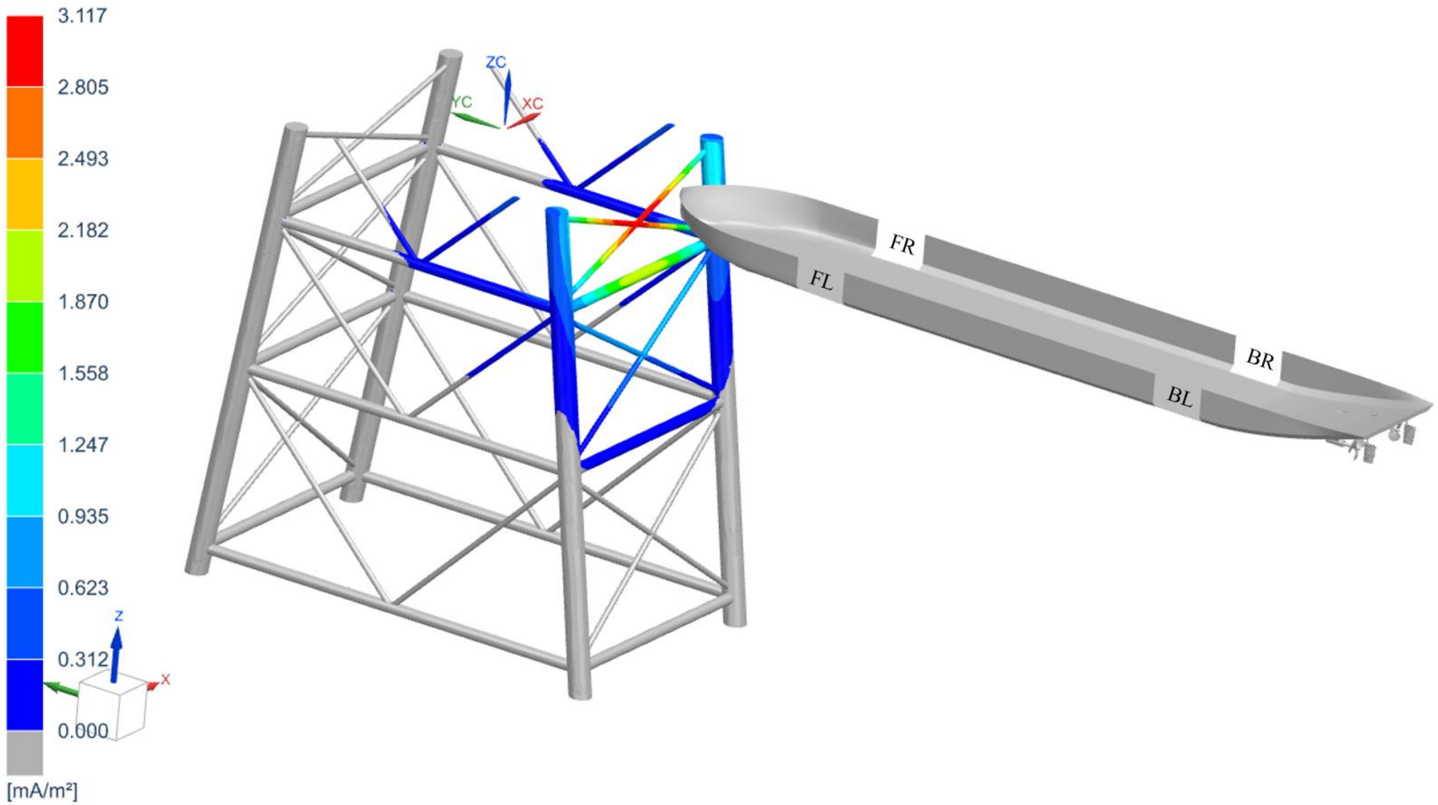

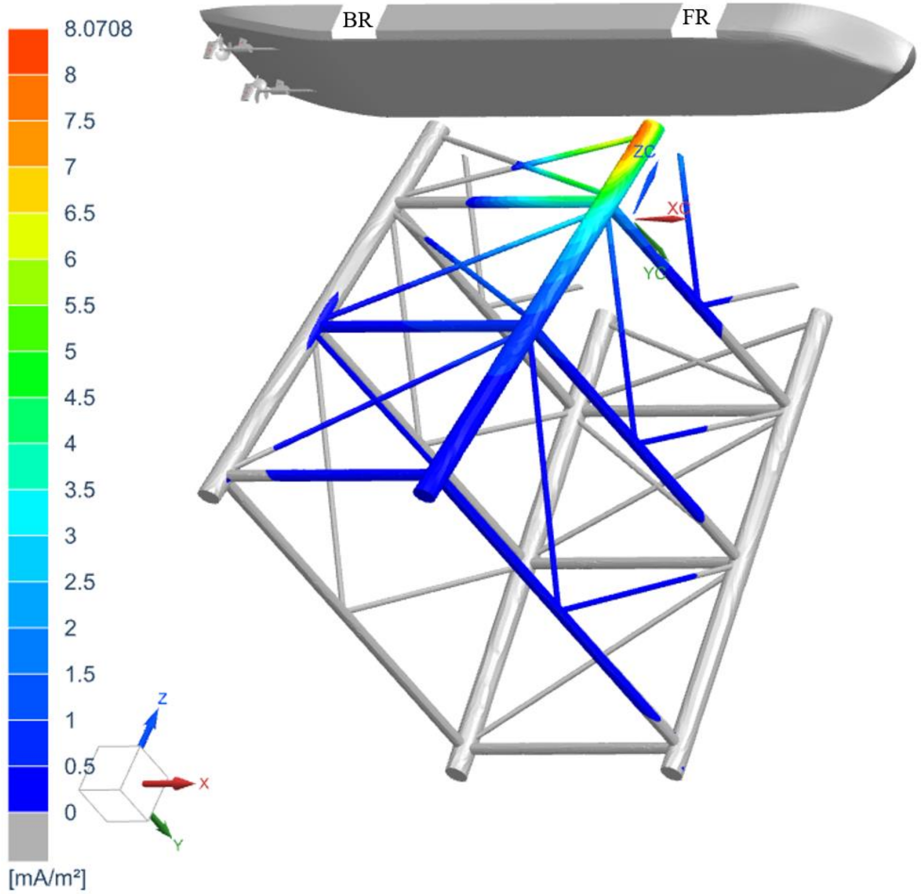

ACA/BEM analysis utilizing PITHIA CP

Stray Current Induced Corrosion

interference

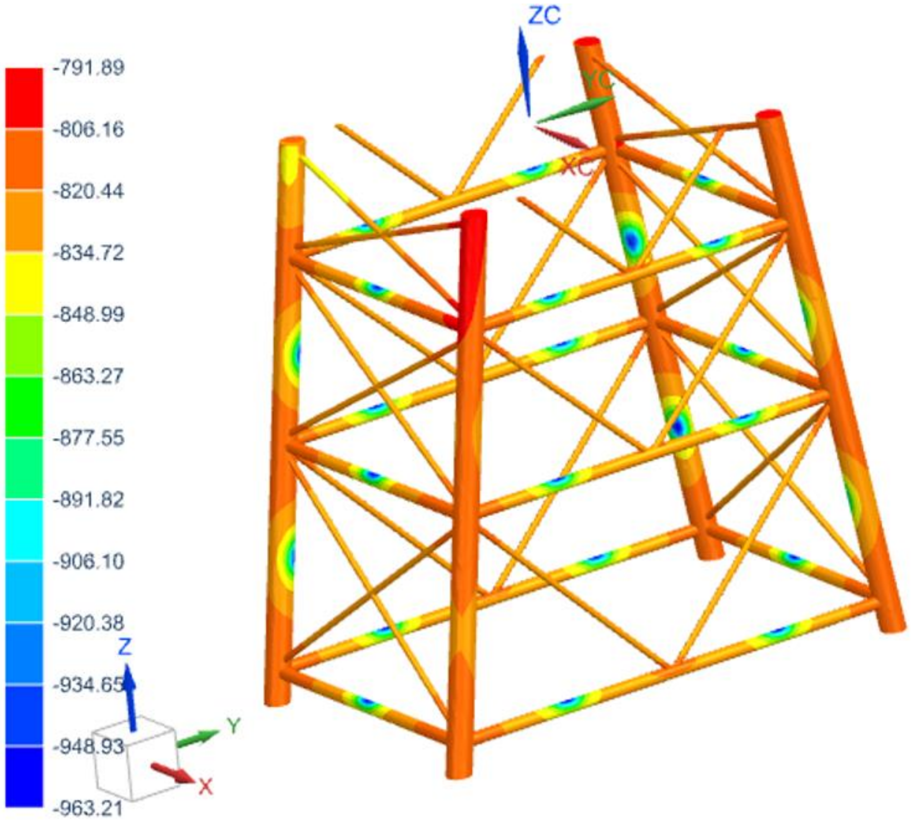

reference

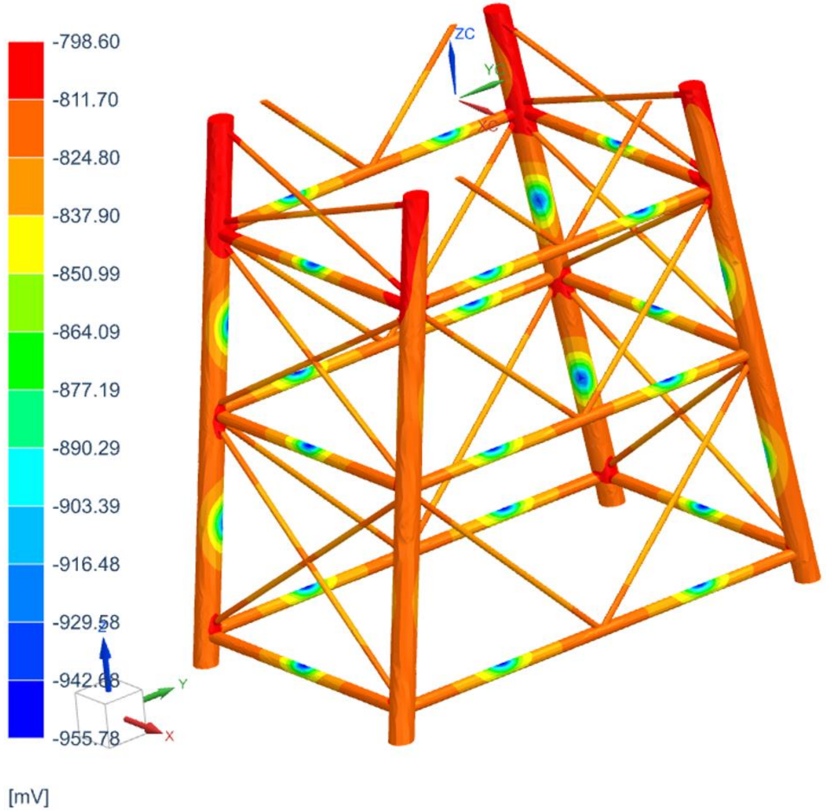

Corrosion Fatigue

- *Assuming **uniform corrosion** (Wang and Zhao, 2016) they found, using a commercial FEA code, a 57% **increase** in the **maximum deflection,** of the steel WT monopipe pile, and a **maximum stress increase** of 63%.*

- *The researches also pointed out that over the course of time, the **reduction** in **strength** and **stability** of the steel WT monopipe pile arising from corrosion exhibits **nonlinear** development.*

- *The impact of **the mechanical stress** and **strain** due to **localized corrosion** is examined by (Wang et.al., 2016) using a commercial FEA code. They found that as the **corrosion rate increases locally** the arising **mechanical stress** and **strain** also **increases** significantly.*

- *The impact of the **pit depth** on the **final crack length** is examined by (Shittu et.al., 2020) using a commercial FEA code. They found that as the **pit depth increases** the **crack length** is **bigger** and they also emerged faster (less loading cycles).*

- *The impact of the **pit depth** on the **crack growth rate** is examined by (Moghaddama et.al., 2019) using a commercial FEA code. They pointed out that the **maximum crack growth rate** is found at the **largest pit**.*

Corrosion Fatigue

- *As discussed previously both, the corrosion degradation of the immersed part, and the emerge of localized corrosion in WTs, threaten their structural integrity. Consequently, during the structural design aspect of WT, the effects of corrosion in the structure surfaces should be taken into account.*
- *Wind Turbines corrosion problems are **large-scale** ones. The accurate approximation of the corrosion rate of such structures as important it is, is a not easy, as it is impossible to run a N-P based simulation through 30+ years, i.e. billions seconds, and possible trillions time steps.*
- *For the immersed part of WT, under cathodic protection a fast and accurate approximation of the corrosion rate can be achieved.*
- *For the exposed part in atmospheric corrosion though, a different strategy has to be employed.*
- *Possibly several smaller problems should be solved to predict potential pitting initiation and/or propagation.*
- *The formulation of reduced order models (ROMs), maybe is the solution to such problems.*
- *In any case more **research** is to be done in that field.*

Corrosion protection

- Corrosion Protection Standards
- Protective Coatings
- Cathodic Protection

LEVELS AND ZONES IN SEAWATER ENVIRONMENT

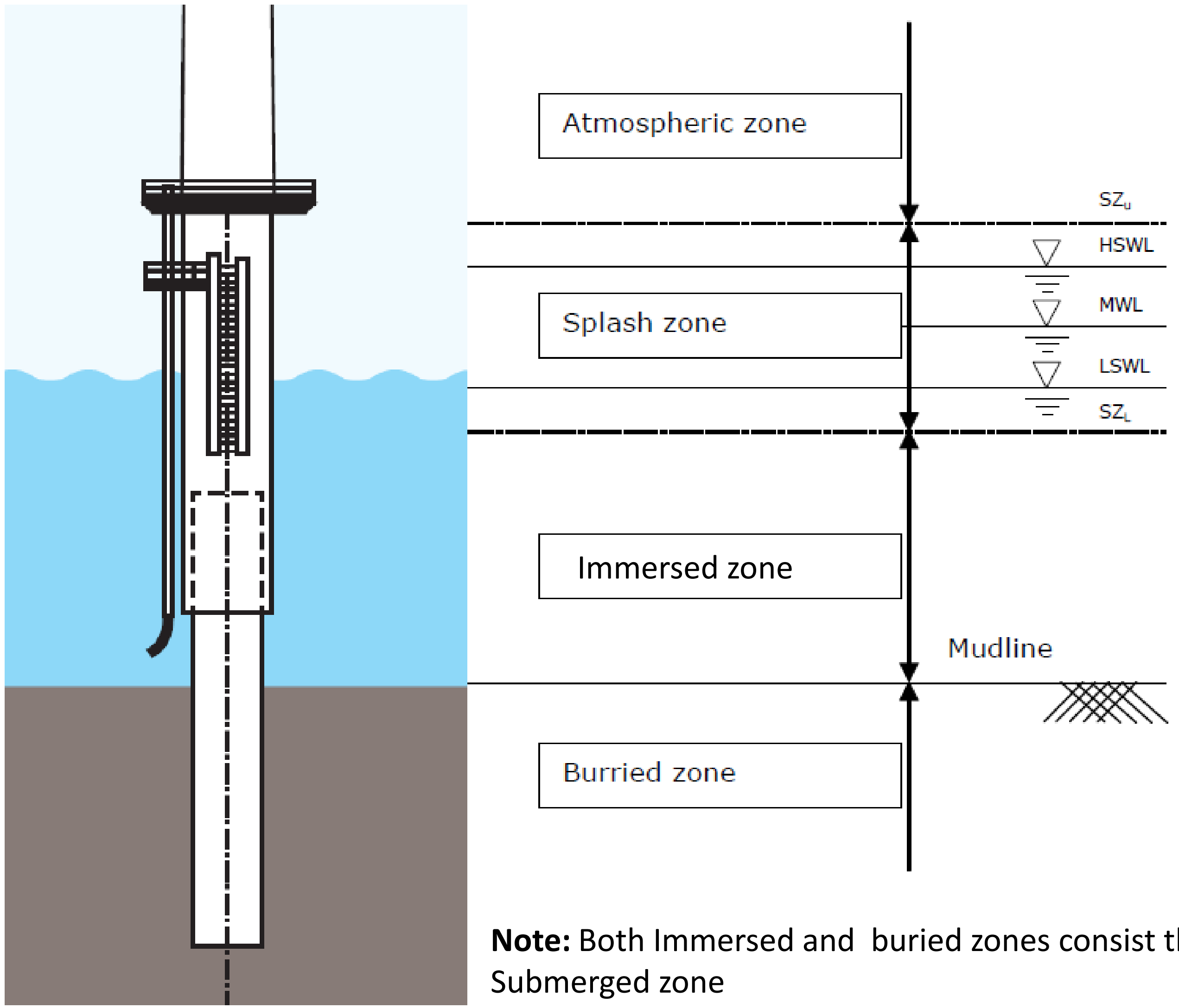

Note: Both Immersed and buried zones consist the Submerged zone

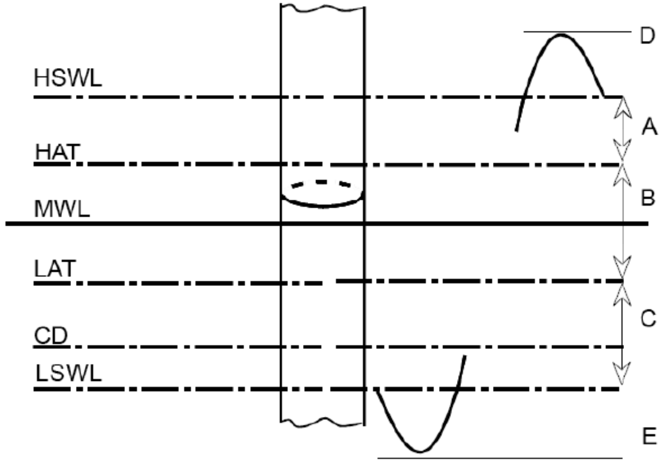

HSWL highest still water level

HAT highest astronomical tide

MWL mean water level

LAT lowest astronomical tide

CD chart datum (often equal to LAT)

LSWL lowest still water level

A positive storm surge

B tidal range

C negative storm surge

D maximum crest elevation

E minimum trough elevation

CORROSION PROTECTION OF ATMOSPHERIC ZONE

At the **atmospheric zone,** the steel tower and topside structure suffer actions from a marine aerosol. Unlike the splash zone, the structure is not directly attacked by water splashes. The winds carry the salts in the form of solid particles or as droplets of saline solution. The quantity of salt present decreases as a function of height distance from the mean water line (MWL).

According to DNV:

- ✓ **External and internal surfaces** of steel structures exposed in the **atmospheric zone shall be protected by the coating**.
- ✓ **Corrosion-resistant materials** are applicable for specific critical components, for example, **stainless steel** for **bolting** and other **fastening devices** and glass-reinforced plastic (GRP) for grating.

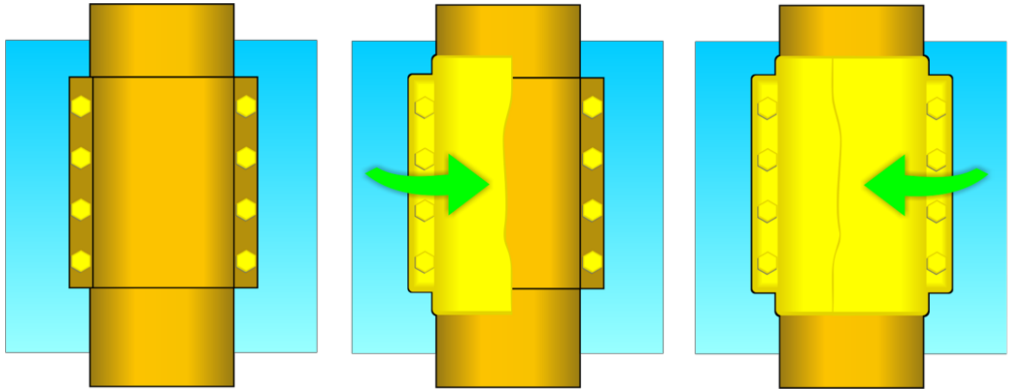

Protection of bolted steel connections

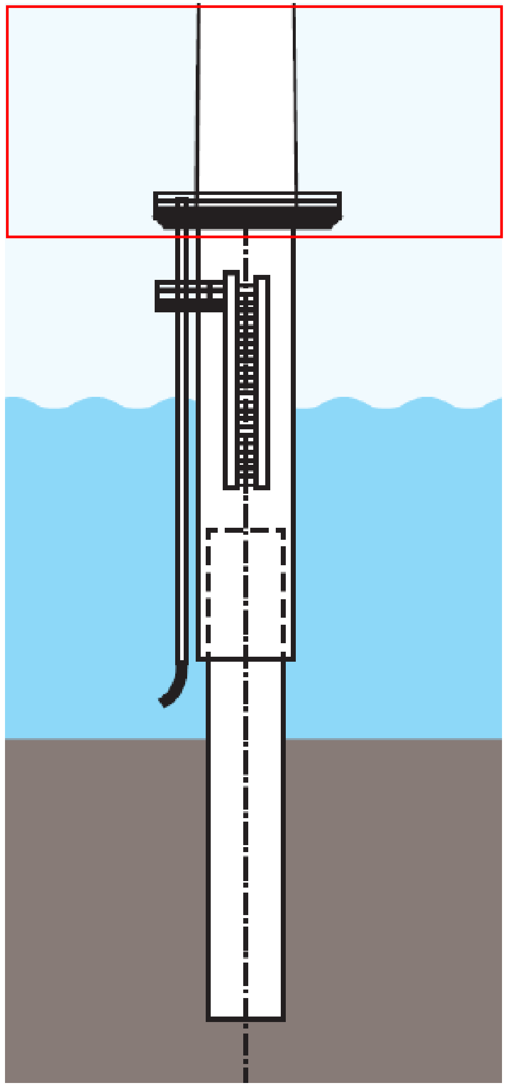

CORROSION PROTECTION OF SPLASH ZONE

At this part of the splash zone, the structure is directly exposed to seawater due to the action of tide and waves (water splash). The **corrosive environment is severe**, the **maintenance of a coating system is not practical** and **cathodic protection is not effective** for parts located **above mean water line** (MWL). Corrosion becomes more significant as water evaporates, and salts remain on the surface of the substrate.

According to DNV:

- ✓ **External and internal surfaces** of steel structures in the splash zone **shall** be protected by a **corrosion control system**. **Coating is mandatory for external surfaces of primary structures**. Maintenance of coating systems in the splash zone is not practical and coating of primary structures shall therefore be combined with a **corrosion allowance**.
- ✓ For **internal surfaces** of primary structures, use of coating is optional. The necessary **corrosion allowance** for internal surfaces shall be calculated assuming $T_C = 0$ when no coating is used.
- ✓ **Coatings** for corrosion control in the splash zone shall as a **minimum extend** to **MWL – 1.0 m**. This zone is often coated using a multi-layer scheme involving glass flakes- reinforced polymer to help protect against mechanical damage.
- ✓ For parts of the splash zone located **below MWL, cathodic protection may be assumed** for design purposes to be fully protective, and **no corrosion allowance** is required.

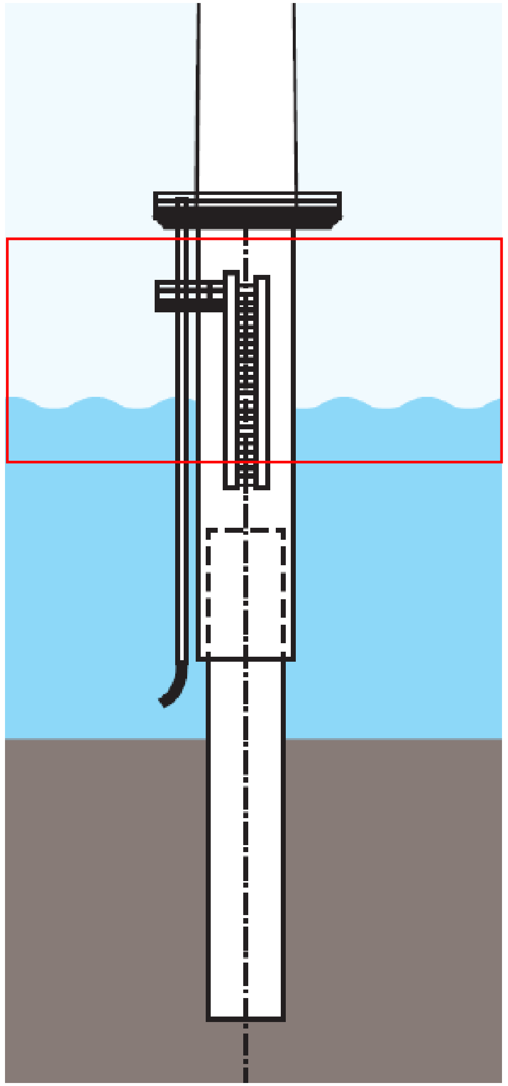

CORROSION PROTECTION OF SUBMERGED ZONE

The **submerged zone** consists of the region below the lower limit of the splash zone (**immersed zone**), including the scour zone and the zone of permanently **buried** structural parts.

According to DNV:

- The **external surfaces of the submerged zone**:
  - ✓ **It is mandatory shall have cathodic protection**.
  - ✓ Use of **coating** is **optional** and is then primarily intended to reduce the required CP capacity.
  - ✓ Use of coating may also be advised to reduce the danger of microbiologically influenced corrosion (MIC) in absence of CP.
  - ✓ The design of CP shall take into account possible scouring causing free exposure to seawater of surfaces initially buried in sediments.
  - ✓ The design of CP shall also take into account current drain to all external surfaces to be buried in sediments. Steel surfaces buried in deep sediments need no corrosion protection, but will still drain current from a CP system due to the electrochemical reduction of water to hydrogen molecules on such surfaces.
- The **Internal surfaces** of the submerged zone **shall be protected** by **either CP or corrosion allowance**, with or without coating in combination.

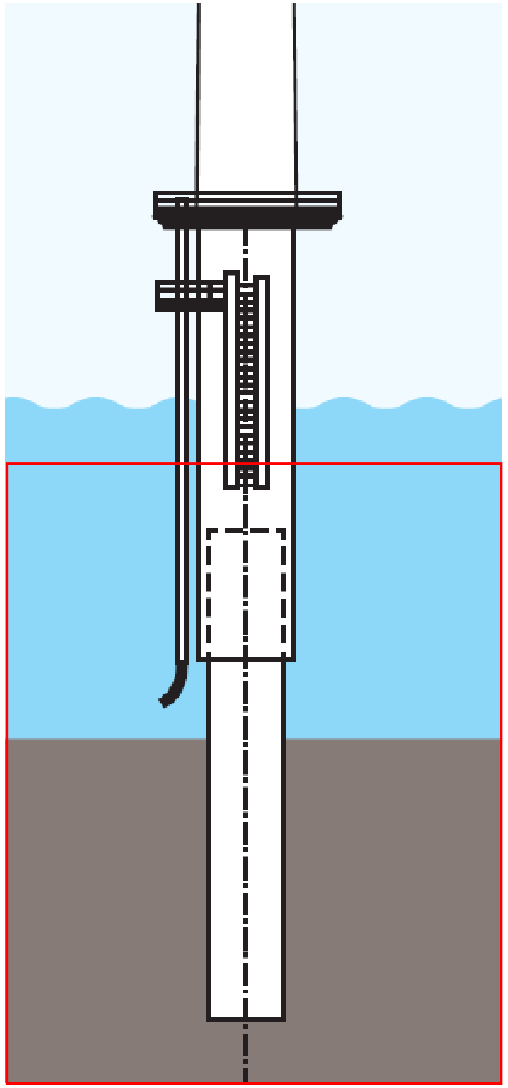

CATHODIC PROTECTION

Either sacrificial anode cathodic protection (SACP) or impressed current cathodic protection (ICCP) can be used.

According to DNV, **SACP** is well established and is **generally preferred for such structures**.

Use of ICCP for offshore structures may offer certain advantages, but there is no generally acknowledged design standard available giving detailed requirements and advice as for galvanic anode systems. Even with adequate design, ICCP systems are more vulnerable to environmental damage and third-party damage than SACP systems, in particular cables to anodes and reference electrodes are vulnerable.

- **Highlights on SACP according to DNV**
  - ✓ The **initial design current density** demands referred in DNV-RP-B401 is recommended to **be increased by 50%** for all initially bare steel surfaces in order to account for the effect of **high seawater currents**, such as in shallow waters with large differences between HAT and LAT.
  - ✓ The **CP system** shall have a **design life** which as a minimum shall **be equal** to the **design life of the structure**.
  - ✓ In areas with **large tidal zones**, the **surface area up to HAT** shall be considered for CP design.
  - ✓ **Anodes** to be used on a structure shall preferably be of **identical or similar size**.
  - ✓ **Anodes** shall be **located** minimum **1.0 m below LAT** and minimum **1.0 m above the seabed**.
  - ✓ **Anodes** shall be **uniformly distributed**, where reasonable practicable, to avoid interference reducing their current output. In case there are reasons to assume a **significant interaction between anodes**, an analysis by a **computer model should be carried out** to determine a reduction factor for the anode current output.
  - ✓ **Anodes** shall be **located close to complex and critical points** such as node areas, but **not closer than 600 mm to nodes**.

CATHODIC PROTECTION

- **Highlights on ICCP according to DNV**
  - ✓ Adequate **potential distribution shall be confirmed by computer-based modelling** of cathodic protection and utilizing some empirical time dependent relation between the cathodic current density and the protection potential (polarization curve). The **CP modelling shall further demonstrate** that **the number and location of fixed reference electrodes** is adequate to confirm that the structure is protected as required by the design.
  - ✓ The steel surfaces must be protected **without exposing** to more negative potentials than **–1.10 V** rel. Ag/AgCl/seawater, which may otherwise lead to damage of any paint coating and possibly also to hydrogen induced damage to the steel structure.
  - ✓ To this end, impressed current **anodes should be located as far as practical from any structure member** (usually a minimum distance of 1.5 m, but proportional to current magnitude).
  - ✓ **Dielectric shields are used to avoid overprotection close to ICCP anodes** and to facilitate adequate current distribution. In the immediate vicinity of anodes, a prefabricated polymeric sheet is normally applied, whilst a relatively thick layer of a special paint coating is applied as an outer shield.
  - ✓ The electric power capacity shall correspond to a minimum of 150% anode current.
  - ✓ ICCP systems shall be designed for remote control of anode current output based on recordings from fixed reference electrodes. Minimum two reference electrodes per rectifier shall be provided.

CORROSION ALLOWANCE

In cases where corrosion cannot be mitigated at an acceptable level (via cathodic protection or/and a protective coating), an additional metal thickness to the wall is added, the so-called corrosion allowance (CA).

Indicatively for offshore wind turbines, DNV recommends the CA of surfaces of primary structural parts exposed in the splash zone with and without coating shall be calculated as

$$CA = V_{corr}\left(T_d - T_c\right)$$

where V_{corr} is the expected maximum rate, T_c is the design life of the coating as provided by the manufacturer and T_d the design life of the structure. Minimum values for design corrosion rate are given in the following table.

Region	V_{corr} External Surface	V_{corr} Internal Surface
Temperate climate (annual mean surface temperature of seawater ≤ 12ºC)	0.30 mm/yr	0.10 mm/yr
Subtropicial and tropical climate	0.40 mm/yr	0.20 mm/yr

According to DNV the resulting acceptable decrease of the metal thickness should be taken to account on the structures fatigue analysis during the structural design.

PROTECTIVE COATINGS

- **Organic coatings**

Organic coatings are semi-permeable membranes. If applied well on the surface to be protected, **act as a barrier** to oxygen and water and delay corrosion.

However, bulk **corrosion occurs** at the base of existing **holidays, bare patches and pinholes**. The paint does the primary protection, but the cathodic protection reinforces it at the weak spots.

The coating, reducing the exposed area to the corrosive environment, decreases the total current requirement for protection, improves the potential distribution and reduces the interference effects.

In fact, coatings and cathodic protection complement each other. The coatings save current, and the cathodic protection acts complementary at mechanically damaged areas, at weak spots and as the coating degrades with time.

Coating systems may integrate several layers of different types of coatings, however, the compatibility between the coats (layers) must be ensured.

- **Metallic coatings**

Metallic coatings are generally composed by non-ferrous metals, usually zinc, aluminum and its alloys. Non-ferrous metals are more electronegative than carbon steel. These metallic coatings provide protection to steel structures against corrosion by both galvanic action and barrier. Moreover, the metallic coatings protect steel sacrificially at damaged areas or at small pores in the coatings.

The ideal coating system should assure the proper performance of the structure during its service life without requiring structural repairs. The major factors to be considered in the selection of a coating system are: 1) the type of structure and its importance, 2) environmental conditions, 3) service life, 4) required durability, 4) coating performance, and 5) costs including its application and surface preparation.

PROTECTIVE COATINGS

- **Classification of paint coating systems according to EN ISO 12944-5:2007**

Paint Coating Types Classification		Typical Examples	Typical Binders
Irreversible coatings	Air-drying paints (oxidative curing)	–	Epoxy ester Alkyd Urethane alkyd
	Water-borne paints (single pack)	– – –	Polyurethane resins (PU) Acrylic polymers Vinyl polymers
	Chemically curing paints	Epoxy paints (two-pack)	Epoxy Epoxy vinyl/epoxy acrylic Epoxy combinations
		Polyurethane paints (two-pack)	Polyester Acrylic Fluoro resin Polyether Polyurethane combinations
	Moisture-curing paints	– – –	Ethyl silicate (one-pack) Ethyl silicate (two-pack) Polyurethane (one-pack)
Reversible coatings	– – –	– – –	Chlorinated rubber Vinyl chloride copolymers Acrylic polymers

PROTECTIVE COATINGS

- Classification of paint coating systems according to DNV

Category	Coating System	Applied Layers	Total nominal dry film thickness (μm)
I	Epoxy paint coating	One	20
II	Marine paint coating (epoxy, polyurethane or vinyl based)	One or more	250
III	Marine paint coating (epoxy, polyurethane or vinyl based)	Two or more	350

PROTECTIVE COATINGS

- **Coating breakdown factors**

Coatings deteriorate with time due to mechanical damage, erosional effects of waves and current and cleaning operations to remove marine growth.

The coating deterioration is considered in the design of a CP system, introducing the **so-called breakdown factor**, f_c. The factor f_c describes the anticipated reduction in cathodic current density due to the application of an electrically insulating coating. When $f_c = 0$, the coating is considered fully (100%) electrically insulating, i.e., the cathodic current density demand becomes zero. When $f_c = 1$ the coating has no protective properties, and the current density would be the same as for a bare steel surface.

DNV recommends the use of a simple linear model to describe coating deterioration, i.e.,

$$f_c(t) = a + b \cdot t$$

where t (years) is the coating age and a and b are constants depended on coating properties and environment. The constant a stands for an initial coating breakdown factor related mainly to mechanical damage occurring during the installation of the structure, while b represents a coating deterioration rate to take into account the coating ageing and possible small mechanical damage occurring to the coating during the structure life.

Recommended by DNV values of *a* and *b* for coating categories I, II and III

Depth (m)	I	II	III
	$a = 0.10$	$a = 0.05$	$a = 0.02$
0-30	$b = 0.10$	$b = 0.025$	$b = 0.012$
>30	$b = 0.05$	$b = 0.015$	$b = 0.008$

Definition of Cathodic Protection

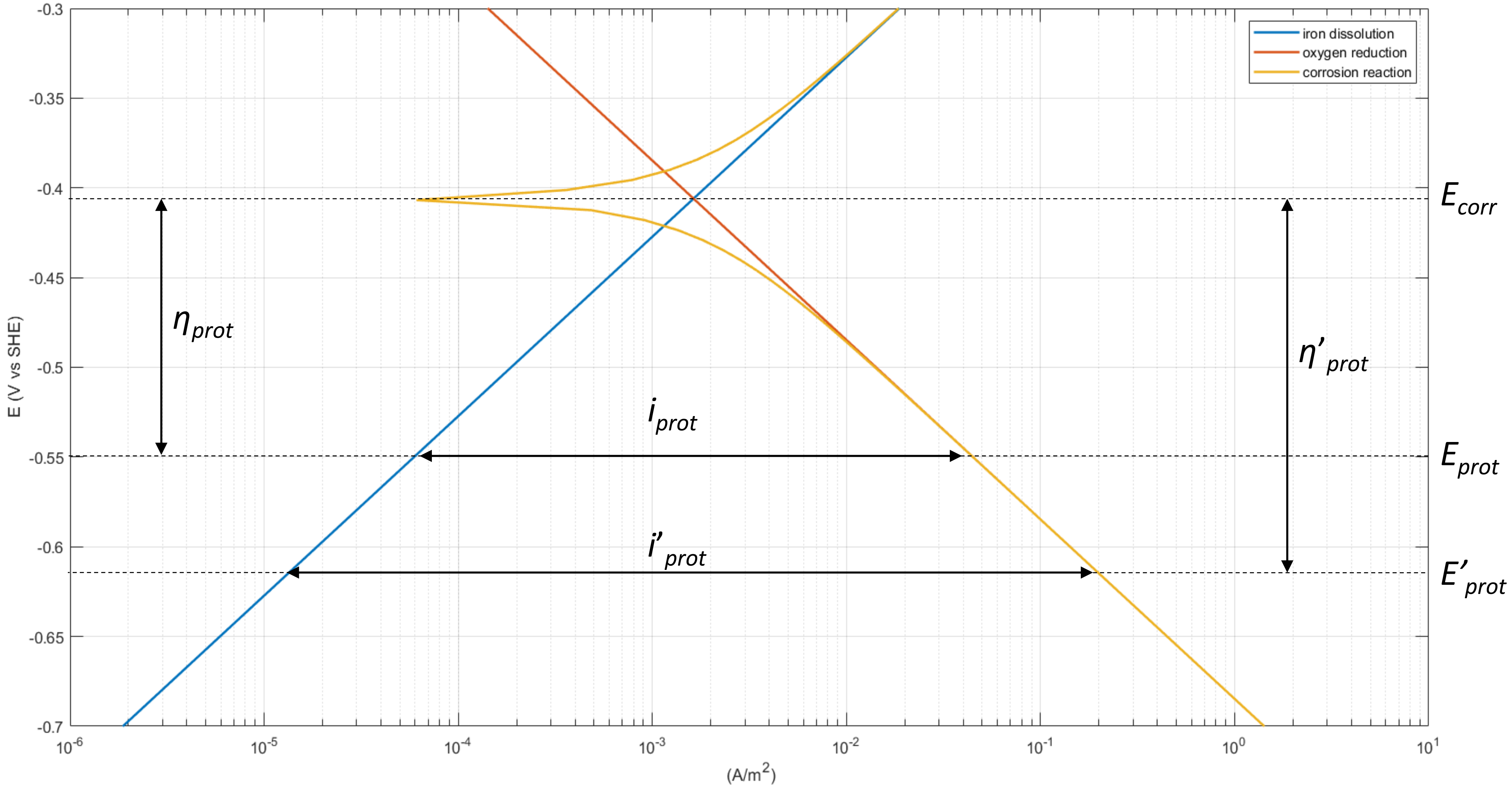

Sacrificial anode cathodic protection (SACP)

- In this method, **the required electrons** to polarize the steel surface to be protected **are provided using another dissimilar metal** immersed in the **same electrolyte**.
- The corresponding **electrodes**, having corrosion potentials E^c_{corr} and E^a_{corr} respectively, **are electrically connected via the electrolyte** and **a metallic connection** and thus, form a **galvanic cell** (close circuit).
- **The initial electromotive force** (emf) to drive the current is the **positive difference (voltage) of the corrosion potentials** E^c_{corr} - E^a_{corr} > 0, with $E^a_{corr} < E^c_{corr}$. I.e., to achieve **positive voltage**, a **more electronegative metal than steel** must be used.
- From an electrochemical point of view, the **more negative electrode** releases electrons to the circuit, dissolves more rapidly than its open circuit equilibrium E^a_{corr}. I.e., **it is sacrificed** and is called that behaves as an **anode**.
- In contrast, **steel** dissolves less, i.e., **it is protected** and acts as a **cathode**.
- To protect steel in seawater **zinc**, **aluminum** or **magnesium** alloys are used as sacrificial anodes.
- They are attached to the steel structure via their steel core, establishing the required metallic connection to transfer the electrons.

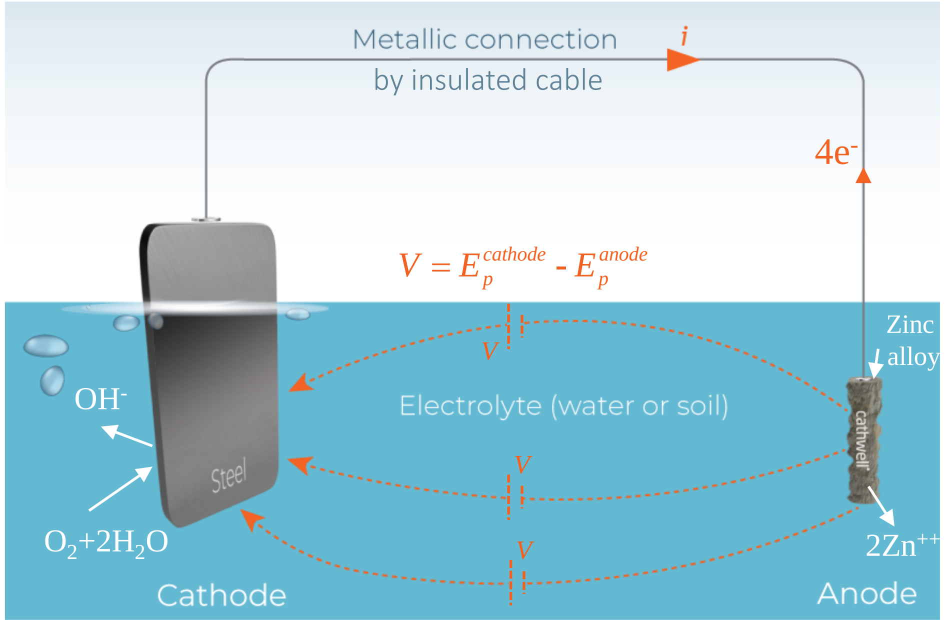

Sacrificial Anodes

Recommended compositional limits for Al-based and Zn-based anode materials (DNV)

Alloying/impurity element	Zn-base	Al-base
Zn	rem.	2.5-5.75
Al	0.10-0.50	rem.
In	na	0.015-0.040
Cd	< 0.07	< 0.002
Si	na	< 0.12
Fe	< 0.005	< 0.09
Cu	< 0.005	< 0.003
Pb	< 0.006	na

Recommended design anode materials properties at seawater (DNV)

Anode material type	Environment	Electrochemical capacity (Ah/kg)	Closed circuit potential (V)
Al-based	seawater	2,000	-1.05
	sediments	1,500	-0.95
Zn-based	seawater	780	-1.00
	sediments	700	-0.95

CATHODIC PROTECION METHODS

❖ Impressed Current cathodic protection (ICCP)

- In this method, **the driving voltage** to polarize the steel surface to be protected is a **direct current (DC) external power source**. Usually, the DC is produced by an altering current transformer rectifier.
- Consequently, there is no need for anodes made by more electronegative metals than steel to be used. Using noble metals for anodes is a significant advantage because these materials do not dissolve on anodic polarization and practically remain unconsumed (inert anodes). The anodic reactions which provide **the required electrons** involve decomposition of the electrolyte compounds, such as:

$$2H_2O \rightarrow O_2 + 4H^+ + 4e^- \quad \text{and} \quad 2Cl^- \rightarrow Cl_2 + 2e^-$$

- Inert anodes are usually made of graphite, thin coatings of platinum, etc.
- The metallic connection must be performed in the right direction, i.e., the **positive pole** of the external power is connected **to the anode**, while its **negative pole** is attached **to the structure**.
- In an **ICCP system**, since the driving voltage can be significantly larger than in an SACP one, **a few anodes are enough** to protect large uncoated surfaces, even if they are embedded in high resistivity electrolytes.
- A **dielectric shield** should usually be applied **in the vicinity of the anodes** to prevent extremely high current densities and **avoid undesired over-polarization** (will be explained later). Dielectric shield materials include epoxy materials, coal-tar epoxy resins, polyurethane coatings, rubber coatings, etc.
- Furthermore, potential sensors (**reference electrodes**) are used, **adjusting the delivered current automatically** to achieve the desired predefined protection potential.

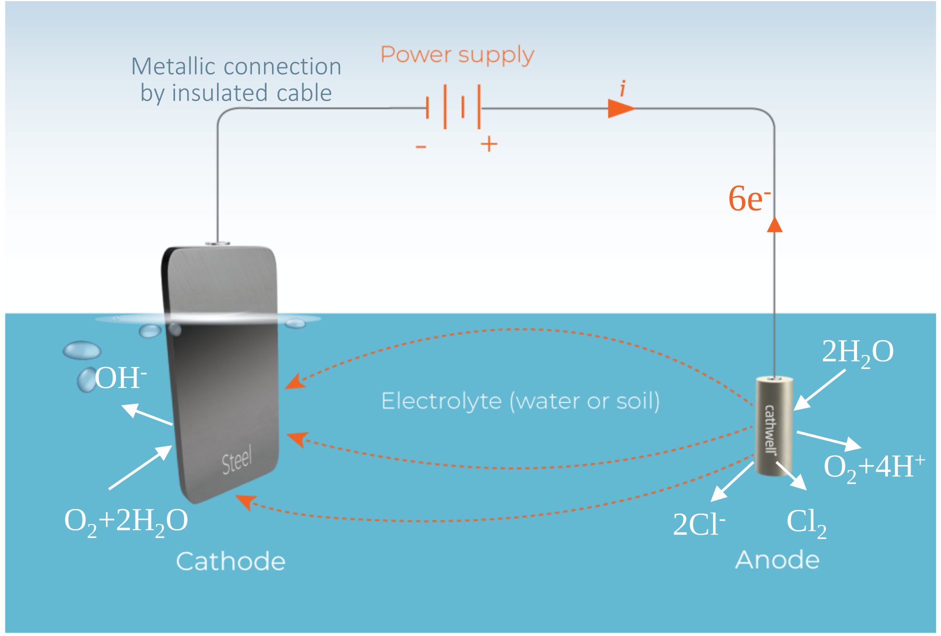

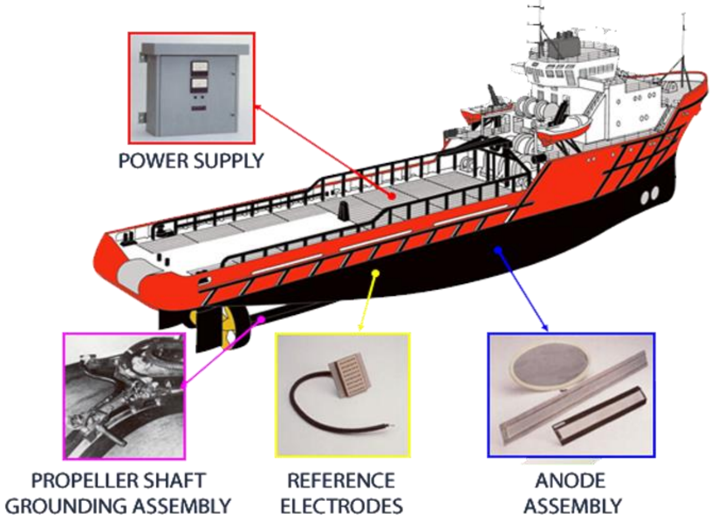

CATHODIC PROTECION SYSTEMS

- **SACP vs. ICCP systems**

Sacrificial Anode Cathodic Protection (SACP)	Advantages	Disadvantages
	No need for external power source	Current output is limited. It has limited driving potential
	Less complex installation	
	Uniform distribution of current	Poorly coated structures need more anodes
	Minimum maintenance	
	Minimum cathodic interference	The system is ineffective in high resistivity environments

Impressed Current Cathodic Protection (ICCP)	Advantages	Disadvantages
	The system is adjustable	Overprotection leads to coating damage and hydrogen embrittlement
	High current can be impressed with a single ground bed	
	Single installation can protect larger metallic surface	The system is affected by interference problems
	Uncoated and poorly coated structures can be effectively protected	
	Voltage and current can be varied to meet changing conditions over time	External power is necessary, thus the system is vulnerable to power failure

REFERENCE ELECTRODES

To measure the potential of an electrode (structure/electrolyte potential), a second electrode, with defined and reproducible potential with respect to its electrolyte (a so-called reference electrode) must be used.

The reference electrodes most used for marine CP systems are Silver/Silver chloride/seawater (Ag/AgCl/seawater) and Zinc/seawater. The latter is cheaper, but the former is more accurate.

The potentials of various reference electrodes with respect to standard hydrogen electrode (SHE or NHE) at 25°C are given in the following table.

Electrode	Potential shift (Volt)
Silver/silver chloride/saturated KCl	+0.20
Silver/silver chloride/seawater	**+0.25**
Calomel (normal KCl)	+0.28
Calomel (saturated KCl)	+0.24
Zinc/seawater	-0.78

Silver/silver chloride reference electrode

Zinc reference electrode

PROTECTION CRITERIA

- **Steel**

  - ***Minimum negative potential level***

As already mentioned, the corrosion is completely stopped at a steel surface, decreasing the potential from E_{corr} to E_a by providing external current. However, to achieve this, an excessive amount of current is required, which is not practical from an economic point of view. Experiments and experience have shown that when **carbon steel in aerated sea water** is polarized up to **-0.80V (Ag/AgCl/sw RE)**, the corrosion rate decreases to an acceptable level. Consequently, this is the general the minimum negative potential level used for the cathodic protection of carbon steel in aerated sea water.

In case of steel in **anaerobic conditions** (e.g. some seabed muds), due to the possibility of microbially-assisted corrosion, the accepted minimum negative potential level is **-0.90V (Ag/AgCl/sw RE).**

  - ***Maximum negative potential level – Over-protection***

Excessive polarization of steel (to values below E_a) energies a second cathodic reaction. This is the **electrolysis of water** that produces hydrogen gas:

$$2H_2O + 2e^- \rightarrow 2OH^- + H_2$$

Beyond the current waste, this situation (so-called **over-protection**) can be highly damaging because the hydrogen gas generation may disrupt the protective calcareous deposits (see slide 20). Furthermore, it can cause delamination of the coating/paint and embrittlement of the steel, especially in the case of high strength steel (yield strengths >700MPa).

For **mild steel**, a maximum negative potential limit of **-1.1V (Ag/AgCl/sw RE)** is generally accepted, while for **high strength steels**, due to the risk of hydrogen embrittlement, this limit is lower, equal to **-0.95V (Ag/AgCl/sw RE)**.

PROTECTION CRITERIA

- **Recommended potentials for the cathodic protection of various metals in seawater (BS EN)**

Material	Minimum negative potential (Volt vs Ag/AgCl/seawater)	Maximum negative potential (Volt vs Ag/AgCl/seawater)
Iron and steel		
Aerobic environment	-0,80	-1,10
Anaerobic environment	-0,90	-1,10
High strength steels	-0,80	-0,95[1]
Aluminum alloys (Al Mg & Al Mg Si)	-0,80 (negative potential swing 0,10 V)	-1,10
Stainless steel Austenitic steel		
(PREN[2] ≥ 40)	-0,30	no limit
(PREN < 40)	-0,60	no limit
Duplex	-0,60	High negative potential should be avoided
Copper alloys		
Without aluminum	-0,45 to -0,60	no limit
With aluminum	-0,45 to -0,60	-1,10
Nickel base alloys	-0,20	High negative potential should be avoided

Notes: 1) For high strength steel susceptible to hydrogen assisted cracking the limit is -0.83V vs Ag/AgCl/seawater.
2) PREN = Cr%+3.3Mo%+16%N

ENVIROMENTAL FACTORS ON CURRENT DEMAND

The current required to achieve the recommended potentials for cathodic protection depends on several environmental factors.

- **Dissolved oxygen**

As already mentioned, the dissolved oxygen in the electrolyte is correlated with the corrosion rate. Consequently, the required current density for protection is proportional to the rate of dissolved oxygen that diffuses to the steel surface. The dissolved **oxygen concentration** in seawater **decreases** as **water depth**, **temperature** and **salinity increase**.

Furthermore, **sea currents and waves increase** the transfer rate of the dissolved oxygen to the steel surface and, thus, the **current density requirement** for cathodic protection.

- **Calcareous deposits**

When the cathodic protection is applied, the anodic reaction rate is lower, but the cathodic one remains energized. Thus, an excess amount of hydroxyl ions is produced at the steel surface. This high concentration of hydroxyl ions triggers a few other reactions, the products of which are calcium carbonate ($CaCO_3$) and magnesium hydroxide ($Mg(OH)_2$).

Both products are insoluble and **form a protective film** at the steel surface, known as **calcareous deposit**, which acts as a paint coating.

Thus, after a high initial temporary current density requirement for a rapid cathodic polarization to form a high protective the calcareous film, a significant decrease in demand is observed.

Note that **mechanical damage** (e.g., during a storm) or **excessive hydrogen** generation may **damage the film**. Thus, the cathodic protection system at any time, even at the end of its design life, must be capable of delivering increased current to depolarize the steel surface and reform the calcareous deposit. The above-mentioned current demands, the first for the initial polarization, the second since the calcareous deposit is formed, and the third for the repolarization after a damage of the film, are referred to standards and recommendations as **initial**, **maintenance or mean** and **final**, respectively.

CURRENT DEMANDS FOR DESIGN CP SYSTEMS

Recommended by **DNV** initial, mean and final design current densities (A/m^2) for seawater exposed bare steel metal surfaces as a function of depth and climatic region based on surface water temperature

Depth (m)	Tropical (> 20 °C)			Sub-tropical (12- 20 °C)			Temperate (7-11 °C)			Arctic (< 7 °C)		
	initial	mean	final	initial	mean	Final	initial	mean	final	initial	mean	Final
0-30	0.150	0.070	0.100	0.170	0.080	0.110	0.200	0.100	0.130	0.250	0.120	0.170
>30-100	0.120	0.060	0.080	0.140	0.070	0.090	0.170	0.080	0.110	0.200	0.100	0.130
>100-300	0.140	0.070	0.090	0.160	0.080	0.110	0.190	0.090	0.140	0.220	0.110	0.170
>300	0.180	0.090	0.130	0.200	0.100	0.150	0.220	0.110	0.170	0.220	0.110	0.170

Recommended by **NACE** initial, mean and final design current densities (mA/m^2) for seawater exposed bare steel metal surfaces for various productive areas

Production Area	Water Resistivity (ohm-cm)	Water Temp. (°C)	Wave Action	Lateral Water Flow	Current density demand (mA/m^2)			Slope ohm-m^2
					Initial	Mean	Final	
Gulf of Mexico	20	22	Moderate	Moderate	110	55	75	4.1
U.S. West Coast	24	15	Moderate	Moderate	150	90	100	3.0
Cook Inlet	50	2	Low	High	430	380	380	1.0
Northern North Sea	26 to 33	0 to 12	High	Moderate	180	90	120	2.5
Southern North Sea	26 to 33	0 to 12	High	Moderate	150	90	100	3.0
Arabian Gulf	15	30	Moderate	Low	130	65	90	3.5
Australia	23 to 30	12 to 18	High	Moderate	130	90	90	3.5
Brazil	20	15 to 20	Moderate	High	180	65	90	2.5
West Africa	20 to 30	5 to 21	Low	Low	130	65	90	3.5
Indonesia	19	24	Moderate	Moderate	110	55	75	4.1
South China Sea	18	30	Low	Low	100	35	35	

CORROSION RATE ALONG DEPTH

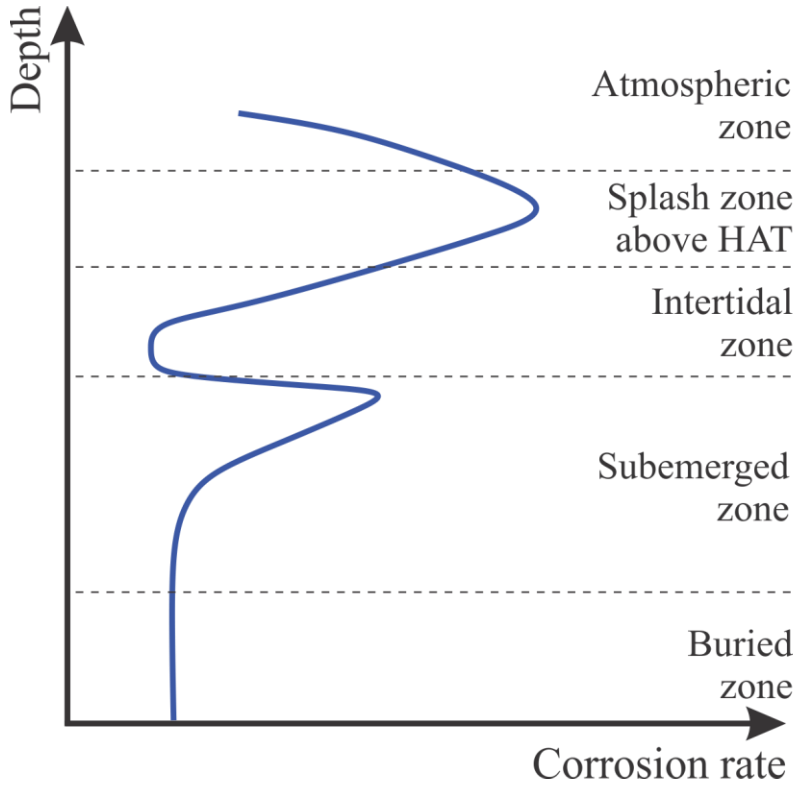

Environmental zone	Corrosion rate (mm/y)
Atmospheric zone	0.050-0.075
Splash zone above high tide	0.20-0.40
Splash zone below high tide (Intertidal zone)	0.05-0.25
Submerged zone	0.10-0.20
Buried in soil	0.06-0.10

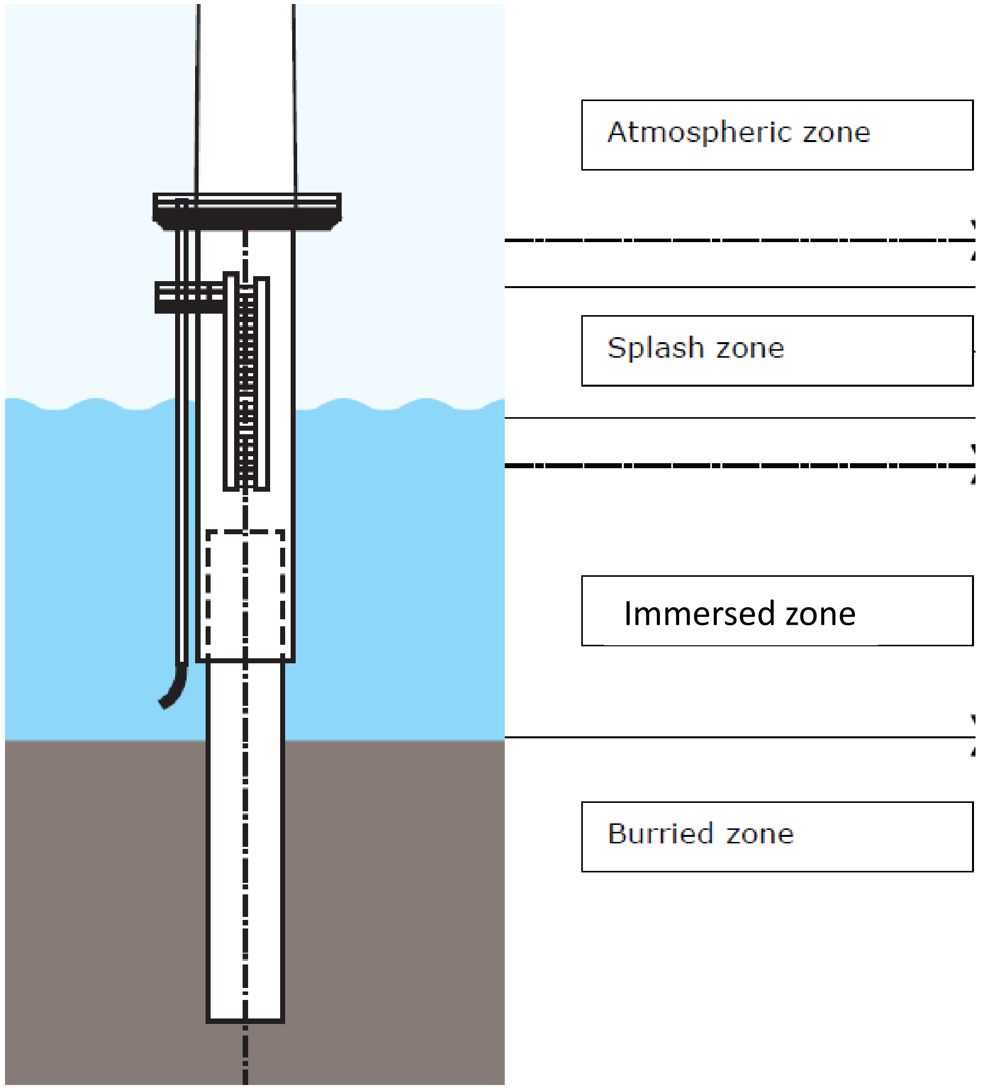

MODELLING FOR THE DESIGN CP SYSTEMS

- Mathematical formulation of a CP problem

Governing Equations

$$\nabla^2 \varphi = 0$$

$$i = \mathbf{n} \cdot \mathbf{J} = -\sigma \, \mathbf{n} \cdot \nabla \varphi = -\sigma \, \partial_n \varphi$$

Boundary conditions

$$i(\mathbf{x}) = -\sigma \, \partial_n \varphi(\mathbf{x}) = 0 \ , \quad \mathbf{x} \in S_\infty \cup S_p$$

Insulated and fictitious boundaries

$$i_c(\mathbf{x}) = f\left(\varphi_c(\mathbf{x})\right), \mathbf{x} \in S_c$$

cathode

$$\left.\begin{array}{c} \varphi_a(x) = \varphi_0 \\ \text{or} \\ i_a(x) = g\left(\varphi_a(x)\right) \end{array}\right\} x \in S_{as}$$

sacrificial anode

$$i_a(\mathbf{x}) = -\sigma \, \partial_n \varphi(\mathbf{x}) = i_0 \ , \quad \mathbf{x} \in S_{ai}$$

impressed anode

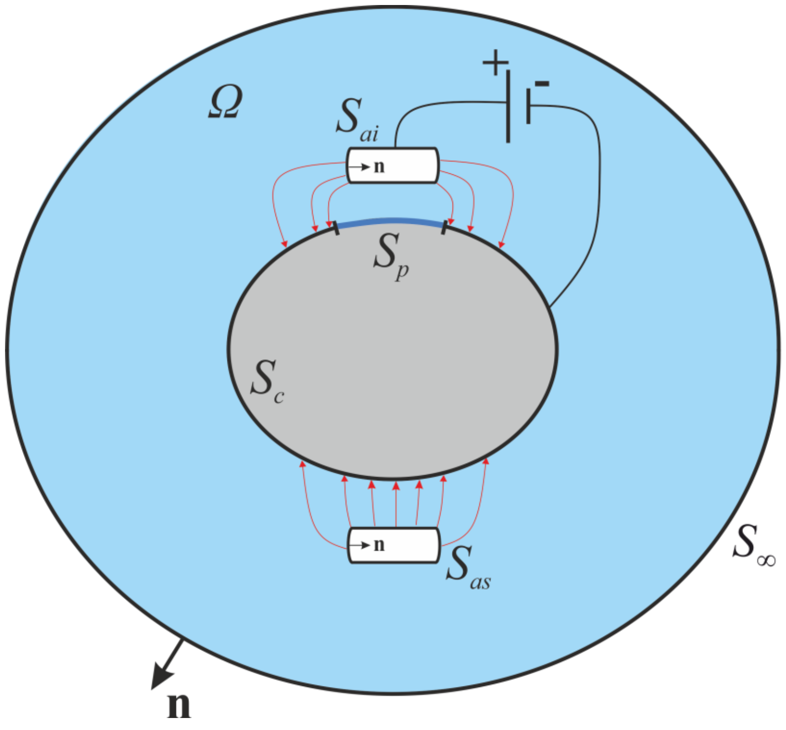

Numerical Methods for solving Cathodic Protection Problems

__FEM__

- ✓ Fast computations
- X Lack of accuracy in the solution of the current density in geometries with corners and curvature.

__BEM__

- ✓ High accuracy
- X Costly computations and high computer memory demand.

__FVM__

- ✓ Fast computations
- X Lack of accuracy in the solution due to inability to handle properly the robin boundary conditions of the polarization curve.

__ACA/BEM__ (Gortsas et.al. , 2021)

- ✓ High accuracy
- ✓ Fast computations and efficient computer memory demand handling.

Calcareous Deposits

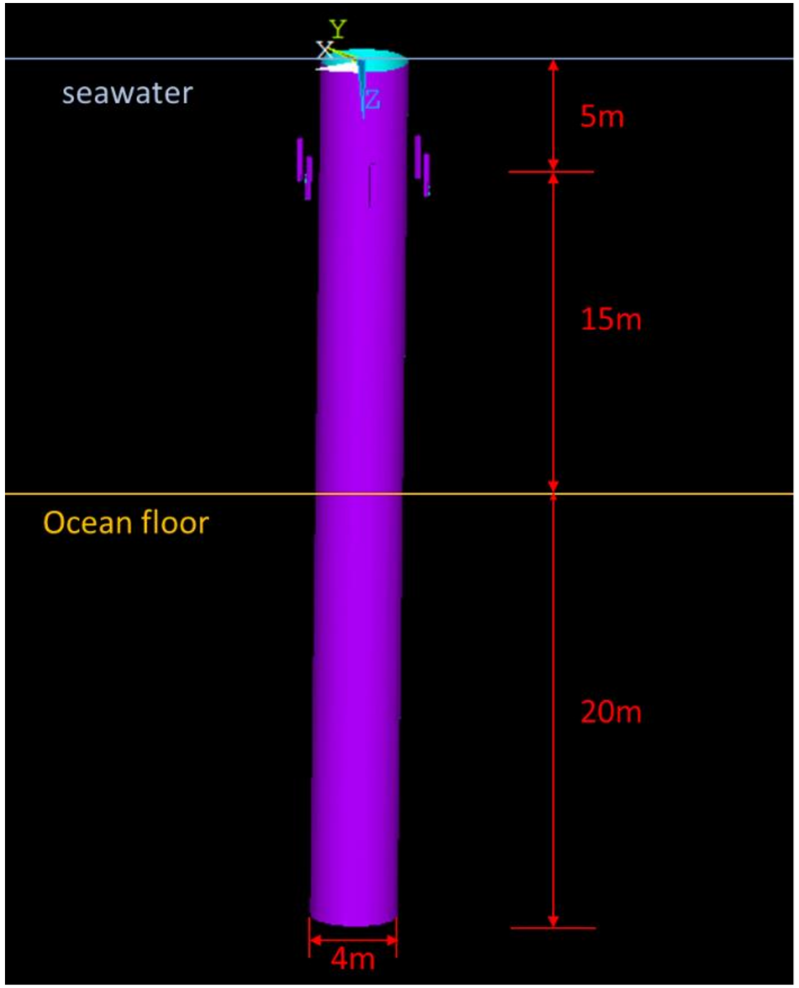

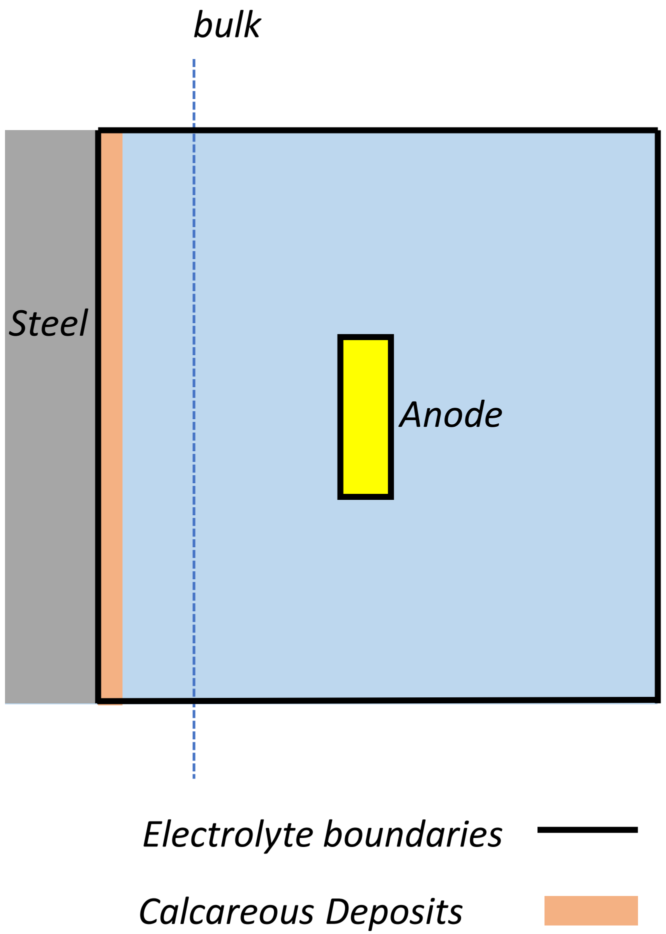

Calcareous Deposits

- *The formed compact calcareous deposits act as a physical barrier impede oxygen diffusion, and thus the current density of the steel decreases with the increase of time.*

- The mechanism for the formation of calcareous deposits is:

$$Mg^{2+} + 2OH^{-} \rightarrow Mg(OH)_2$$

$$HCO_3^{-} + OH^{-} \leftrightarrow H_2O + CO_3^{2-}$$

$$Ca^{2+} + CO_3^{2-} \rightarrow CaCO_3$$

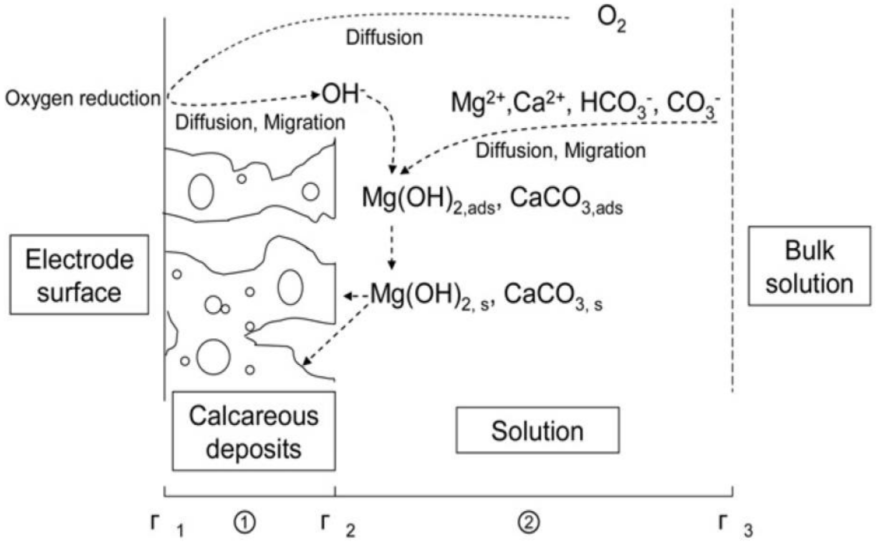

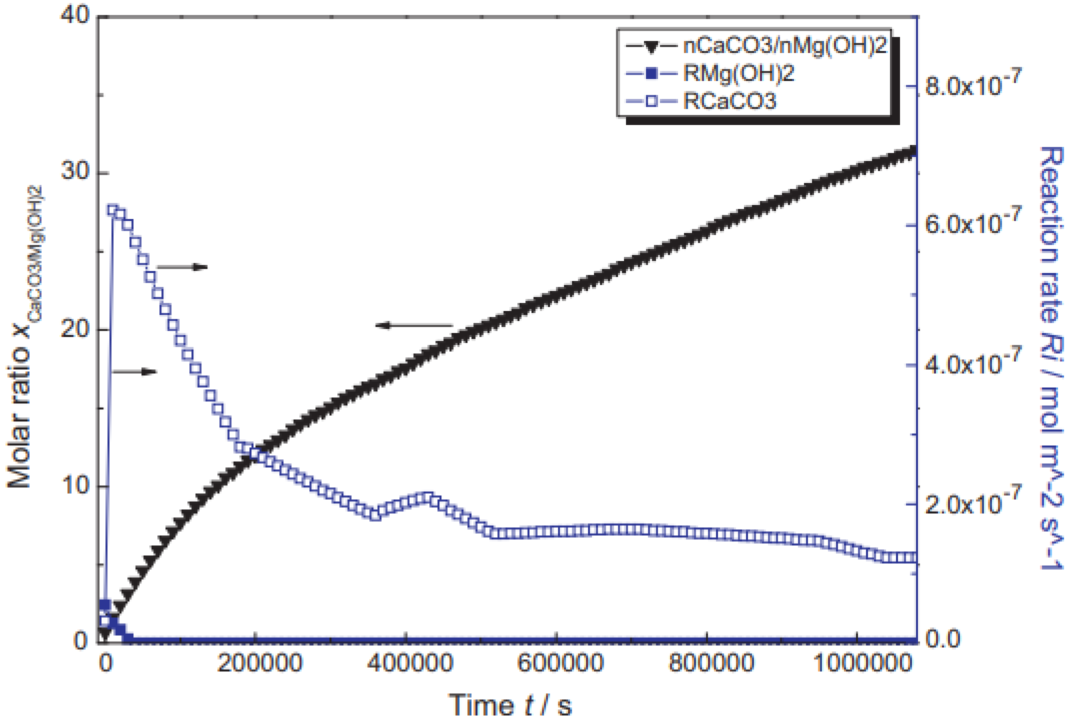

Sun, W., Liu, G., Wang, L., & Li, Y. (2012). A mathematical model for modeling the formation of calcareous deposits on cathodically protected steel in seawater. Electrochimica Acta, 78, 597–608.

Calcareous Deposits

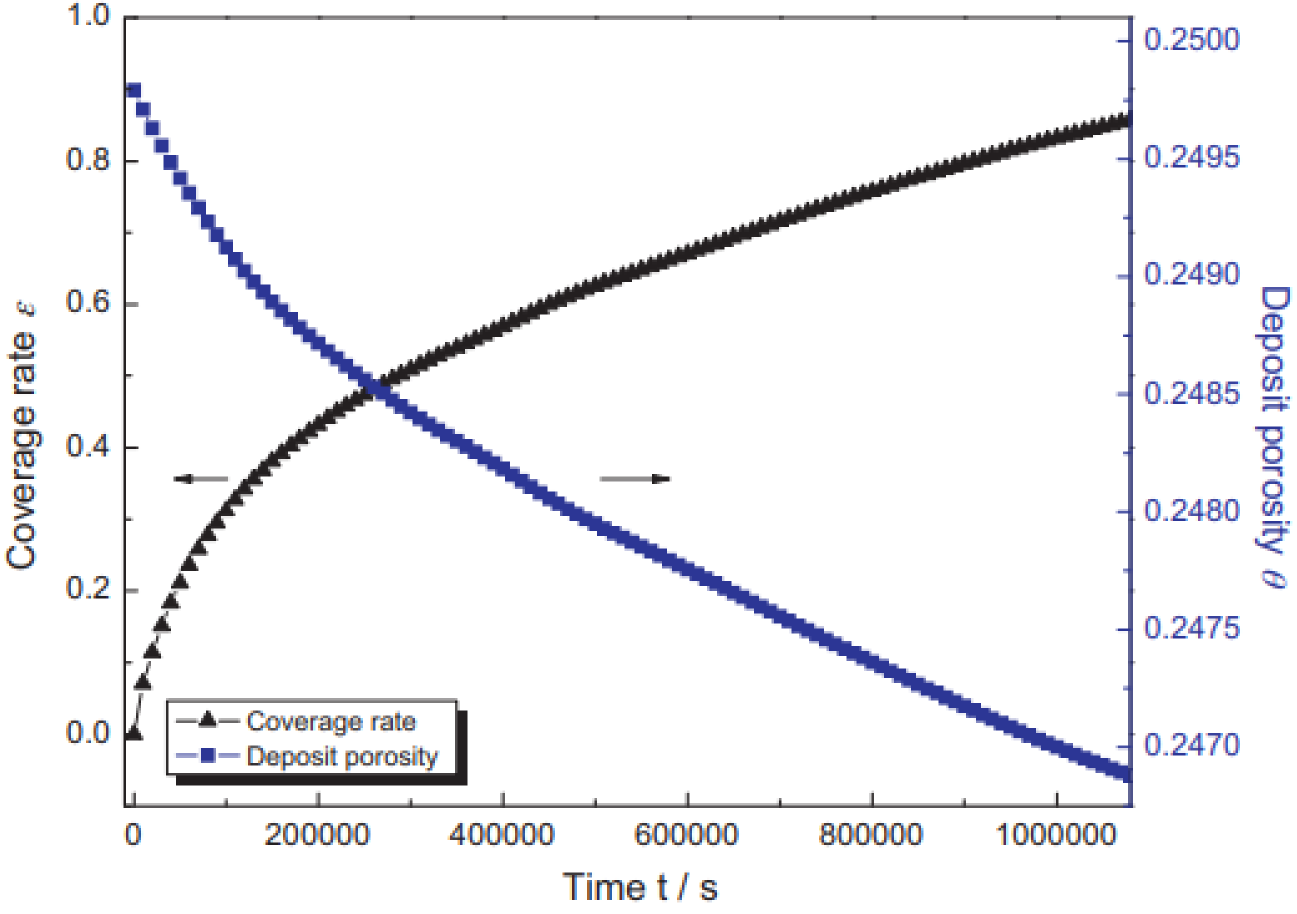

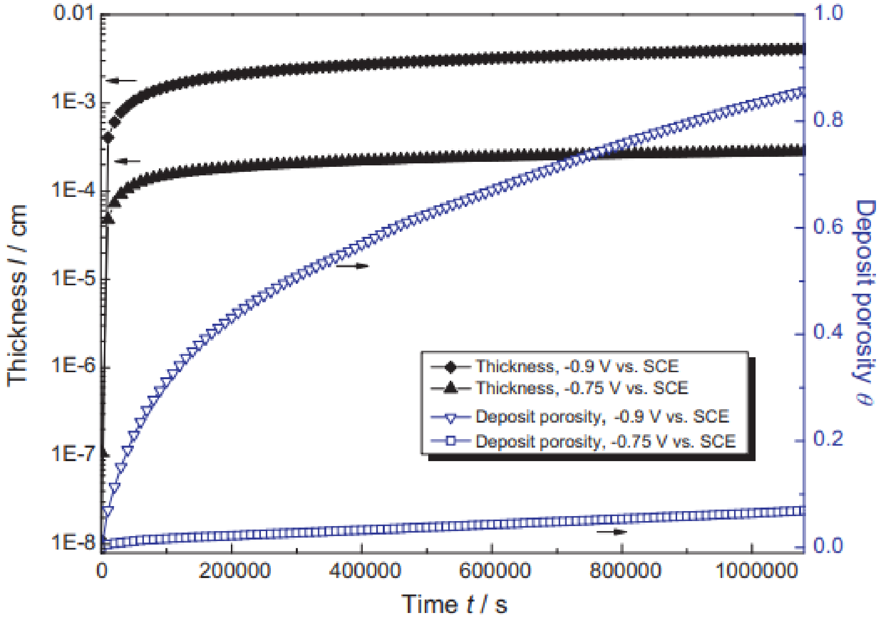

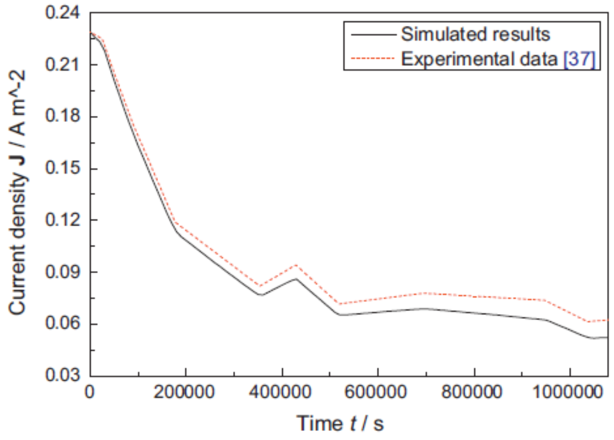

Sun, W., Liu, G., Wang, L., & Li, Y. (2012). A mathematical model for modeling the formation of calcareous deposits on cathodically protected steel in seawater. Electrochimica Acta, 78, 597–608.

Calcareous Deposits

FEA utilizing COMSOL Multiphysics

Potential

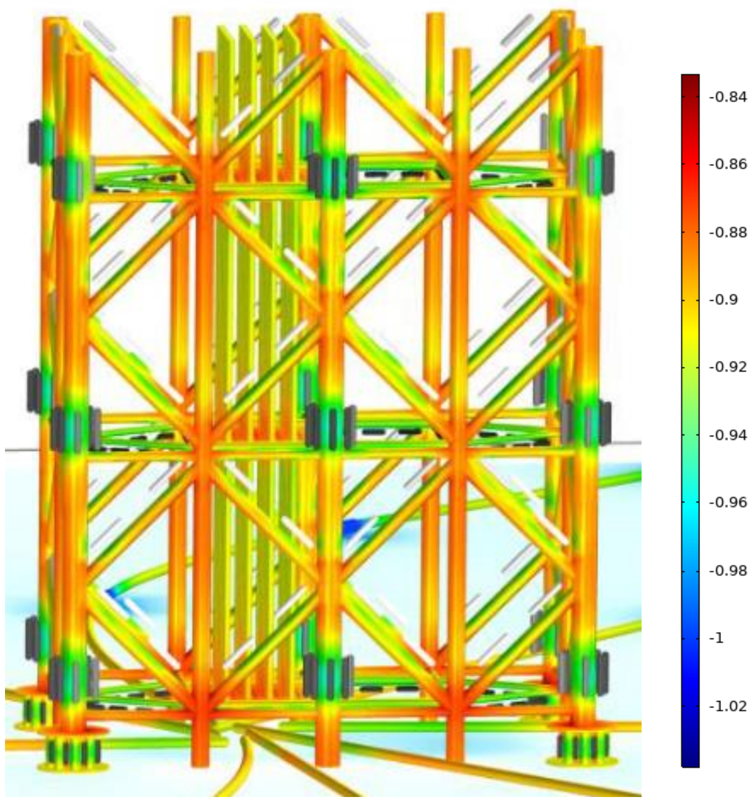

Thickness

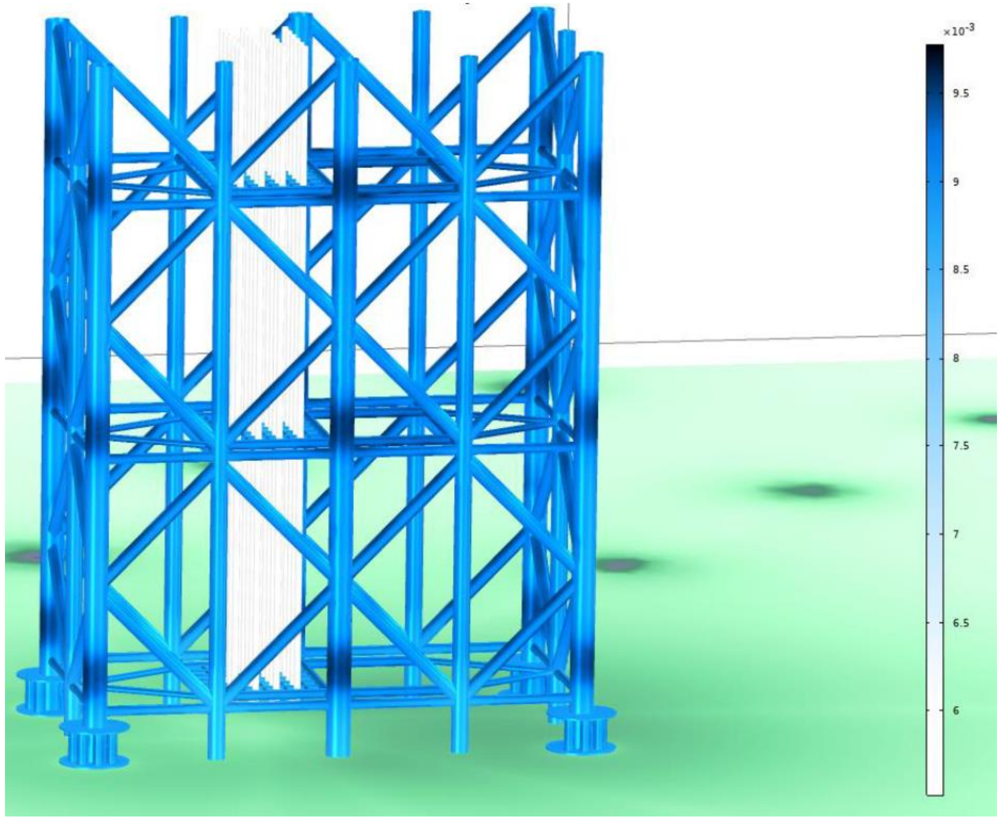

CASE STUDY:
PRELIMINARY DESIGN OF A SACP SYSTEM FOR A MONOPILE

- **Data and design criteria according to DNV**

Geometry	
Wall:	Pipe Pile
Diameter (m) D =	1.3
Coating	
Total thickness (μm):	350
DNV Category:	III
Coating Break down factor constants	
a =	0.02
b =	0.012
Design Life	
Design Life (yrs) t_f =	35
Protection Potential (V vs Ag/AgCl/sw)	
Seawater E^c_{sw} =	-0.8
Mud E^c_{mu}=	-0.9
Conductivity σ (S/m)	
Seawater σ_{sw} =	4.5
Mud σ_{cm}=	1.0

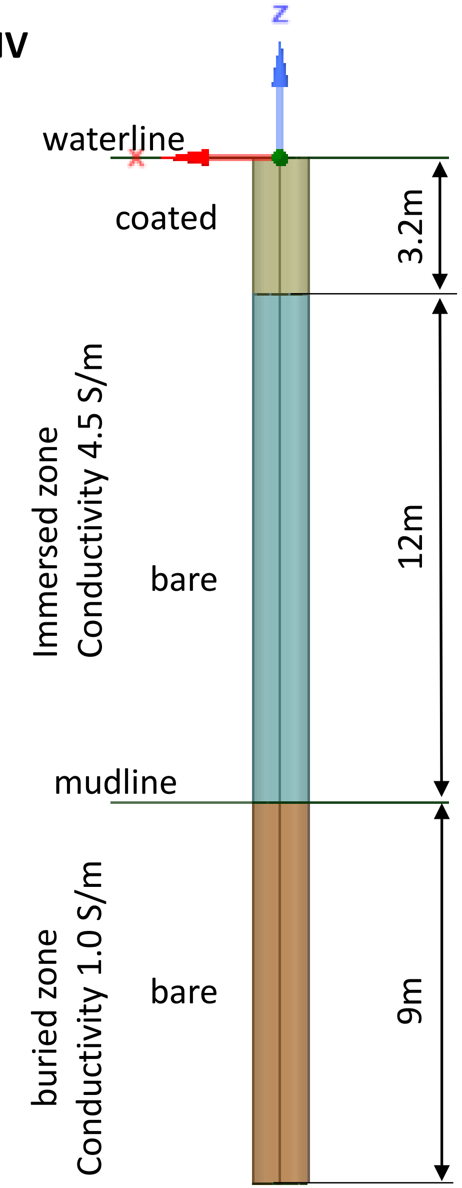

Protection Current Density (mA/m^2) for bare metal			
Region:	Tropical		
Depth (m):	0-30		
Increment (%) for seawater currents:	50%		
	Tidal Zone (Coated)	Immersed Zone (Uncoated)	Buried Zone (Uncoated)
Initial i_{ci} =	225	150	25
Mean i_{cm} =	70	70	20
Final i_{cf} =	100	100	20

Anodes	
Material:	Aluminum Alloy
Alloy Density (kg/m^3) ρ =	2750
Electrochemical Capacity (Ah/kg) ε =	2500
Closed circuit potential (V vs Ag/AgCl/sw) E_a =	-1.05
Length (m) L =	1.21
Section:	Square
Side (m) a =	0.25
Utilization factor ($L \geq 4r$) u =	0.9
Distance (mm) from wall :	300

CASE STUDY:
PRELIMINARY DESIGN OF A SACP SYSTEM FOR A MONOPILE

The used artificial polarization curves to fulfil the design criteria of DNV are shown in the following figure.

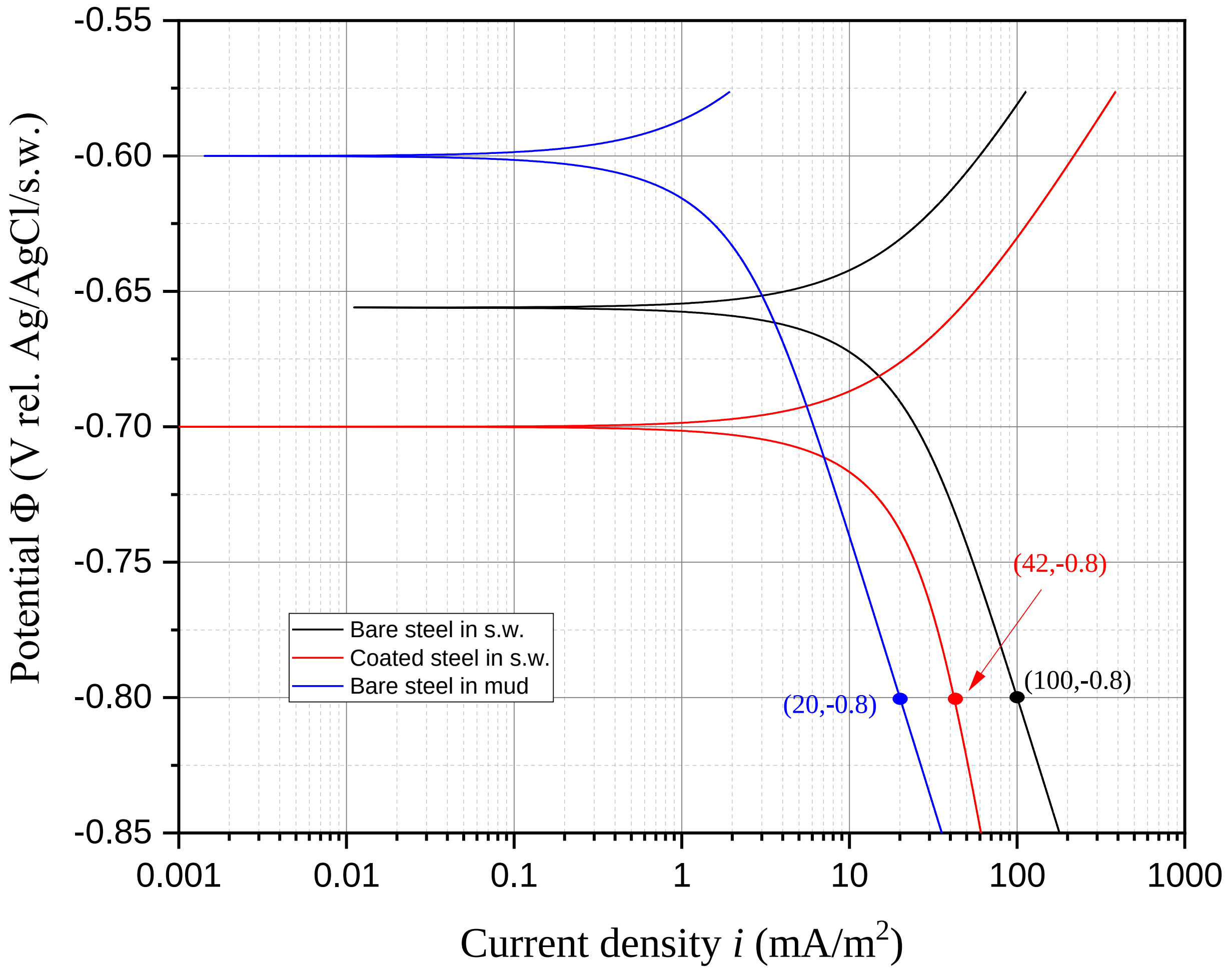

CASE STUDY:
PRELIMINARY DESIGN OF A SACP SYSTEM FOR A MONOPILE

ACA/BEM analysis utilizing PITHIA CP

Four (4) anodes (1.21x0.3x0.3) placed at z=-12m

t = 0 **t = 39 years**

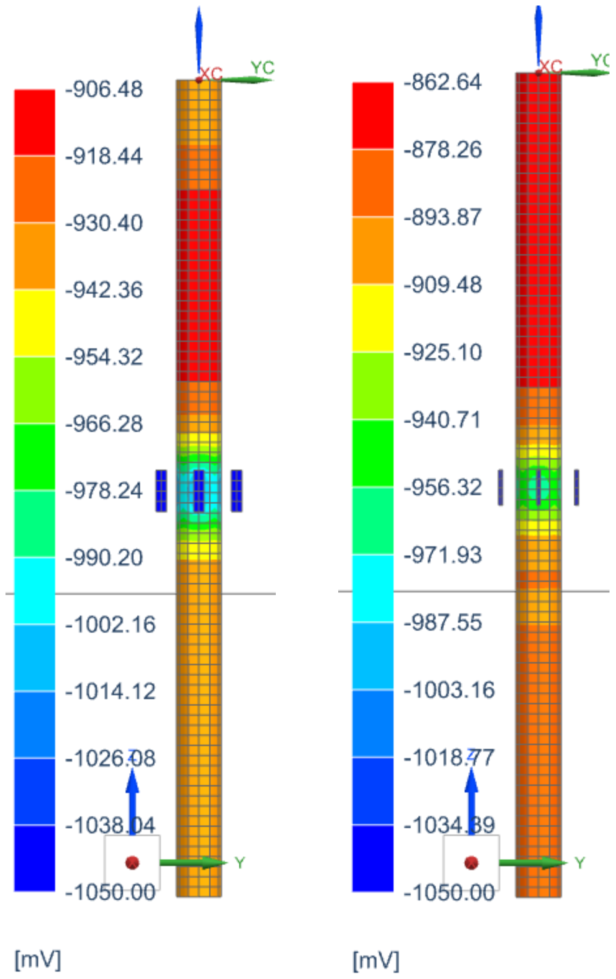

SERVICE LIFE: 39 years

t = 0 **t = 39 years**

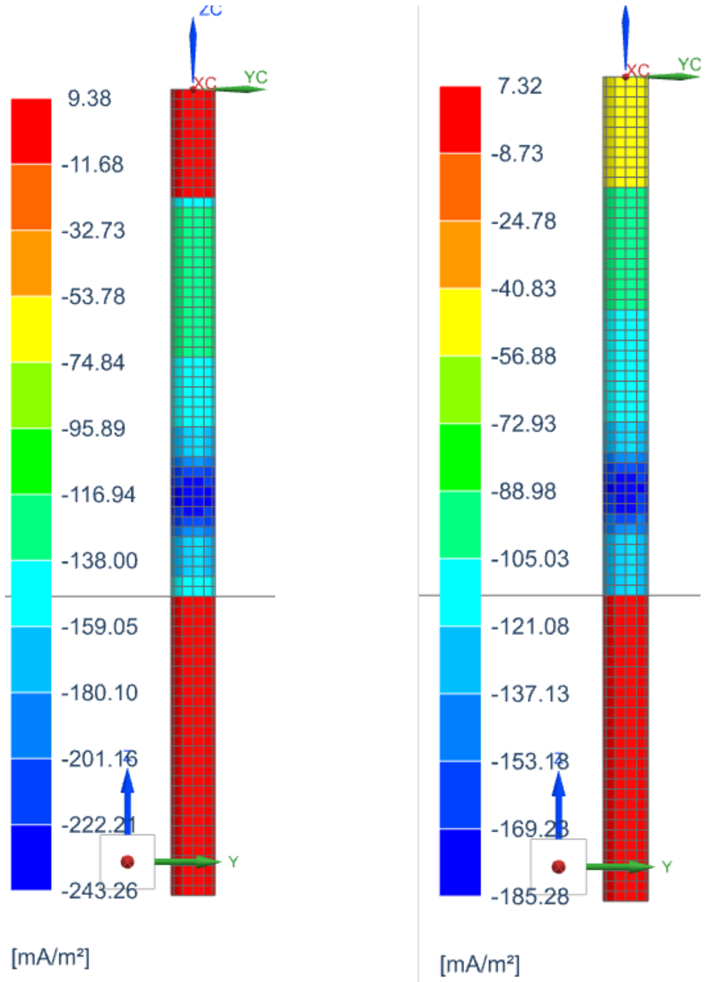

Case Study:
Anodes Current and Consumption Rate

ACA/BEM analysis utilizing PITHIA CP

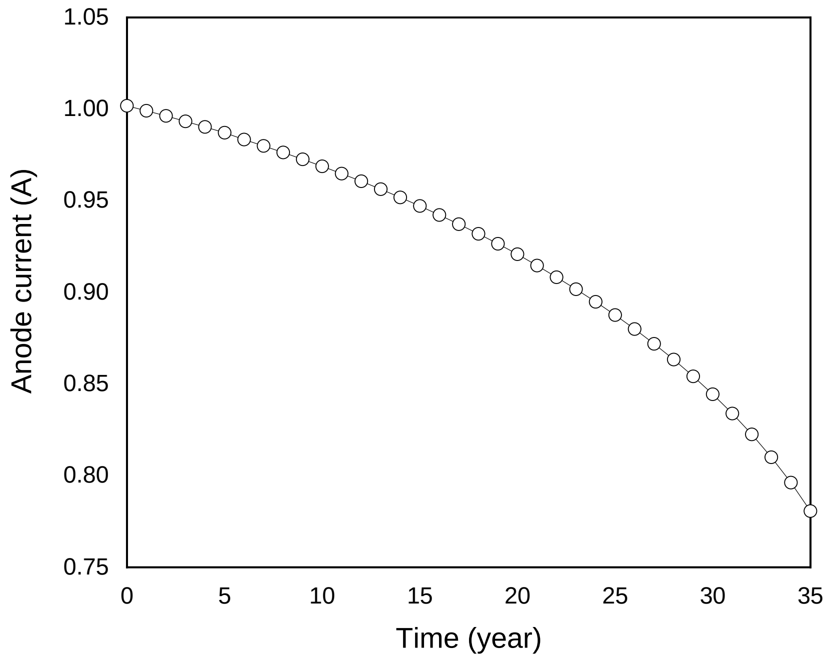

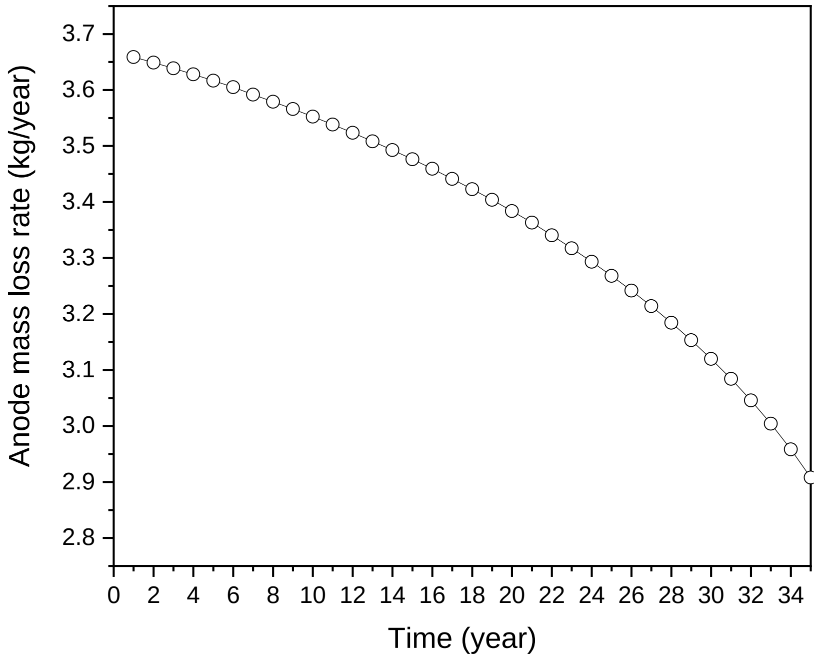

t = 0

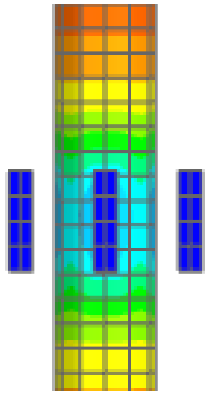

t = 39 years

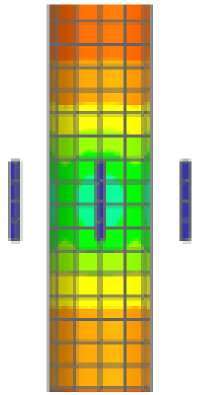

Optimization of CP systems

The design of a CP system is a multiparametric process. During the design process engineers often should define the anodes:

- *number*
- *position*
- *Size*
- *Impressed current density*

Consequently, the design of a CP is a ***multi-objective*** *optimization problem!*

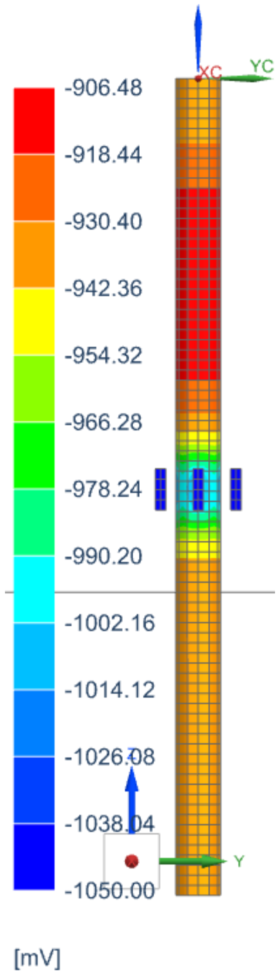

Methods for Optimization of Cathodic Protection Problems

SOP Methods

1. EA algorithms such as GA and SA
2. Methods of the Pattern Search family such as GPS and MADS with its LTMADS and ORTHOMADS instances
3. Swarm intelligence such as PSO
4. Machine Learning

MOP Methods

1. Elitist EA algorithms such as NSGA-II SPEA2 and PAES with their controlled elitist instances
2. Methods of the Pattern Search family such as DMS and DMulti – MADS
3. Machine Learning

Combined with various and flexible constraint handling techniques.

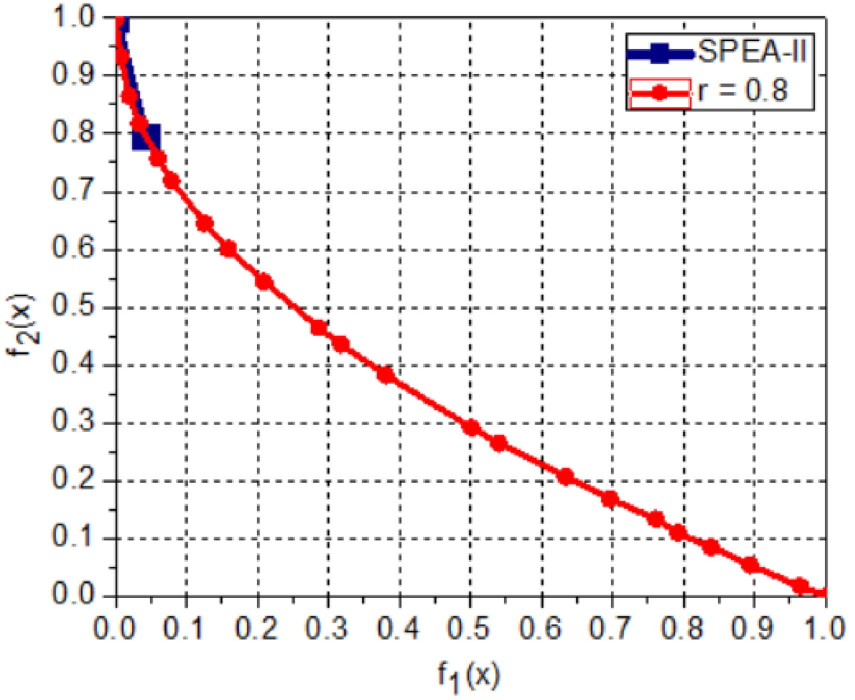

Optimal design of the SACP of a wind turbine Jacket

ACA/BEM analysis utilizing PITHIA CP

Parameters

26 anodes mounted at a distance of 0.35m from the jacket.

Unknowns

- *Anode size*
- *Anode position*

Results

- *Anodes of dimensions 1X0.12X0.12 m*
- *One anode located in $L/2$ short bars*
- *Two anodes in the long and thin bars located in $H/4$ and $3H/4$*
- *Two anodes in the long bars located in $S/5$ and $3S/5$*

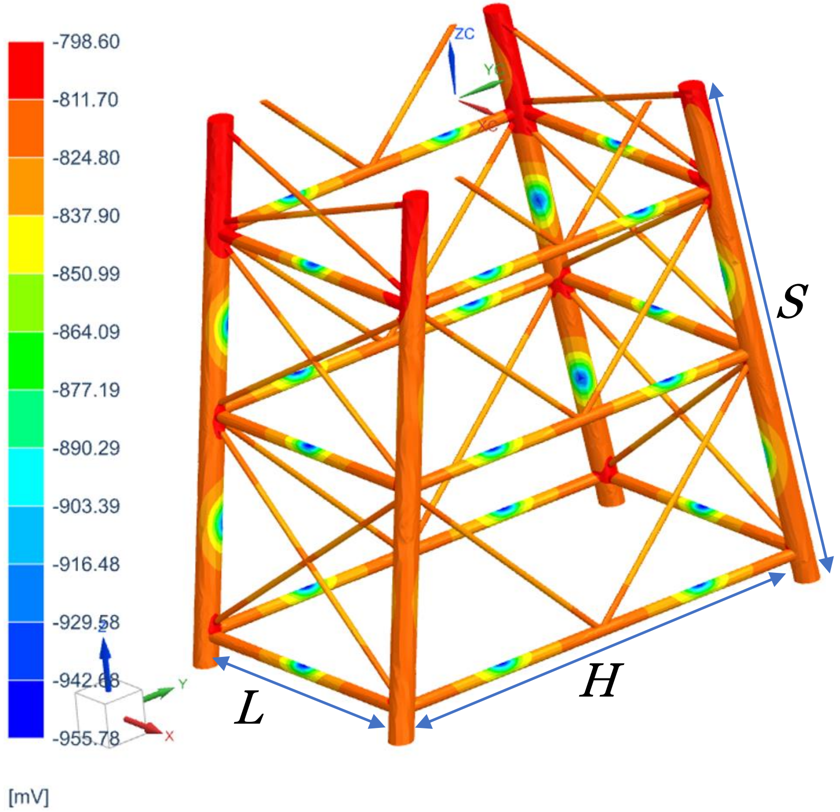

References

1. Popov, B.N., 2015. Corrosion Engineering Principles and Solved Problems. Elsevier, Amsterdam.
2. Rodopoulos, D.C., Gortsas T.V., Tsinopoulos, S. V., Polyzos, D., 2019. ACA/BEM for solving large-scale cathodic protection problems. Eng. Anal. Bound. Elem. 106, 139-148. https://doi.org/10.1016/j.enganabound.2019.05.011.
3. Kalovelonis, D.T., Rodopoulos, D.C., Gortsas, T.V., Tsinopoulos, S.V., Polyzos, D., 2020. Cathodic protection of a container ship using a detailed BEM model. J. Mar. Sci. Eng. 8, 359-373. https://doi.org/10.3390/jmse8050359.
4. Gortsas, T.V., Tsinopoulos, S.V., Polyzos., 2021. An accelerated boundary element method via cross approximation of integral kernels for large-scale cathodic protection problems. ComputAided Civ Inf. 1-16. https://doi.org/10.1111/mice.12687
5. Kalovelonis, D. T., Gortsas, T. v, Tsinopoulos, S. v, & Polyzos, D. (2022). Accelerated boundary element method for direct current interference of cathodic protections systems. Ocean Engineering, 258, 111705. https://doi.org/https://doi.org/10.1016/j.oceaneng.2022.111705
6. Siemens Digital Industries Software. Simcenter STAR-CCM+, version 2022.1, Siemens 2022.
7. Macdonald, D.D., Qiu, J., Zhu, Y., Yang, J., Engelhardt, G.R., Sagüés, A., 2020. Corrosion of rebar in concrete. Part I: Calculation of the corrosion potential in the passive state, Cor.Sci. 177, 109018. https://doi.org/10.1016/j.corsci.2020.109018.
8. COMSOL Multiphysics® v. 5.6. www.comsol.com. COMSOL AB, Stockholm, Sweden.
9. Revie, R.W., Uhlig, H.H., 2008. Corrosion and corrosion: control an introduction to corrosion science and engineering. John Wiley & Sons
10. Newman, J., Thomas-Alyea, K.E., 2004. Electrochemical Systems. third ed. John Wiley & Sons, New Jersey.
11. King, P., Uhlig, H. , J. Phys. Chem, 63 , 2026 (1959)

References

12. Macdonald, D.D., Zhu, Y., Yang, J., Qiu, J., Engelhardt, G.R., Sagüés, A., Sun, L., Xiong, Z., 2021. Corrosion of rebar in concrete. Part IV. On the theoretical basis of the chloride threshold, Cor. Sci. 185, 109460. https://doi.org/10.1016/j.corsci.2021.109460.

13. Bockris, J. O'M., Reddy, A. K. N., Gamboa-Aldeco, M., 2000. Modern Electrochemistry 2A: Fundamentals of Electrodics, Springer New York, NY. https://doi.org/10.1007/b113922

14. Det Norske Veritas (2017), Recommended Practice DNVGL-RP-B401: Cathodic protection design, DNV, Oslo, Norway

15. Det Norske Veritas (2016), Recommended Practice DNVGL-RP-0416: Cathodic protection for wind turbines, DNV, Oslo, Norway

16. British Standards Institution (2000), BS EN 12473:2000: General principles of cathodic protection in sea waters , BSI, London, UK

17. British Standards Institution (2000), BS EN 12495:2000: Cathodic protection for fixed steel offshore structures, BSI, London, UK

18. British Standards Institution (2001), BS EN 13174:2001: Cathodic protection for harbour installations, BSI, London, UK

19. NACE International (2003), NACE Standard RP0176-2003: Corrosion control pf steel fixed offshore structures associated with petroleum production, Houston, Texas, USA

20. Brooks, C.L., Prost-Domasky, S. A., K. T. Honeycutt, K. T. and T. B. Mills, T. B., 2003. Predictive modeling of structure service life, ASM Handbook Volume 13A.

21. Sun, W., Liu, G., Wang, L., & Li, Y. (2012). A mathematical model for modeling the formation of calcareous deposits on cathodically protected steel in seawater. Electrochimica Acta, 78, 597–608. https://doi.org/https://doi.org/10.1016/j.electacta.2012.06.056

22. Wang, K., Li, C., Li, Y., Lu, J., Wang, Y., & Luo, X. (2021). Multi-physics analysis of the galvanic corrosion of Mg-steel couple under the influence of time-dependent anisotropic deposition film. Journal of Magnesium and Alloys, 9(3), 866–882. https://doi.org/https://doi.org/10.1016/j.jma.2020.11.022

References

23. Thébault, F., Vuillemin, B., Oltra, R., Allely, C., & Ogle, K. (2012). Reliability of numerical models for simulating galvanic corrosion processes. Electrochimica Acta, 82, 349–355. https://doi.org/https://doi.org/10.1016/j.electacta.2012.04.068

24. Bauer, G., Gravemeier, V., & Wall, W. A. (2012). A stabilized finite element method for the numerical simulation of multi-ion transport in electrochemical systems. Computer Methods in Applied Mechanics and Engineering, 223–224, 199–210. https://doi.org/https://doi.org/10.1016/j.cma.2012.02.003

25. Duddu, R. (2014). Numerical modeling of corrosion pit propagation using the combined extended finite element and level set method. Computational Mechanics, 54(3), 613–627. https://doi.org/10.1007/s00466-014-1010-8

26. Gortsas, T. v, Tsinopoulos, S. v, & Polyzos, D. (2022). A local domain boundary element method for solving the nonlinear fisher KPP diffusion-reaction equation. Engineering Analysis with Boundary Elements, 138, 177–188. https://doi.org/https://doi.org/10.1016/j.enganabound.2022.02.008

27. Gortsas, T. v, & Tsinopoulos, S. v. (2022). A local domain BEM for solving transient convection-diffusion-reaction problems. International Journal of Heat and Mass Transfer, 194, 123029. https://doi.org/https://doi.org/10.1016/j.ijheatmasstransfer.2022.123029

28. Giera, B., Henson, N., Kober, E. M., Shell, M. S., & Squires, T. M. (2015). Electric Double-Layer Structure in Primitive Model Electrolytes: Comparing Molecular Dynamics with Local-Density Approximations. Langmuir, 31(11), 3553–3562. https://doi.org/10.1021/la5048936

29. Wang, X., Wang, Y., Wang, B., Xing, Y., Lu, M., Qiao, L., & Zhang, L. (2022). Effect of scratches on hydrogen embrittlement sensitivity of carbon steel in cathodic protection and dynamic DC stray current interference environments. International Journal of Pressure Vessels and Piping, 199, 104712. https://doi.org/https://doi.org/10.1016/j.ijpvp.2022.104712

30. Huang, C. (2020). NUMERICAL MODELING OF HYDROGEN EMBRITTLEMENT [University of Akron]. http://rave.ohiolink.edu/etdc/view?acc_num=akron1588597670254056

References

31. Hägg Mameng, S., Pettersson, R., & Leygraf, C. (2019). Localised corrosion and atmospheric corrosion of stainless steels [KTH]. In TRITA-CBH-FOU. http://urn.kb.se/resolve?urn=urn:nbn:se:kth:diva-263756

32. G. Masi, F. Matteucci, J. Tacq, A. Balbo (2018), State of the art study on materials and solutions against corrosion in offshore structures, North sea solutions for innovation in corrosion for energy (NeSSIE) project.

33. Wang, K., & Zhao, M. (2016). Mathematical Model of Homogeneous Corrosion of Steel Pipe Pile Foundation for Offshore Wind Turbines and Corrosive Action. Advances in Materials Science and Engineering, 2016, 9014317. https://doi.org/10.1155/2016/9014317

34. Wang, K., Li, Z., & Zhao, M. (2016). Mechanism of Localized Corrosion of Steel Pipe Pile Foundation for Offshore Wind Turbines and Corrosive Action. The Open Civil Engineering Journal, 10, 685–694. https://doi.org/10.2174/1874149501610010685

35. Shittu, A. A., Mehmanparast, A., Shafiee, M., Kolios, A., Hart, P., & Pilario, K. (2020). Structural reliability assessment of offshore wind turbine support structures subjected to pitting corrosion-fatigue: A damage tolerance modelling approach. Wind Energy, 23(11), 2004–2026. https://doi.org/https://doi.org/10.1002/we.2542

36. Moghaddam, B. T., Hamedany, A. M., Mehmanparast, A., Brennan, F., Nikbin, K., & Davies, C. M. (2019). Numerical analysis of pitting corrosion fatigue in floating offshore wind turbine foundations. Procedia Structural Integrity, 17, 64–71. https://doi.org/https://doi.org/10.1016/j.prostr.2019.08.010

Thank you for your attention!